

Aus der Medizinischen Poliklinik – Innenstadt
der Ludwig-Maximilians-Universität München
ehem. Direktor: Prof. Dr. med. Detlef Schlöndorff
jetziger komm. Direktor: Prof. Dr. med. Martin Reincke

***The role of chemokine receptor CCR1-dependent
macrophage recruitment for the progression of
chronic kidney disease in murine Alport
syndrome or type 2 diabetes***

Dissertation

Zum Erwerb des Doktorgrades der Humanbiologie
an der Medizinischen Fakultät der
Ludwig-Maximilians-Universität zu München

Vorgelegt von: **Volha Ninichuk**

Minsk, Weissrussland

2008

Mit Genehmigung der Medizinischen Fakultät der Universität München

1. Berichterstatter:	PD Dr. H.- J. Anders
2. Berichterstatter:	PD Dr. H. Engelmann
1. Mitberichterstatter:	PD Dr. St. Lederer
2. Mitberichterstatter:	Prof. Dr. F. Krombach
Dekan:	Prof. Dr. med. D. Reinhard
Tag der mündlichen Prüfung:	15.01.2008

Die vorliegende Arbeit wurde in der Zeit von Oktober 2003 bis Januar 2007 in der Abteilung für Klinische Biochemie in der Medizinischen Poliklinik der Ludwig-Maximilians-Universität durchgeführt.
(Direktor: Prof. Dr. Med. Detlef Schlöndorff)

Betreut wurde die Arbeit von Herrn PD Dr. med. Hans-Joachim Anders

ACKNOWLEDGEMENTS

First and foremost, my profound gratitude is addressed to my supervisor PD Dr. med. Hans-Joachim Anders for his leadership, valuable help and kind support. It would be impossible to complete this work without his editorial advices, suggestions, discussions and guidance.

I am also heartily grateful to Prof. Dr. med. Detlef Schlöndorff for accepting me at the research laboratories of the Medical Policlinic, for his critical reading of our manuscripts and his positive influence on my work.

Moreover, I would like to acknowledge the skilful technical assistance of Ewa Radomska, Stephanie Pfeiffer, Dan Draganovici and Jana Mandelbaum from the groups of Dr. Hans-Joachim Anders and Dr. Stephan Segerer.

I also express my thanks to our collaborators for their significant and fruitful contribution to a number of our experiments: Prof. Fritz Krombach from the Institute for Surgical Research (Munich, Germany) and members of his group; Dr. Richard Horuk and his team from Berlex Biosciences, Richmond, California, USA and Dr. Pius Loetscher from Novartis Institute for Biomedical Research, Basel, Switzerland for providing us with CCR1 antagonists; PD Dr. Oliver Gross from the Department of Nephrology and Rheumatology, University of Göttingen (Göttingen, Germany) supplying us with Col4A3-deficient mice.

For organizing the GRK438 course “Vascular Biology in Medicine” I want to thank Prof. Dr. Wolfgang Siess (Institut für Prophylaxe und Epidemiologie der Kreislaufkrankheiten, Klinikum der LMU, Munich, Germany). It was a great chance for me to improve my scientific skills and I want also to warmly thank all members and students of the Department of Clinical Biochemistry of the Ludwig Maximilians University (Munich) who monitored my work and helped me during my stay in the lab.

Furthermore, I would like to express my deepest gratitude and thanks to all members of my group for having shared with me their experience and creation a wonderful working environment.

I especially thank my family and all my friends. Their faith, love and support are the keys of all my achievements.

Publications Related to the Dissertation Work

1. **Ninichuk V**, Gross O, Reichel C, Khandoga A, Pawar RD, Ciubar R, Segerer S, Belezmezova E, Radomska E, Luckow B, de Lema GP, Murphy PM, Gao JL, Henger A, Kretzler M, Horuk R, Weber M, Krombach F, Schlöndorff D, Anders HJ: Delayed chemokine receptor 1 blockade prolongs survival in collagen 4A3-deficient mice with Alport disease. *J Am Soc Nephrol* 16:977-985, 2005
2. **Ninichuk V**, Anders HJ: Chemokine receptor CCR1: a new target for progressive kidney disease. *Am J Nephrol* 25:365-372, 2005
3. Anders HJ, **Ninichuk V**, Schlöndorff D: Progression of kidney disease: blocking leukocyte recruitment with chemokine receptor CCR1 antagonists. *Kidney International* 69:29-32, 2006
4. **Ninichuk V**, Segerer S, Khandoga AG, Loetscher P, Schlapbach A, Revesz L, Feifel R, Khandoga A, Krombach F, Nelson PJ, Schlöndorff D, Anders HJ: The role of interstitial macrophages in nephropathy of type 2 diabetic db/db mice. (*Am J Pathol* 2007, in press)
5. **Ninichuk V**, Kulkarni O, Clauss S, Anders HJ: Tubular atrophy, interstitial fibrosis, and inflammation in type 2 diabetic db/db mice. An accelerated model of advanced diabetic nephropathy. (under revision)

Additional Publications

6. **Ninichuk V**, Gross O, Segerer S, Hoffmann R, Radomska E, Buchstaller A, Huss R, Akis N, Schlöndorff D, Anders HJ: Multipotent mesenchymal stem cells reduce interstitial fibrosis but do not delay progression of chronic kidney disease in collagen4A3-deficient mice. *Kidney International* 70:121-129, 2006
7. Kulkarni O, Purschke W, Eulberg D, Selve N, Buchner K, **Ninichuk V**, Segerer S, Vielhauer V, Klusmann S, Anders HJ: Spiegelmer therapy of lupus-like disease in MRL-(Fas)lpr mice. (under revision)

Presentation of this Project

Oral presentations

1. 3-d Herrsching-Symposium of the Graduate Program “Vascular Biology in Medicine“ (GRK 438)

March 2005, Munich, Germany

Ninichuk V, Reichel CA, Khandoga A, Krombach F, Schlöndorff D, and Anders HJ:

Antagonism of chemokine receptor CCR-1 prolongs survival in Alport disease.

2. Nephrologisches Forum München “Fellow’s night 2006”

June 2006, Munich, Germany

Ninichuk V, Schlöndorff D, and Anders HJ: The role of interstitial macrophages in nephropathy of type 2 diabetic db/db mice.

Posters

1. 1-st Students’ meeting “DECIPHERING THE CELL MIGRATION CODE”,

May 2005, Gwatt-Zentrum am Thunersee, Thun, Switzerland

Ninichuk V, Reichel CA, Khandoga A, Krombach F, Schlöndorff D, and Anders HJ:

Antagonism of chemokine receptor CCR-1 prolongs survival in Alport disease.

2. 2-nd Students’ meeting “DECIPHERING THE CELL MIGRATION CODE”,

May 2006, Gwatt-Zentrum am Thunersee, Thun, Switzerland

Ninichuk V, Khandoga A.G, Krombach F, Schlöndorff D, and Anders HJ:

Blocking chemokine receptor CCR1 reduces interstitial macrophage infiltrates in diabetic nephropathy.

CONTENTS

1.	SUMMARY	1
2.	INTRODUCTION	5
2.1	Chronic kidney disease	5
2.1.1	Alport syndrome	8
2.1.2	Diabetes	14
2.2	Pathophysiology of the progression of chronic kidney disease	18
2.2.1	Chemokines and chemokine receptors in renal inflammation	18
2.2.2	Chemokines and chemokine receptors	23
2.2.3	Chemokine receptor CCR1 as a potential target in kidney disease	26
2.2.3.1	Chemokine receptor CCR1	26
2.2.3.2	CCR1 antagonism in models of kidney disease	28
2.3	Research hypothesis	32
3.	MATERIAL AND METHODS	33
3.1	Materials	33
3.1.1	Equipment	33
3.1.2	Chemicals and materials	34
3.1.3	Oligonucleotide primers and probes for RT-PCR	37
3.1.4	Computer programs	38
3.1.5	Solutions	38
3.2	Methods	41
3.2.1	Animal studies	41
3.2.1.1	Homing conditions and animal procedures	41
3.2.1.2	Study design and experimental procedures	41
3.2.1.3	Determination of BL5923 blood levels	43
3.2.1.4	Cremaster muscle intravital microscopy	43
3.2.1.5	Cell transfer study	45
3.2.1.5.1	Cell isolation	45
3.2.1.5.2	Fluorescent labeling	46
3.2.1.5.3	Intravenous injection protocol	46
3.2.2	In vitro methods	47
3.2.2.1	Culture of mammalian cells	47
3.2.2.2	Cell freezing and thawing	47
3.2.2.3	Stimulation experiments	48
3.2.2.4	Cytokine Elisa	48
3.2.3	Immunohistochemical methods and histopathological evaluation	49
3.2.5	RNA analysis	50
3.2.5.1	RNA isolation	50
3.2.5.2	cDNA synthesis and real-time RT-PCR	51
3.2.6	Statistical analysis	52

4.	RESULTS	53
4.1	Role of CCR1 for the progression of Alport disease	53
4.1.1	CCR1 blockade and survival of COL4A3-deficient mice	53
4.1.2	Interstitial macrophages and tubulointerstitial injury in COL4A3-deficient mice	54
4.1.3	Renal infiltration of labeled macrophages in kidneys of COL4A3-deficient mice	57
4.1.4	Interstitial renal fibrosis	59
4.1.5	Renal CCL5 expression in COL4A3-deficient mice	61
4.1.6	CCL5 production by J774 macrophages	62
4.1.7	CCR1 mediates intravascular adhesion and transendothelial migration of leukocytes	64
4.2	Role of CCR1 for the progression of type 2 diabetic nephropathy	67
4.2.1	Effect of uninephrectomy on diabetic nephropathy of db/db mice	67
4.2.2	CCR1 antagonist reduces recruitment of macrophages to the renal interstitium of uninephrectomized db/db mice	69
4.2.3	CCR1 antagonist reduces interstitial macrophage counts and tubulointerstitial injury in uninephrectomized db/db mice	71
4.2.4	CCR1 blockade reduces renal expression of proinflammatory mediators in uninephrectomized db/db mice	78
4.2.5	CCR1 blockade inhibits the proliferation of J774 but not of tubular epithelial cells	80
5.	DISCUSSION	82
6.	REFERENCES	87
7.	ABBREVIATIONS	102
8.	CURRICULUM VITAE	107

1. SUMMARY

The global burden of chronic kidney diseases remains an ongoing medical challenge. Therapies that can halt or reverse advanced renal injury are not yet available. Increasing numbers of patients progress to the end-stage renal failure and require renal replacement therapy, the latter being associated with significant mortality, a lower quality of life, and high costs for national health systems. Thus, new treatment strategies that slow down, halt or even revert progressive renal damage are requested.

Chemokines and their receptors are involved in the pathogenesis of renal diseases. They mediate leukocytes and macrophages recruitment and activation during initiation as well as progression of renal inflammation. Infiltrating leukocytes are the major source for proinflammatory and profibrotic cytokines and are therefore critical for mediating fibroblast proliferation, differentiation into myofibroblasts, matrix production, and tubular atrophy.

Recent advances in the understanding of the molecular mechanisms that regulate renal leukocyte recruitment suggest chemokines and chemokine receptors as novel targets for specific pharmacological intervention.

The aim of the present thesis was to investigate the role of chemokine receptor CCR1 for the progression of chronic kidney diseases, e.g. Alport disease and diabetic nephropathy. Two different animal models were used: Col4A3-deficient mice and type 2 diabetic db/db mice with advanced diabetic nephropathy. We blocked CCR1 in Col4A3-deficient mice with BX417, a small molecule CCR1 antagonist, and BL5923, a novel orally available antagonist with a high specificity for human and murine CCR1 in uninephrectomized type 2 diabetic db/db mice, respectively.

Treatment with BX471 (25mg/kg) from weeks 6 to 10 of life improved survival of COL4A3-deficient mice, characterized by glomerulosclerosis and subsequent progressive tubulointerstitial injury, leading to fatal end-stage renal disease (ESRD). Improvement was associated with less interstitial macrophages, apoptotic tubular epithelial cells, tubular atrophy, interstitial fibrosis, and less globally sclerotic glomeruli. BX471 reduced total renal *Ccl5* mRNA expression by reducing the number of interstitial CCL5-positive cells in inflammatory cell infiltrates. Intravital microscopy of the cremaster muscle in male mice identified that BX471 or lack of CCR1 impaired leukocyte adhesion to activated vascular endothelium and transendothelial leukocyte migration, whereas leukocyte rolling and interstitial migration were not affected. Furthermore, in activated murine macrophages, BX471 completely blocked CCL3-induced CCL5 production.

When CCR1 was blocked with BL5923 (60mg/kg, b.i.d), the interstitial recruitment of ex vivo labeled macrophages was markedly decreased in uninephrectomized male db/db mice with type 2 diabetes. Similarly, BL5923 orally administered from month 5 to 6 of life reduced the numbers of interstitial macrophages in uninephrectomized db/db mice. This was associated with reduced numbers of Ki-67 proliferating tubular epithelial and interstitial cells, tubular atrophy, and interstitial fibrosis in uninephrectomized db/db mice. Glomerular pathology and proteinuria were not affected by the CCR1 antagonist. BL5923 reduced renal mRNA expression of Ccl2, Ccr1, Ccr2, Ccr5, Tgf- β 1, and collagen I- α 1 when compared to untreated uninephrectomized male db/db mice of the same age.

Thus, we identified a previously unrecognized role for CCR1-dependent recruitment of interstitial macrophages for the progression of chronic kidney disease in Alport disease and diabetic nephropathy. These data identify CCR1 as a potential therapeutic target for Alport disease and late stage diabetic nephropathy or other progressive nephropathies associated with interstitial macrophage infiltrates.

1. ZUSAMMENFASSUNG

Die zunehmende Prävalenz der Chronischen Niereninsuffizienz bleibt eine medizinische Herausforderung. Behandlungsmöglichkeiten, die einen Stop oder eine Heilung der Chronischen Niereninsuffizienz erlauben, sind bisher nicht verfügbar. Bei immer mehr Patienten schreitet die Chronische Niereninsuffizienz bis zum terminalen Nierenversagen voran, die letztlich nur durch Nierenersatz am Leben erhalten werden können, Verfahren, die mit einer erheblichen Morbidität, Kosten und Einschränkungen der Lebensqualität einhergehen. Daher sind neue Behandlungsverfahren, die die Progression der Chronischen Niereninsuffizienz aufhalten oder gar rückgängig machen können dringend notwendig.

Chemokine und ihre Rezeptoren sind an der Pathogenese von Nierenkrankheiten beteiligt. Die vermitteln die Rekrutierung und Aktivierung von Leukozyten und Makrophagen and während der Initiation und Progression der renalen Entzündung. Infiltrierende Leukozyten sind die Hauptquelle von proinflammatorischen und profibrotischen Zytokinen und tragen so zur Fibroblastenproliferation, Differenzierung in Myofibroblasten, Matrixproduktion und Tubulusatrophie bei.

Fortschritte zum Verständnis der molekularen Mechanismen der renalen Leukozytenrekrutierung deuten daraufhin, dass Chemokine und Chemokinrezeptoren als neue Targets für eine spezifische pharmakologische Intervention in Frage kommen.

Das Ziel der vorgelegten Arbeit ist, die funktionelle Bedeutung des Chemokinrezeptors CCR1 für die Progression der Chronischen Niereninsuffizienz z.B. beim Alport Syndrom und der Diabetischen Nephropathie zu untersuchen. Es wurden zwei verschiedene Tiermodelle verwendet: Col4A3-defiziente Mäuse und db/db Mäuse mit Typ 2 Diabetes und fortgeschrittener Diabetischer Nephropathie. Wir verwendeten BX471 als CCR1 Antagonisten bei Col4A3-defizienten Mäusen, und BL5923, einen oral verfügbaren CCR1 Antagonist bei uninephrektomierten db/db Mäusen.

BX471 (25mg/kg) von der 6. bis 10. Lebenswoche gegeben, verbesserte das Überleben von COL4A3-defizienten Mäusen, durch Reduktion der Glomerulosklerose und der nachfolgenden progredienten tubulointerstitiellen Schädigung. BX471 reduzierte die Zahl der interstitiellen Makrophagen, der apoptotischen Tubulusepithelzellen, die Tubulusatrophie und die interstitielle Fibrose. BX471 reduzierte auch die totale renale *Ccl5* mRNA Expression durch Reduktion der Zahl der interstitiellen CCL5-positiven Zellen. Durch Intravitalmikroskopie konnte gezeigt werden, dass nach Gabe von BX471 oder genetischer

Verlust von CCR1 die Leukozytenadhäsion und die transendotheliale Migration behindert ist, wohingegen das Leukozytenrolling und die interstitielle Migration nicht beeinträchtigt waren. Darüberhinaus, blockierte BX471 in aktivierten Makrophagen die CCL3-induzierte CCL5 Produktion.

CCR1 Blockade mit BL5923 (60mg/kg alle 12h) reduzierte die Rekrutierung ex vivo markierter Makrophagen in das renale Interstitium uninephrektomierter männlicher db/db Mäuse mit Typ 2 Diabetes. Wurde BL5923 ab dem 5. Lebensmonat für 4 Wochen oral gegeben kam es zu einer Abnahme der Zahl interstitieller Makrophagen sowie Ki-67 positiver proliferierender Tubulusepithelzellen in uninephrektomierten db/db Mäusen. Die glomeruläre Pathologie und die Proteinurie wurden durch den CCR1 Antagonisten nicht verbessert. BL5923 reduzierte zudem die renale mRNA Expression von Ccl2, Ccr1, Ccr2, Ccr5, Tgf- β 1 und collagen I- α 1.

Zusammengefasst konnten wir durch Blockade von CCR1 bislang unbekannt Funktionen für interstitielle Makrophagen bei der Progression der Chronischen Niereninsuffizienz von Mäusen mit Alport Syndrom oder Diabetischer Nephropathie beschreiben. Diese Daten identifizieren CCR1 als ein potentiell Therapietarget für das Alportsyndrom und die fortgeschrittene Diabetische Nephropathie oder andere progrediente Nierenkrankheiten, bei denen interstitielle Makrophageninfiltrate auftreten.

2. INTRODUCTION

2.1 Chronic kidney disease

Chronic renal failure

Chronic renal failure (CFR) defined by gradual and progressive loss of the ability of the kidneys to excrete wastes, concentrate urine, and conserve electrolytes. It usually occurs over a number of years as the internal structures of the kidney are slowly damaged. In the early stages, there may be no symptoms. In fact, progression may be so gradual that symptoms do not occur until kidney function is less than one-tenth of normal.

The incidence and prevalence of chronic kidney disease (CKD) is on the rise worldwide. ESRD is the most advanced form of CKD, requiring some form of renal replacement therapy to ensure survival. Interventions to prevent or slow the progression of CKD, irrespective of the original cause, are thus of significant importance (1). For example, ESRD affects more than 2 out of 1,000 people in the United States. Diabetes and hypertension are the two commonest causes and account for approximately two thirds of the cases of chronic renal failure and ESRD (2). In fact, by the time dialysis is initiated, more than 70% of patients with CKD have four or six comorbidities. Besides diabetes and hypertension, dialysis patients often have congestive heart failure, atherosclerotic heart disease, and transient ischemic attack (TIA) or stroke (3). In addition to vascular risk factors and diseases, patients with CKD are predisposed to oxidative stress, inflammation, elevated homocysteine levels, anemia, and vascular calcification (4, 5) all of which have been associated with impaired neurologic functions (6). In the USA in 2002, the Kidney Disease Outcomes Quality Initiative (K/DOQI) of the National Kidney Foundation established a classification of CKD (7), which has become increasingly accepted by the international nephrology community (8) (Table 1). This classification defines CKD as a GFR <60 ml/min/1.73 m² or a GFR ≥ 60 ml/min/1.73 m² together with the presence of kidney damage, present for ≥ 3 months (9).

Table 1. The USA National Kidney Foundation's K/DOQI classification (with minor adaptations, ref. 9).

Stage	Description	GFR (ml/min/1.73m ²)	Prevalence	Focus of care
1	Kidney damage with normal	>90	3.3%	Diagnosis and disease-specific therapies
2	Kidney damage with mildly	60–89	3.0%	Slowing of progression and reduction
3	Moderately impaired GFR	30–59	4.3%	Addressing complications of CKD
4	Severely impaired GFR	15–29	0.2%	Preparation for dialysis
5	Established renal failure	<15 or on dialysis	0.2%	Dialysis, transplantation or conservative care

Chronic renal failure (CRF) is a progressive process. It may result from any major cause of renal dysfunction. Progression may continue to ESRD, requiring dialysis or a kidney transplant. According to the “Annual Report on Dialysis Treatment and Renal Transplantation in Germany for 2005/2006” on 31 December 2005 a total of 87,151 patients were treated with renal replacement therapy (RRT), corresponding to a prevalence of 1,057 RRT per million population (pmp) (Table 2) (<http://www.quasi-niere.de>).

Table 2. Summary overview on ESRD therapy in Germany for the years 2005, 2004, 2003 (<http://www.quasi-niere.de>)

	2005	2004	2003
Response rate (%)	89	90	90
Total number of ESRD patients	87, 151	82, 305	78,281
children<15 years	578	523	564
adolescents 15-18 years	349	348	326
Prevalence of ESRD therapy / pmp	1057	998	949
Total number of dialysis patients	63,427	60,992	58,579
Prevalence / pmp	769	739	710
- Patients on haemodialysis	60,411	58,168	55,871
- Patients on peritoneal dialysis	3,016	2,824	2,708
Patients with a functional transplant	23,724	21,313	19,702
Prevalence functioning transplant / pmp	288	258	239
Commencement of ESRD therapy	16, 766	16,027	15,360
Incidence / pmp	203	194	186
- Haemodialysis treatment (adults)	15,578	14,953	14,402
- Peritoneal dialysis treatment (adults)	973	856	802
- Children and adolescents (on dialysis)	108	137	103
- Preemptive transplantation	107	81	53
Deceased patients	11,519	10, 992	10,654

2.1.1 Alport syndrome

Alport syndrome (AS) is a hereditary nephropathy characterized by a family history of hematuria and proteinuria, progressive renal failure, sensorineural deafness and typical ocular changes (10, 11).

The combination of a progressive hereditary nephritis with sensorineural deafness was first described by A. Cecil Alport in 1927. Alport's syndrome develops from mutations of either the α_3 , α_4 or α_5 chain of type IV collagen, i.e. collagen types that constitute basement membranes in the renal glomerulus, the ear and the eye (12).

Alport syndrome is clinically heterogeneous, and patients have been classified by their age at ESRD and by the presence of accompanying features, such as sensorineural deafness and ocular lesions (lenticonus and perimacular flecks) (13, 14). More rarely, patients develop diffuse esophageal and vulvar leiomyomatosis (15, 16) or macrothrombocytopenia (17, 18). Among patients with diffuse leiomyomatosis, severe congenital and bilateral cataracts are frequent. Alport syndrome is characterized by hematuria progressing in males to renal failure at young or adult age (19). Clinical features are usually less severe in females (20, 21). Alport patients who reach ESRD are dialyzed or undergo renal transplantation. Some transplanted patients develop a posttransplant anti-GBM nephritis, leading to irreversible graft failure (22).

The involvement of type IV collagen in Alport syndrome was indicated by immunohistochemical analysis of renal biopsies using anti-type IV collagen antibodies. The antibodies directed against type IV α_3 and α_5 collagen chains did not bind to the GBM in most Alport patients (23, 24). Further evidence came from studies of collagenase treated renal basement membranes from Alport patients, in which type IV collagen NC domains were absent (25, 26). The type IV collagen COL4A3 and COL4A5 NC domains were also the targets of anti-GBM antibodies, which occurred in some patients after renal transplantation (27, 28). These data also point to a possible type IV collagen defect as the cause of Alport syndrome.

Structure and function of type IV collagen

Type IV collagen is a multimeric protein composed of three so-called α chains. To date, six different α chains have been identified ($\alpha 1$ – $\alpha 6$) with molecular weights of 170–185 kDa. Each of the six chains of collagen IV has three domains: there is a short 7S domain at the N-terminal; a long, collagenous domain occupies the midsection of the molecule; and a noncollagenous domain (NC1) is positioned at the C-terminal (Figure 1) (29).

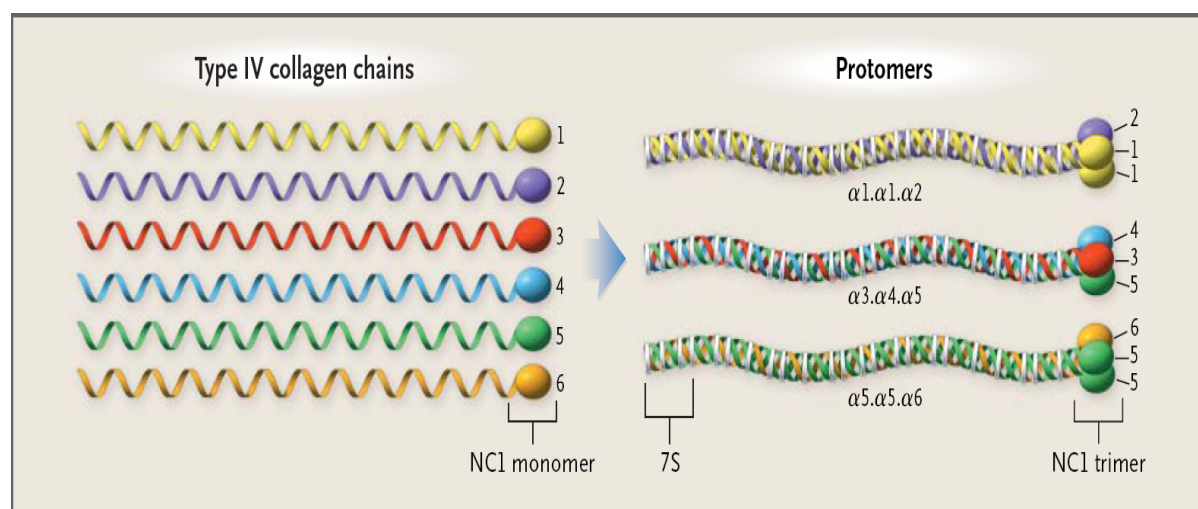


Figure 1. Triple helical organization of the type IV collagen family (ref. 29).

Six genetically distinct α chains are arranged into three triple helical protomers that differ in their chain composition. Each protomer has a 7S triple helical domain at the N-terminal; a long, triple helical, collagenous domain in the middle of the molecule; and a noncollagenous (NC1) trimer at the C-terminal. Interruptions in the Gly–Xaa–Yaa amino acid sequence at multiple sites along the collagenous domain (white rings) confer flexibility, allowing for looping and supercoiling of protomers into networks. The selection of α chains for association into trimeric protomers is governed by molecular recognition sequences encoded within the hypervariable regions of NC1 domains (30, 31).

In spite of many potential permutations, the six chains of collagen IV apparently form only three sets of triple helical molecules called protomers, which are designated as $\alpha 1.\alpha 1.\alpha 2(\text{IV})$, $\alpha 3.\alpha 4.\alpha 5(\text{IV})$ and $\alpha 5.\alpha 5.\alpha 6(\text{IV})$ (30-33). These protomers create collagenous networks by uniting two NC1 trimers to form hexamers and uniting four 7S domains to form tetramers with other protomers, as shown in the $\alpha 3.\alpha 4.\alpha 5(\text{IV})$ network in Figure 2. Only three canonical sets of hexamers form networks: $\alpha 1.\alpha 1.\alpha 2(\text{IV})$ - $\alpha 1.\alpha 1.\alpha 2(\text{IV})$, $\alpha 3.\alpha 4.\alpha 5(\text{IV})$ -

$\alpha3.\alpha4.\alpha5(\text{IV})$, and $\alpha1.\alpha1.\alpha2(\text{IV})$ - $\alpha5.\alpha5.\alpha6(\text{IV})$. The x-ray crystallographic structure of the $\alpha1.\alpha1.\alpha2(\text{IV})$ NC1 hexamer provides novel insight into the molecular interactions that govern chain assembly and the pathophysiological mechanisms underlying Goodpasture's and Alport's syndromes (34, 35).

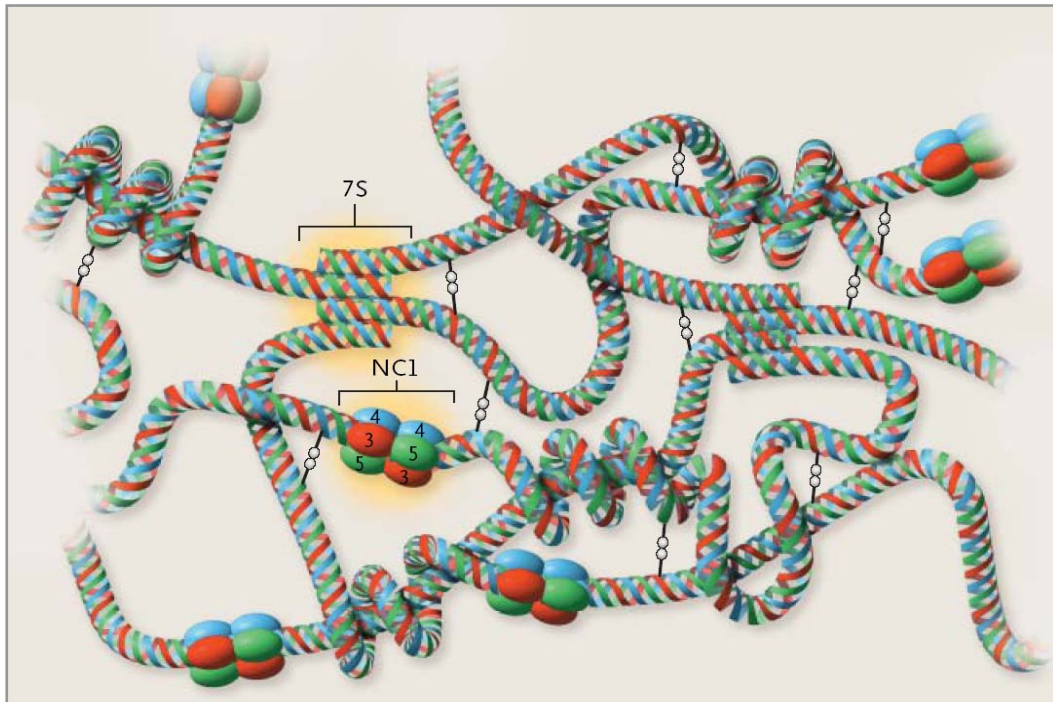


Figure 2. Assembly and network organization of collagen IV protomers (ref. 29).

Protomers create basement-membrane networks with other protomers by uniting two NC1 trimers to form an interface hexamer at the C-terminal and by uniting four triple helical 7S domains at the N-terminal. A network composed of $\alpha3.\alpha4.\alpha5(\text{IV})$ protomers is illustrated, showing end-to-end connections of individual protomer units, supercoiling and looping of the triple helixes, and disulfide cross-links between triple helical domains (30-33). The structure of the NC1 hexamer is determined by the particular α chains that form a triple helical protomer and by the particular canonical protomers that can connect to adjoining protomers (NC1 box). Molecular recognition sequences encoded within NC1 domains govern the selection of partner chains for both protomer and network assembly. The 7S domains also play a key part in determining the specificity, affinity, and geometry of the tetramer formed through the connection of four protomers (7S box) (33, 36, 37). Two other networks are composed of pairs of $\alpha1.\alpha1.\alpha2(\text{IV})$ hexamers or $\alpha1.\alpha1.\alpha2(\text{IV})$ - $\alpha5.\alpha5.\alpha6(\text{IV})$ NC1 hexamers (30-33). The $\alpha3.\alpha4.\alpha5(\text{IV})$ - $\alpha3.\alpha4.\alpha5(\text{IV})$ network differs from the others in that it has a greater number of disulfide cross-links between triple helical domains, which increases its resistance to proteolysis (38).

Assembly of collagen IV networks is regulated developmentally. The $\alpha1.\alpha1.\alpha2(\text{IV})$ - $\alpha1.\alpha1.\alpha2(\text{IV})$ network is $\alpha1.\alpha1.\alpha2(\text{IV})$ is a component of all basement membranes of all animal phyla (39-42), whereas the $\alpha3.\alpha4.\alpha5(\text{IV})$ - $\alpha3.\alpha4.\alpha5(\text{IV})$ and $\alpha1.\alpha1.\alpha2(\text{IV})$ - $\alpha5.\alpha5.\alpha6(\text{IV})$ networks have a restricted distribution in mammalian tissues. The $\alpha3.\alpha4.\alpha5(\text{IV})$ network occurs in the kidney (in glomerular basement membrane and some tubular basement membranes), lung, testis, cochlea, and eye (38, 43, 44) and the $\alpha5.\alpha5.\alpha6(\text{IV})$ network is a feature of skin, smooth muscle, esophagus, and kidney (Bowman's capsule) (31, 32, 45, 46).

Alport genetics

There are three genetic forms of Alport syndrome: XLAS (X-linked Alport syndrome), ARAS (autosomal recessive Alport syndrome) and ADAS (autosomal dominant Alport syndrome).

The estimated gene frequency of Alport syndrome is 1:5000. The disorder is genetically heterogeneous (20), but the vast majority (85%) of Alport pedigrees showed X-linked dominant inheritance. The X-linked Alport gene was mapped to the Xq22–24 region (19, 47, 48), in which the COL4A5 and COL4A6 genes were subsequently localized (49). Mutations in the COL4A5 gene turned out to be the main cause of Alport syndrome. The autosomal recessive (AR) form comprises about 10–15% of the pedigrees and is linked to the COL4A3 and COL4A4 locus (50). Mutations were identified in the COL4A3 and COL4A4 genes in AR Alport families (51, 52). In these families, female patients were clinically indistinguishable from affected male siblings; carriers were asymptomatic and often consanguinous. ADAS accounts for perhaps 5% of Alport patients, at most (Figure 3) (53).

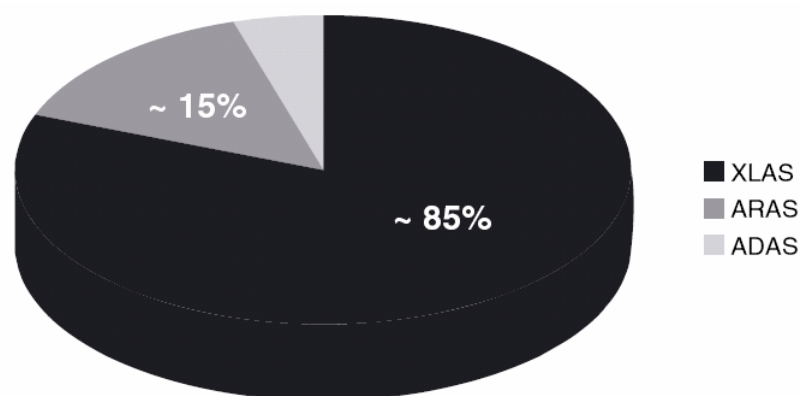


Figure 3. Genetic forms of Alport syndrome. (ref. 53)

Animal models of Alport syndrome

Animal models of genetic disorders provide opportunities for investigating both pathogenesis and treatment of disease. Several excellent animal models of Alport syndrome have been developed (Table 3) (54).

Table 3. Animal models of Alport syndrome (with minor adaptation, ref. 54).

Model	Genetics	Mutation	Onset of proteinuria	Timing of ESRD
Canine				
Samoyed	X-linked	G to T in exon 35 of Col4A5, creating premature stop	4 months	8-10 months
Navasota	X-linked	10-bp deletion in exon 9 shift and premature stop	3-4 months	10-15 months
English cocker spaniel	Autosomal recessive	?	5-8 months	12-18 months
Bull terrier	Autosomal dominant	?	?	Years
Murine				
COL4A3 -/-	Autosomal recessive	COL4A3 deactivated	6 weeks	9-10 weeks
tg/tg mice	Autosomal recessive	COL4A3 & COL4A4 deactivated	2 weeks	8-12 weeks

Murine models have the advantage of a short gestation period. The murine forms of Alport syndrome progress very rapidly (Table 3). Mice that are genetically deficient of the $\alpha 3(\text{IV})$ -chain (“Alport mice”) develop a renal phenotype very similar to that of Alport patients, i.e. proteinuria, glomerulonephritis and subsequent tubulointerstitial fibrosis starting at 8 weeks of age and leading to death due to renal failure at 20–23 weeks (Figure 4) (12).

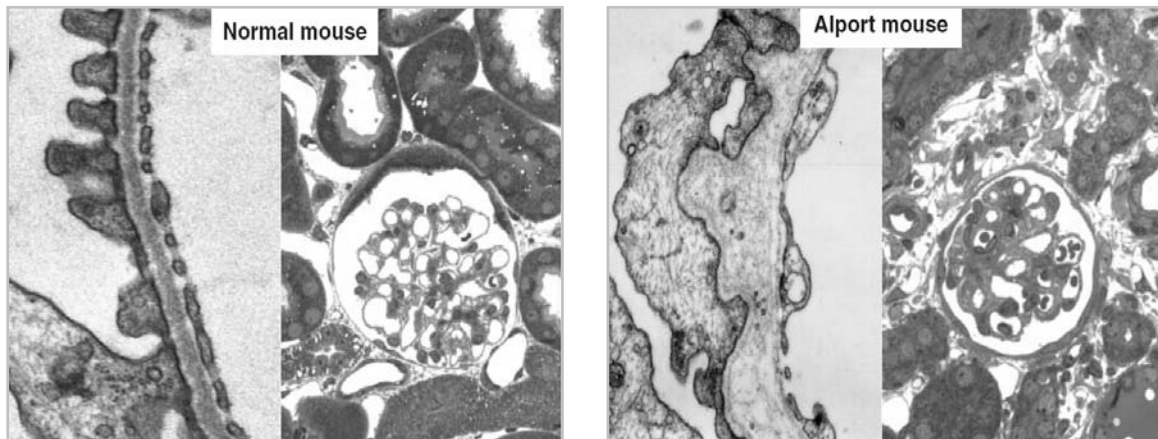


Figure 4. Typical renal morphology in a normal (left) vs an Alport mouse at 8 weeks of age (right).

In the Alport mouse typical splitting of the glomerular basement membrane and pronounced glomerular matrix accumulation is present. Magnification: x20 000 (left) and x800 (right) (12).

2.1.2 Diabetes

Definition

Diabetes results from hyperglycemia associated with defects in insulin secretion, insulin action, or both.

Type 1 diabetes is characterized by beta cell destruction, usually leading to absolute insulin deficiency. This type of diabetes, also known as juvenile-onset diabetes is usually diagnosed in childhood, accounts for 10-15% of all people with the disease. It can appear at any age, although commonly under 40, and its etiology is either immune mediated, related to physical destruction of the pancreas (as in pancreatitis or pancreatic cancer) or idiopathic. Due to the lack of insulin daily injections of insulin are required to sustain life.

Type 2 diabetes is the most common type of diabetes, affecting 85-90% of all people with the disease. This type of diabetes, also known as late-onset diabetes, is characterized by insulin resistance and relative insulin deficiency (55). The disease is strongly genetic in origin but lifestyle factors such as excess weight, inactivity, high blood pressure and poor diet are major risk factors for its development. It usually occurs in adulthood. Symptoms may not show for many years and, by the time they appear, significant problems may have developed. People with type 2 diabetes are twice as likely to suffer cardiovascular disease.

The effect of diabetes is not limited to carbohydrate metabolism. Lipid and protein metabolism play an important role in the progression of the disease. Abnormal glucose metabolism accounts for poorly regulated biochemical processes that glycosylate hemoglobin and other proteins and lipids throughout the body. The progression of diabetes is caused by numerous metabolic events that occur over a period of years (56). Diabetes is a leading cause of blindness, renal failure, and foot and leg amputations in adults.

Epidemiology of type 2 diabetes and Diabetic Nephropathy

The global figure of people with diabetes is set to rise from the current estimate of 150 million to 220 million in 2010, and 300 million in 2025 (57, 58). Most cases will be of type 2 diabetes, which is strongly associated with a sedentary lifestyle and obesity (59). This trend of increasing prevalence of diabetes and obesity has already imposed a huge burden on health-care systems and this will continue to increase in the future (60, 61). In Germany it has been estimated that the point prevalence of type 2 diabetes in the adult population is 6% depending on age; the point prevalence rises to 20% at the age 80 years. The same is also seen in most developed countries (62).

Diabetic nephropathy is a leading cause of ESRD in the Western world, and is one of the most significant long-term complications leading to increased morbidity and mortality in patients with Type 2 diabetes (63). The characteristic renal changes occurring in early stages of diabetic nephropathy include an increase in glomerular filtration rate (GFR) due to hyperfiltration, renal and glomerular hypertrophy, and accumulation of extracellular matrix (ECM) proteins (64). Glomerular hypertrophy precedes GBM thickening, leading to glomerular hyperfiltration, microalbuminuria and the development of proteinuria. Advanced mesangial matrix expansion reduces the surface area of glomerular capillaries available for filtration, leading to declining glomerular function (65). Progressive loss of renal function correlates with the development of tubulointerstitial fibrosis in addition to glomerulosclerosis (66). Glomerular hypertrophy occurs in both Type 1 and Type 2 diabetic patients in both the early and the late stages of disease, although the mechanisms leading to increase in glomerular size may differ (67, 68). Previous studies (69-71) provide convincing evidence of glomerular capillary growth and glomerular hypertrophy as an earliest response to hyperglycaemia in diabetic nephropathy. Evidence from both human and animal studies indicates that glomerular filtration surface area is increased in the early stages of diabetes, and quantitative morphological (stereological) studies have shown this to be the result of increases in length, surface area and number of capillaries per glomerulus (69, 71). Results from several studies indicate that capillary growth contributes to glomerular growth prior to FSGS (72-76). Nagata *et al.* (77) found an increase in the length of capillaries in glomeruli following unilateral nephrectomy, and Nyengaard *et al.* (71) demonstrated a significant increase in the surface area, length and number of capillaries in streptozotocin (STZ)-induced diabetic rats at 10 days. Cahill *et al.* (78) reported that glomerular hypertrophy and glomerular capillary growth in a rat model of FSGS where glomerular hypertrophy preceded

FSGS by several weeks. However, the alterations in the glomerular capillary dimensions associated with advanced diabetic nephropathy have not yet been described (79). Approximately 30% of patients with type 1 diabetes develop DN (80, 81). Barkis *et al.* (82) reported that approximately 25 to 30% of patients with type 2 diabetes will develop overt DN (83). Diabetic nephropathy is generally considered a non-immune disease; however, examination of human biopsies and animal models has shown the presence of macrophages in diabetic kidney (84-89). Macrophages are known to cause renal injury in experimental models of immune-mediated kidney disease and they correlate with renal impairment in human glomerulonephritis (90), but the role in diabetic nephropathy is poorly understood (91).

Animal models of Diabetes

There are several genetic mouse models of diabetes. These include the hypoinsulinemic non-obese diabetic mouse, the Kkay mouse, the New Zealand obese mouse, the hyperinsulinemic ob/ob mouse, and the different strains of obese hyperinsulinemic db/db mouse. Each of these models displays some renal changes, but the most studied is the db/db mouse.

The db/db mouse was identified initially in 1966 in Jackson Labs as an obese mouse that was hyperphagic soon on weaning (92). The diabetic gene (*db*) is transmitted as an autosomal recessive trait. The *db* gene encodes for a G-to-T point mutation of the leptin receptor, leading to abnormal splicing and defective signaling of the adipocyte-derived hormone leptin (93, 94). Lack of leptin signaling in the hypothalamus will lead to persistent hyperphagia and obesity with consequently high leptin and insulin levels. The recognition of diabetes initially was recognized in mice from the C57BLKS/J strain. The C57BLKS/J mouse shares 84% of its alleles with the common C57BL/6 strain and 16% with the DBA/2J strain and was initially maintained by Dr. N. Kaliss (KS). The updated nomenclature from Jackson Labs uses the term C57BLKS/J^{L^{ep}r} (KS for Kaliss) to designate the *db/db* mouse in the C57 black Kaliss background (Jackson Labs, http://jaxmice.jax.org/jaxmicedb/html/model_66.shtml). The *db/db* mouse has a long history as a model of human diabetic nephropathy. Key common features with the human condition are renal hypertrophy, glomerular enlargement, albuminuria, and mesangial matrix expansion. Occasionally, arteriolar hyalinosis is observed in the glomerular arterioles. Features that are not as reproducibly altered in the *db/db* mouse with respect to the human condition are the increase in GBM thickening in relation to albuminuria and the lack of progressive increase in albuminuria. Chow *et al.* (91) showed an

increase in interstitial leukocytes in kidneys from these diabetic mice at 6 to 8 months of age. By 8 months of age, there was a threefold rise in interstitial macrophages in diabetic db/db mice versus db/+ control mice (Figure 5). By 6 months of age, an increase in tubular dilation, atrophy, apoptosis, and early interstitial fibrosis as assessed by an increase in interstitial volume and type IV collagen deposition were also observed (91).

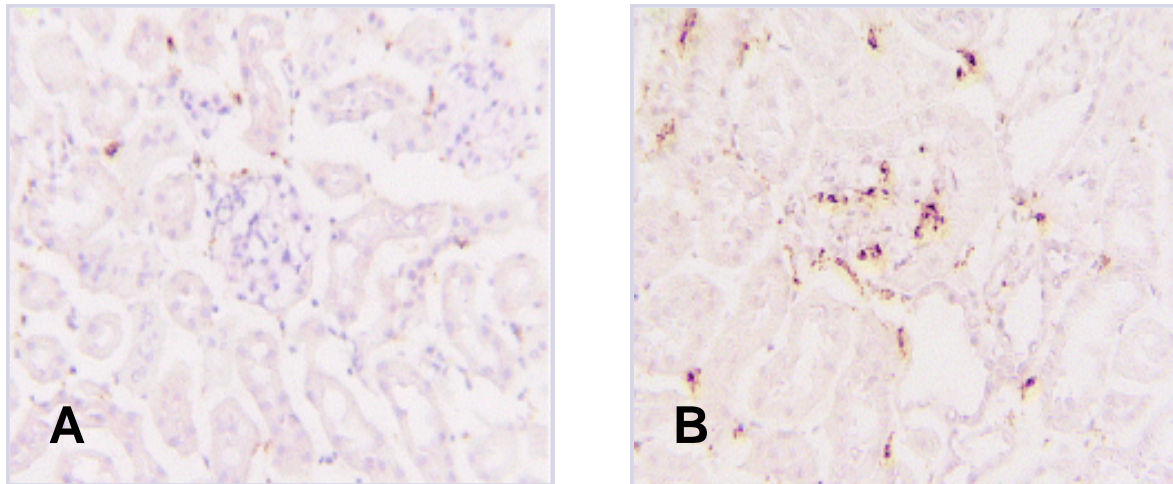


Figure 5. Macrophage association with renal damage in diabetic db/db kidneys.

Immunostaining shows only a few macrophages (brown) in a db/+ kidney at 8 months of age (A), and many glomerular and interstitial macrophages in a diabetic db/db kidney at 8 months (B) (91).

2.2 Pathophysiology of the progression of chronic kidney disease

2.2.1 Chemokines and chemokine receptors in renal inflammation

Chronic inflammation and tissue fibrosis are common causes of progressive organ dysfunction. In the kidney, the extent of leukocyte infiltration and tubulointerstitial fibrosis are strong prognostic factors for the degree of renal insufficiency and the progression to end-stage renal disease (95). Interstitial fibrosis is characterized by the accumulation of interstitial T cells, macrophages, and fibroblasts that contribute to extracellular matrix production and tubular atrophy (96). In this process the accumulation of interstitial leukocytes is critical for mediating fibroblast proliferation, differentiation into myofibroblasts, matrix production, and lymphocytes are the major sources for proinflammatory and profibrotic cytokines (97). All types of renal cells can produce chemokines upon stimulation (reviewed by ref. 98). Proinflammatory stimuli including reactive oxygen species, growth factors and vasoactive agents like angiotensin II can stimulate chemokine production of renal cells. Furthermore, immune complexes and complement activation cause mesangial production of chemokines. In proximal tubular cells chemokines can be induced by LPS (99), high concentrations of albumin (110, 101) or exposure to both calcium oxalate and calcium phosphate crystals (102). Besides intrinsic renal cells, infiltrating leukocytes are a major source of local chemokine production in a positive amplification loop (103, 104), as chemokines secreted by infiltrating leukocytes promote additional leukocyte recruitment (105). It is important to note that chemokine expression is restricted to the injured compartment of the kidney (reviewed in ref. 22). The spatial expression of chemokines in the kidney correlates with the local accumulation of inflammatory cell infiltrates and renal damage (106, 104). Data from animal models have been confirmed by human renal biopsy studies (107-110).

Termination of the trigger injury correlates with a reduction of chemokine expression by intrinsic renal cells and infiltrating leukocytes (111). As further influx of leukocytes does not occur, the number of infiltrating leukocytes declines in parallel to the resolution of disease. Termination of the chemokine signal is critical for the resolution of the inflammatory process. If local chemokine expression is augmented by another trigger of chemokine release, a pre-existing renal disease may eventually progress to severe renal damage. For example, intercurrent infections frequently result in a deterioration of renal diseases including chronic transplant nephropathy. The proinflammatory signals of bacterial and viral invasion are mediated by Toll-like receptors (TLR) (112). TLRs recognize pathogen-associated molecules

such as LPS, peptidoglycans, and unmethylated CpG-DNA (112). It has been found that injection of unmethylated CpG-DNA into mice with otherwise self-limiting immune complex glomerulonephritis resulted in progression instead of resolution of the disease process. This was associated with increased chemokine expression and subsequent glomerular macrophage recruitment (113). Even if the triggering injury subsides, renal chemokine expression can be maintained by other mechanisms such as infection, renin-angiotensin activation, hypoxia or proteinuria, and contribute to persistent leukocyte infiltration and tissue damage. Many studies addressed the functional role of single chemokines or chemokine receptors in defined renal disease models by applying either neutralizing antibodies, DNA vaccination, chemokine receptor antagonists, or by using mutant mice (reviewed in ref. 104). Among those only a few studies have administered specific antagonists late in the disease process, which most appropriately mimics treatment of established kidney disease. Such data is only available for specific blockade of CCR1 (197).

Model of stages of progressive renal disorders

- **Early-stage disease (initiation phase)**

Injury to any type of renal parenchymal cells leads to the secretion of proinflammatory mediators that induce leukocyte infiltration and activation at the place of injury (Figure 6a). If the inflammatory process is restricted either to the glomerulus or to the tubulointerstitium the leukocyte infiltration will be restricted to the respective compartment (111, 114). The selective recruitment of certain leukocyte subsets to different compartments of the kidney further illustrates the complexity of this process. For example, except for transplant glomerulitis, T cells are rarely found within the glomerular tuft as long as Bowman's capsule is intact, whereas T cells are commonly present in interstitial infiltrates (115). Compared to peritubular vessels glomerular capillaries may not support the binding and transmigration of T cells, a phenomenon that could be related to a different expression of adhesion molecules and chemokines or simply to higher shear stress in the glomerular microcirculation. On the other hand, macrophages can be found intraglomerularly during proliferative and especially crescentic glomerulonephritis. Microthrombosis of glomerular capillaries, which is commonly present in focal necrotic or crescentic lesions, may contribute to this phenomenon.

- **Mid-stage disease (amplification phase)**

Infiltration and local proliferation of leukocytes further enhance the local production of cytokines and chemokines (Figure 6b). Furthermore, neutrophils and macrophages generate radical oxygen species and lipid mediators that contribute to local tissue damage, supporting positive feedback mechanisms. Macrophages themselves may secrete extracellular matrix components, but they also are the major source of growth factors such as fibroblast growth factor (FGF), transforming growth factor- β (TGF- β), tumor necrosis factor- α (TNF- α), epithelial growth factor (EGF), and platelet-derived growth factor (PDGF) (97). These cytokines stimulate mesangial cell proliferation and matrix synthesis in the glomerulus leading to the typical pictures of mesangioproliferative GN (116). Activation of podocytes leads to rearrangement of the complex secondary structure, including the slit membrane leading to foot process effacement and proteinuria. Extensive podocyte damage leads to focal adhesions of the denuded GBM to Bowman's capsule and to focal glomerulosclerosis. In the tubulointerstitium, fibroblast proliferation and secretion of extracellular matrix leads to widening of the interstitial space and renal fibrogenesis. Sources of the heterogeneous fibroblast population include proliferation of resident fibroblasts and myofibroblasts derived from tubular epithelial cells by a process described as epithelial-mesenchymal transformation, two mechanisms that are induced by macrophage derived profibrotic cytokines such as FGF-2 (117). In addition, blood borne immature, monocyte-like cells, referred to as fibrocytes, rapidly enter sites of tissue injury and contribute to the local fibrosis (118). However, their role in renal fibrosis has not yet been determined. Another common observation leading to interstitial fibrosis is the appearance of an interstitial cell infiltrate in primary glomerulopathies such as membranous GN, focal glomerulosclerosis or mesangioproliferative GN. The tubular epithelial cell may have an important role in mediating the progression from glomerular to tubulointerstitial nephritis. Spillover of proinflammatory mediators, growth factors, and even albumin into the glomerular ultrafiltrate appear as stimulators for tubular epithelial cells to secrete additional proinflammatory profibrotic cytokines and chemokines (98). Furthermore, proinflammatory mediators secreted within the glomerulus will reach the post-glomerular peritubular circulation, thereby activating peritubular endothelial and tubular epithelial cells (119). In addition, focal capsular adhesions develop "misdirected" ultrafiltrate that may result in local generation of mediators (120). All of these mechanisms may enhance interstitial mononuclear cell recruitment secondary to primary glomerular injury and thus expand the lesion from the glomerulus to the tubulointerstitium.

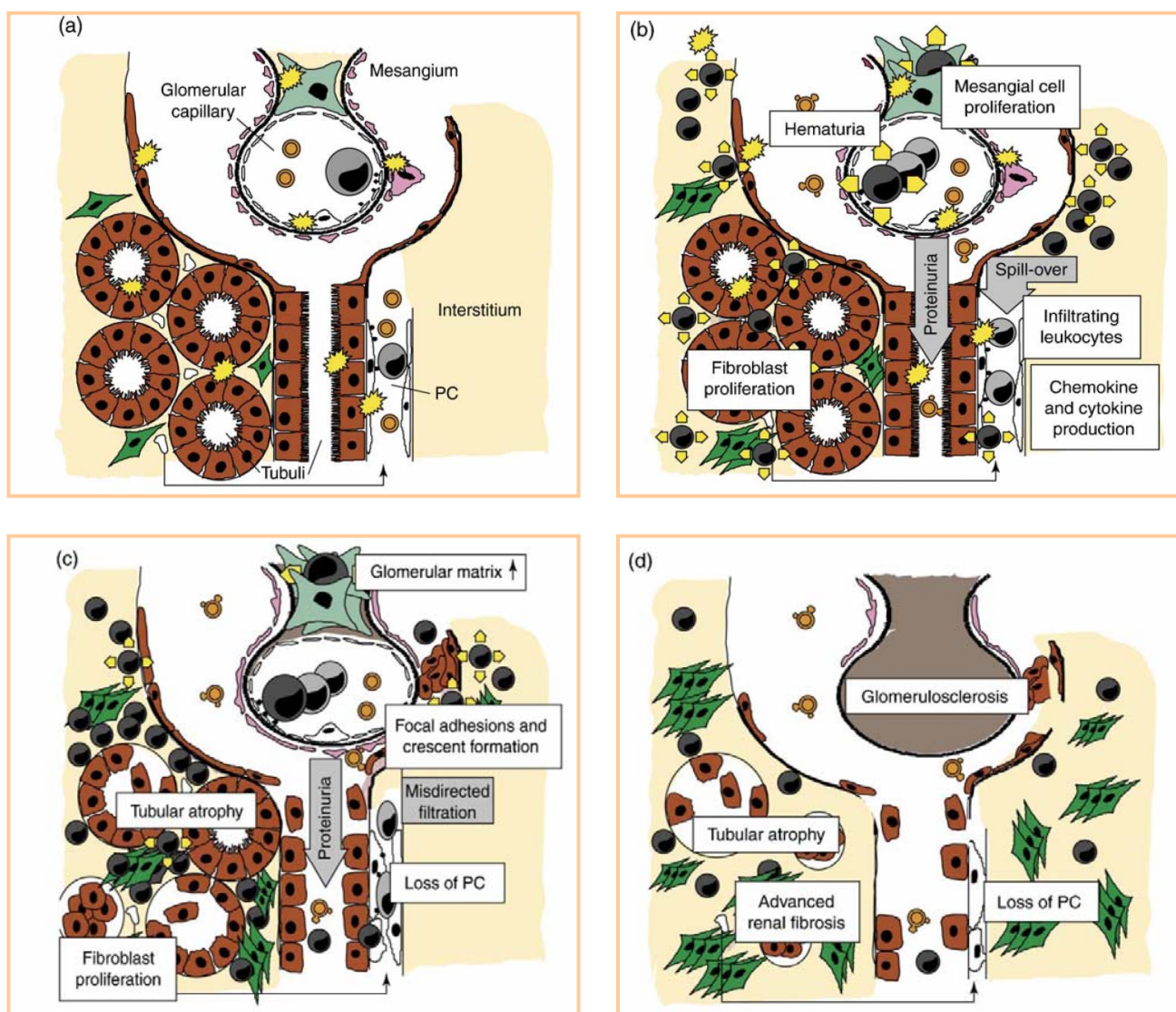


Figure 6. Proposed model of chemokine involvement in progressive disease and fibrosis.

Details are in the text.

(a) Early-stage disease (initiation phase). (b) Mid-stage disease (amplification phase).

(c) Late-stage disease (progression phase). (d) Final-stage disease (terminal phase). Modified, with permission, from ref. 106.

- **Late-stage disease (progression phase)**

The continuous stimulation of intrinsic renal parenchymal cells by infiltrating leukocytes, proteinuria, and secreted cytokines results in ongoing synthesis of extracellular matrix components and irreversible structural damage (Figure 6c). In the glomerulus infiltrating macrophages stimulate mesangial cells to secrete collagen type IV, laminin, and fibronectin that contribute to the development of glomerulosclerosis (121). Mesangial expansion also

leads to narrowing or obliteration of single glomerular capillaries as well as dilation of others (122). Eventually this will not only result in podocyte damage and glomerular sclerosis, but also in destruction of the entire nephron, including downstream peritubular capillaries (120, 122). Thus, the tubulointerstitial compartment undergoes major structural rearrangement. The accumulation of T cells and macrophages provides continuous release of profibrotic mediators that induce the accumulation of fibroblasts, and the ongoing production of extracellular matrix. Activated tubular epithelial cells themselves contribute to this phenomenon by matrix production chemokine-cytokine release, and even to transdifferentiate to myofibroblasts that migrate into the interstitial space (117). The interstitial cell infiltrate itself, together with the increasing amount of extracellular matrix, lead to critical widening of the interstitial space, thereby increasing the distance of the remaining peritubular capillaries to their respective tubular segments, impairing oxygen diffusion as well as tubular reabsorption and excretory function (123). The tubulointerstitial ischemia is considered to be an important factor for tubular cell apoptosis, necrosis, and, finally, tubular atrophy (124, 125). Thus, progressive glomerular and interstitial injuries are tightly linked and aggravate each other by multiple mechanisms, including ischemia.

- **Final-stage disease (terminal phase)**

Finally, vascular rarification and diffuse scarring lead to extensive tubular atrophy, and glomerulosclerosis (Figure 6d). The extensive loss of renal parenchyma and structural integrity finally results in end-stage renal disease with the clinical signs and symptoms of uremia. Leukocytic cell infiltrates resolve, but renal fibroblasts maintain the synthesis of extracellular matrix due to sustained hypoxia and autocrine stimulation (126, 127). Myofibroblasts contribute to contraction of the fibrous tissue with scarring, resulting in the ultimate stage, the shrunken kidney. In the above process there are roles for chemokines at multiple steps. The contribution of the chemokines cannot be viewed in isolation, but as part of an integral system together with adhesion molecules and cytokines (106).

2.2.2 Chemokines and chemokine receptors

Chemokines

Chemoattractant cyto**kines** (**chemokines**) are a family of low-molecular-weight cytokines that induce migration of leukocytes and modulate multiple functions of immune and non-immune cells (128) as well as involve in a number of biological processes, including growth regulation, hematopoiesis, embryonic development, angiogenesis, and HIV-1 infection (129). Although chemokines have a relatively low level of sequence identity, their three-dimensional structure is highly homolog in that they all have the same monomeric fold. This fold results from a four-cysteine motif that forms two characteristic disulfide bridges. Depending on the relative position of the first two cysteines, chemokines are divided into **CC**, **CXC**, **C**, and **CX3C** subfamilies (128). The systematic nomenclature describes individual chemokines (ligands L) and their receptors (R) on the basis of subgroups they belong to (Table 4) (128, 130, 131). Chemokines can be further categorized into two classes depending on whether they are constitutively produced or are inducible (132, 133). The first group, the homeostatic chemokines, are instrumental in basal leukocyte development and trafficking during immune surveillance. For example, chemokines such as CCL21 or CCL19 are involved in physiological homing of leukocytes to lymphoid tissues (130, 134), and in lymphocyte and dendritic cell trafficking during immune surveillance (135). In contrast, inflammatory chemokines are induced by proinflammatory stimuli and orchestrate innate and adaptive immune responses, for example by recruitment of leukocytes to sites of tissue injury (CCL2, CCL3, CCL5, and CXCL10) and regulation of T cell, monocyte and dendritic cell differentiation. All members of the chemokine family work in concert with selectins and integrins to sort and direct effector leukocyte migration (136, 137). Chemokines mediate their biological effects by binding to cell surface receptors that belong to the GPCR superfamily (138). Receptor binding initiates a cascade of intracellular events mediated by the receptor associated heterotrimeric G proteins. These G protein subunits trigger various effector enzymes, which leads to the activation not only of chemotaxis but also to a wide range of functions in different leukocytes, such as an increase in the respiratory burst, degranulation, phagocytosis, and lipid mediator synthesis. Chemokines can interact with only one receptor or a single chemokine binds to multiple receptors (136). Increased chemokine

expression has been shown to be associated with a number of autoinflammatory diseases, including multiple sclerosis, rheumatoid arthritis, diabetes, endometriosis, transplant rejection, multiple myeloma, etc. (139).

Chemokine Receptors

All chemokines signal through G-protein-coupled seven-transmembrane receptors. Chemokine receptors are named and classified according to their chemokine ligand(s), that is C, CC, CXC, and CX3C receptors (Table 4) (128, 130, 131). Each chemokine receptor has a distinct chemokine specificity and a restricted expression on subclasses of leukocytes (and non-hematopoietic cells). However, ligand specificities of the receptors can substantially overlap within a chemokine class leading to redundancy in the system. Some receptors bind multiple chemokines, and others share the same ligands (Table 4). The receptor binding involves high affinity interactions and signal transduction initiated by the dissociation of G-protein complex into $G\alpha$ and $G\beta\gamma$ subunits. $G\alpha$ induces the activation of the phosphoinositide 3-kinase pathway, while the $G\beta\gamma$ subunits activate phospholipase C and induce Ca^{2+} influx and protein kinase C activation. The involvement of MAP kinases as well as JAK/STAT signaling also has been shown (140). In general, the proinflammatory chemokine receptors have more promiscuous ligand-binding specificities, while receptors involved in basal leukocyte development and trafficking have fewer ligands. Although *in vitro* binding and activation studies suggest a high degree of redundancy in the chemokine system, this might actually be not true *in vivo*. Indeed, genetic and an increasing number of functional studies have largely confirmed that single chemokines and receptors play non-redundant roles in immune biology (133, 141). The complexity of the system may be further enhanced by the fact that chemokine receptors can form heterodimers with new ligand specificities and that some chemokines or their metabolites can even act as antagonists for their receptors (142).

Table 4. Classification of chemokines and chemokine receptors (with minor adaptation 128, 130, 131, abbreviations see page 102).

<i>Systematic name</i>	<i>Common names</i>	<i>Chemokine receptors</i>
Alpha (CXC) chemokine-receptor family		
CXCL1	Gro- α , KC, MIP-2	CXCR1, CXCR2
CXCL2	Gro- β , CINC-2 α	CXCR2
CXCL3	Gro- γ , CINC-2 β	CXCR2
CXCL4	PF4	Unknown
CXCL5	ENA-78	CXCR2
CXCL6	GCP-2	CXCR1, CXCR2
CXCL7	NAP-2	CXCR2
CXCL8	IL-8	CXCR1, CXCR2
CXCL9	Mig	CXCR3
CXCL10	IP-10	CXCR3
CXCL11	I-TAC	CXCR3
CXCL12	SDF-1 (α / β)	CXCR4
CXCL13	BCA-1	CXCR5
CXCL14	BRAK/bolekine	Unknown
CXCL15	Lungkine	Unknown
CXCL16	CR-PSOX	CXCR6
Beta (CC) chemokine-receptor family		
CCL1	I-309, TCA-3	CCR8
CCL2	MCP-1	CCR2
CCL3	MIP-1 α	CCR1, CCR5
CCL4	MIP-1 β	CCR5
CCL5	RANTES	CCR1, CCR3, CCR5
CCL7	MCP-3	CCR1, CCR2, CCR3
CCL8	MCP-2	CCR2, CCR3, CCR5
(CCL9/10)	Unknown	CCR1
CCL11	Eotaxin	CCR3
(CCL12)	Unknown	CCR2
CCL13	MCP-4	CCR1, CCR2, CCR3
CCL14	HCC-1	CCR1, CCR5
CCL15	HCC-2	CCR1, CCR3
CCL16	HCC-4	CCR1, CCR2
CCL17	TARC	CCR4
CCL18	DC-CK1	Unknown
CCL19	MIP-3 β /ELC	CCR7
CCL20	MIP-3 α /LARC	CCR6
CCL21	SLC/6Ckine	CCR7
CCL22	MDC	CCR4
CCL23	MPIF-1	CCR1
CCL24	Eotaxin-2/ MPIF-2	CCR3
CCL25	TECK	CCR9
CCL26	MIP-3 α /Eotaxin-3	CCR3
CCL27	CTACK/Eskine	CCR10
CCL28	MEC	CCR3/CCR10
Gamma (C) chemokine-receptor family		
XCL1	Lymphotactin/SCM-1 α	XCR1
XCL2	SCM-1 β	XCR1
Delta (CX3C) chemokine-receptor family		
CX3CL1	Fractalkine/neuroactin	CX3CR1

2.2.3 Chemokine receptor CCR1 as a potential target in kidney disease

2.2.3.1 Chemokine receptor CCR1

CC chemokine receptor 1 (CCR1) was the first CC chemokine receptor identified (143, 144). Initially this receptor was identified as the CCL3/MIP-1 α and CCL5/RANTES receptor, but later studies have shown it to bind and signal in response to a variety of chemokines including CCL8/MCP-2, CCL7/MCP-3, CCL15/Lkn-1, CCL24/MPIF-1 (myeloid progenitor inhibitory factor), and CCL14/HCC-1 (hemofiltrate CC-chemokine) (145, 146). The gene is on human chromosome 3p21 in a cluster with CCR2, CCR3, CCR4, CCR5, CCR8, CCR9, XCR1, CX3CR1 (147). The open reading frame (ORF) is on a single exon, and the predicted polypeptide is 355 aminoacids in a length. The strong association with a wide variety of autoimmune and pro-inflammatory diseases has made the CCR1 protein an attractive therapeutic target, and Berlex has developed a potent, specific, orally available antagonist, BX 471, currently in a phase II clinical trial (148) (Figure 7, ref. 157).

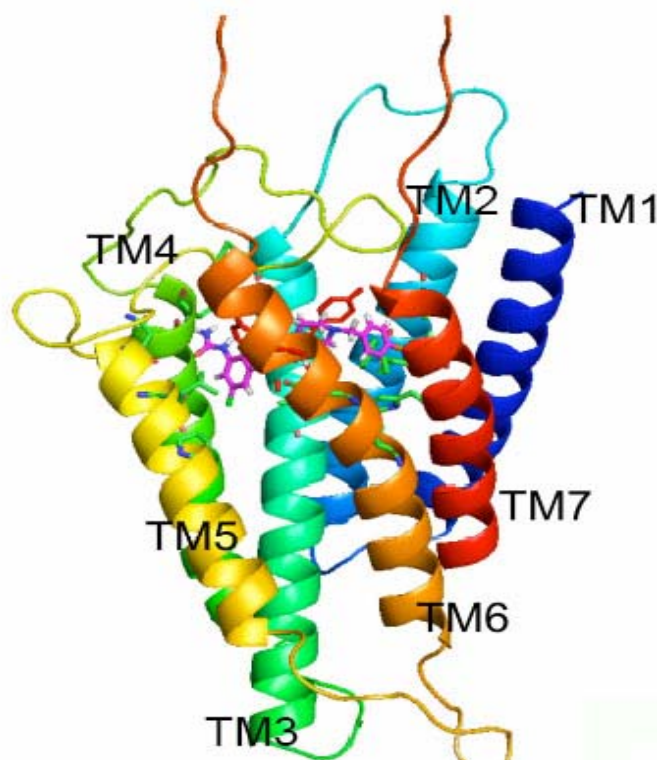


Figure 7. The structure of human CCR1 predicted using MembStruk computational method showing the BX 471 antagonist binding site predicted using HierDock computational protocol. A side view with the extracellular region at the top (157).

Human CCR1 binds several CC chemokines, including CCL3, CCL5, CCL7, CCL8, CCL13, CCL14, CCL15, CCL16, and CCL23 (Table 4). The amino acid sequence of human CCR1 has a high degree of homology to murine CCR1 (Figure 8). However, species-specific pharmacodynamics need to be defined for each antagonist when to be tested in another species (149).

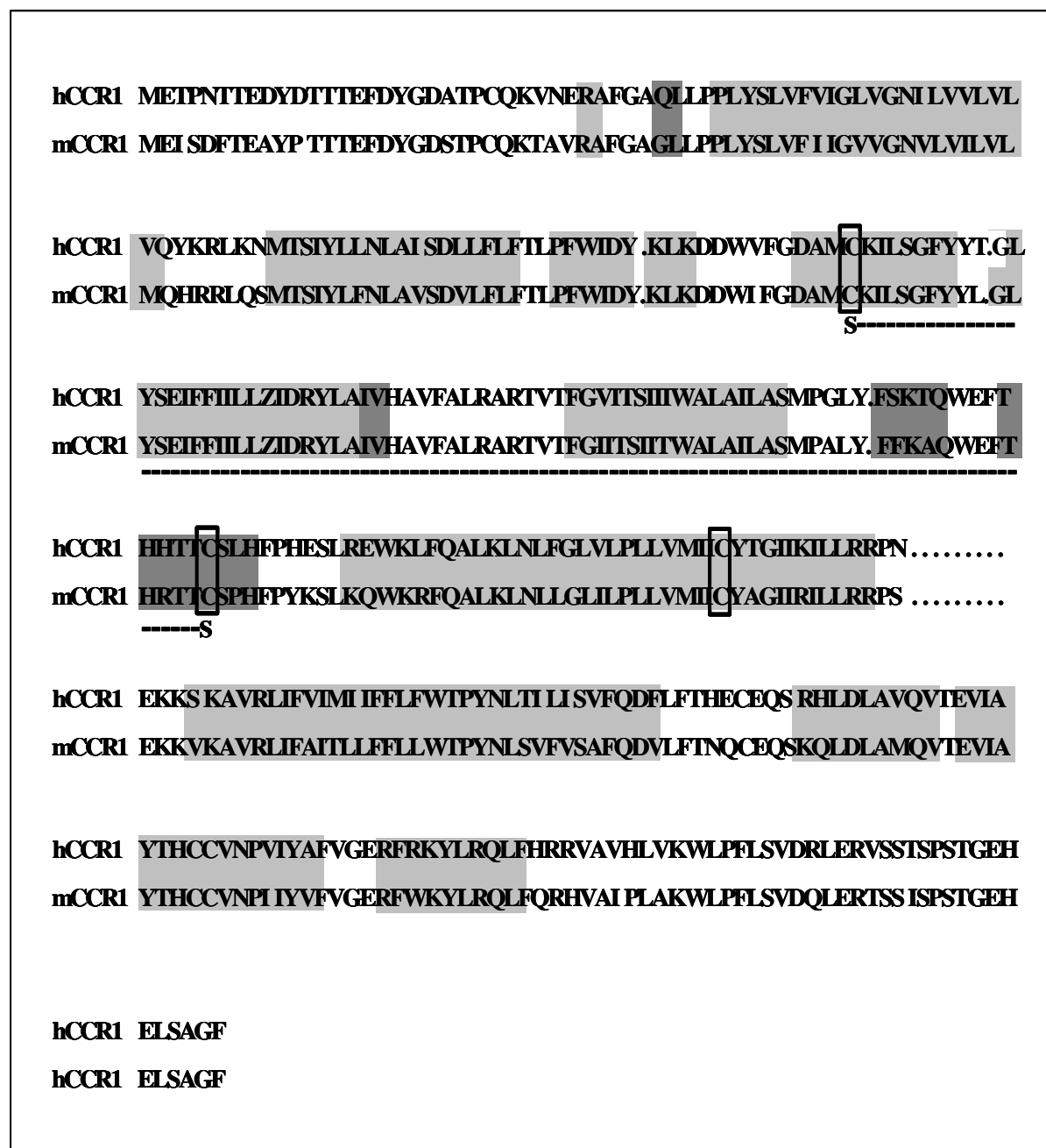


Figure 8. Alignment of human and mouse CCR1.

Known or predicted helices are highlighted in light gray. Known or predicted-strands are highlighted in dark gray. Cysteine residues are encircled. Disulfide bonds is indicated by the letter 'S'.

The latter often compromises the interpretation of data generated in rodents that apply chemokine antagonists designed for the human system. CCR1 is expressed at low levels on T cells. By contrast, human and murine blood monocytes, tissue macrophages, neutrophils, and eosinophils express CCR1 at high levels (128, 110, 150). Upon ligation with its ligands a conformational change of the seven transmembrane elements of CCR1 leads to intracellular activation of G-protein subunits (Figure 8). CCR1 signaling includes calcium flux, inhibition of adenylyl cyclase, and chemotaxis (151, 152). Studies using an *in vitro* flow chamber system first identified a critical role for CCR1 for adhesion of rolling macrophages or T cells to activated endothelium using established human cell lines (141). These findings were validated *in vivo* by two approaches. First, intravital microscopy of the cremaster muscle in mice was used to study the role of CCR1 for leukocyte rolling, firm adhesion, transendothelial migration, and interstitial migration. Either by applying a specific CCR1 antagonist or performing intravital microscopy in CCR1-deficient mice has been found that CCR1 is required for leukocyte adhesion and transendothelial migration during the recruitment process (153). The coherent findings in antagonist-treated mice or CCR1 deficient mice argue for a non-redundant role of CCR1 in that processes. Because organ-specific roles of chemokines and chemokine receptors have been reported, studies performed on cremaster muscles do not allow a safe conclusion upon the role of CCR1 in the kidney. Thus, as a second approach macrophages were isolated and T cells from spleens of CCR1-deficient or wild-type mice. After *ex vivo* labelling with fluorescence dye cells were injected into mice with renal fibrosis after unilateral ureteral obstruction (UUO) (154). CCR1-deficient macrophages and T cells showed markedly reduced recruitment to the interstitial compartment of diseased kidneys as compared to cells isolated from wild-type mice (154). These data show that CCR1 on macrophages and T cells is required for interstitial leukocyte recruitment in renal fibrosis in mice.

2.2.3.2 CCR1 antagonism in models of kidney disease

The functional roles of various chemokines during renal inflammation were examined by either blocking chemokine activity with neutralizing antibodies, chemokine receptor antagonists, or targeted disruption of genes encoding chemokines and their receptors in various animal models (106). It turned out that within the large family of chemokines and chemokine receptors, CCR1 appears to be particularly suitable target for an antagonistic strategy in progressive renal disease (155).

Acute and Chronic Renal Allograft Rejection

The first study that used the small molecule CCR1 antagonist BX471 in kidney disease was reported by Horuk et al. (156) in 2001.

BX471 (**(R-N-[5-chloro-2-[2-[4-[(4-fluorophenyl)methyl]-2-methyl-1-piperazinyl]-2-oxoethoxy]phenyl]urea hydrochloric salt**), non-peptide CCR1 antagonist (Figure 9), is able to displace the CCR1 ligands CCL3, CCL5, and CCL7 (MCP-3) with high affinity (K_i ranged from 1nM to 5.5 nM) and is potent functional antagonist based on its ability to inhibit a number of CCR1-mediated effects, including Ca^{2+} mobilization, increase in extracellular acidification rate, CD11b expression, and leukocyte migration. BX 471 demonstrated a greater than 10, 000-fold selectivity for CCR1 *versus* other GPCR in both receptor binding assays and functional assays (158).

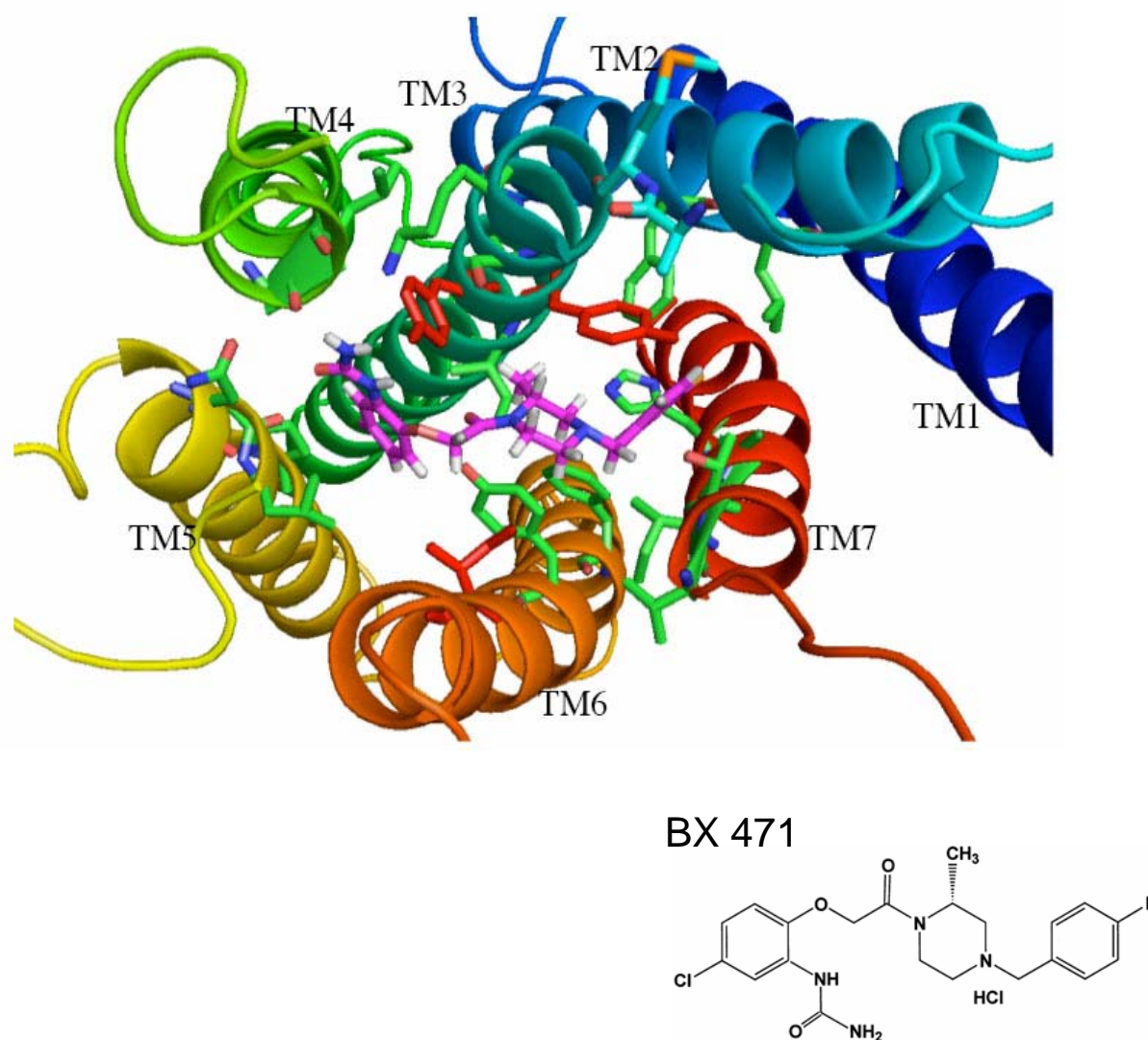


Figure 9. A top view of the predicted structure of BX 471 in the CCR1 binding pocket. (157).

In this study, BX471 monotherapy had beneficial effects on serum creatinine levels and renal survival in a model of kidney transplantation in rabbits. Pathologic analysis showed that BX471 was similar to cyclosporine in its ability to prevent extensive infarction of transplanted kidneys (156). Furthermore, BX471 prevented chronic allograft nephropathy in a Fischer 344 into Lewis rat model of acute and chronic allograft rejection (159). BX471 given from day 21 to 42 after kidney transplantation reduced the number of ED-1-positive macrophages in renal allografts in association with a reduction of markers of renal fibrosis.

Obstructive Nephropathy

Experimental UUO represents a model for obstructive nephropathy but also allows insight into the process of interstitial fibrosis that is a common characteristic of many chronic nephropathies. UUO kidneys show increased CCR1 expression as compared to their respective non-obstructed contralateral kidneys (114). UUO kidneys from mice treated with the CCR1 antagonist BX471 revealed a marked reduction of interstitial leukocyte counts (160). Markers of renal fibrosis, such as interstitial fibroblasts, interstitial volume, mRNA and protein expression for collagen I, were all significantly reduced by BX471 compared to vehicle-treated controls. Most interestingly, the beneficial effect was comparable when BX471 was given not before day 6, indicating that late onset of CCR1 blockade may still be effective. By contrast, treatment was ineffective when the drug was supplied only from day 0 to day 5. These data were confirmed by inducing UUO in CCR1-deficient mice (154).

Immune Complex Glomerulonephritis

Chemokines are also involved in systemic immune responses (128), so that data from the UUO model may not apply to renal manifestations of systemic autoimmunity, e.g. lupus nephritis. In fact, lack of CCR1 has been reported to be associated with an enhanced Th1-like immune response and aggravation of nephrotoxic serum nephritis (161). It has been studied the effects of therapeutic CCR1 blockade in progressive lupus-like immune complex glomerulonephritis of MRL ^{lpr/lpr} mice. BX471 treatment initiated late during the course of disease (weeks 20–24 of age) improved blood urea nitrogen levels and reduced the amount of macrophages and lymphocytes in the interstitium (162). Furthermore, BX471 reduced the extent of interstitial fibrosis as evaluated by interstitial smooth muscle actin expression and collagen I deposits, as well as mRNA expression for collagen I and TGF- β 1. BX471 did not affect serum DNA autoantibodies despite potential roles of CC chemokines and their

receptors in systemic immune responses. As CCR1 blockade does not reduce glomerular macrophage recruitment, it was found to be ineffective in modulating glomerular pathology and proteinuria in MRL ^{lpr/lpr} mice.

Focal Segmental Glomerulosclerosis

Proteinuria represents a major prognostic factor for the progression of renal disease, because unselective proteinuria can induce chemokine expression in renal tubular cells (163). Thereby proteinuria serves as a major factor for tubulointerstitial inflammation. The authors hypothesized that CCR1 antagonism would be able to improve interstitial fibrosis in the presence of massive proteinuria caused by FSGS. FSGS was induced in BALB/c mice by two intravenous injections of adriamycin at day 0 and 14. BX471 was started from day 14 when nephrotic syndrome was established. Again, BX471 reduced the amount of interstitial macrophages and T cells and markers of renal fibrosis including interstitial fibroblasts and interstitial volume (164). These findings demonstrate that therapeutic CCR1 blockade is effective in the presence of heavy proteinuria. Consistent with our previous findings, BX471 did not affect glomerular pathology in adriamycin-injected BALB/c mice.

CCR1 blockade can effectively prevent recruitment of monocytes and lymphocytes into the renal interstitium. BX471 is effective in multiple models of progressive kidney disease in mice even when treatment was started late in the disease process. Thus, interfering with renal leukocyte recruitment by targeting CCR1 may represent a promising strategy to prevent disease progression in chronic nephropathies characterized by interstitial leukocytic cell infiltrates (197).

2.3 Research hypothesis

The aim of my thesis was to investigate the role of chemokine receptor CCR1 for the progression of chronic kidney disease in murine Alport syndrome and type 2 diabetes, because the molecular and cellular mechanisms of intrarenal inflammation in Alport disease and diabetic nephropathy remain poorly characterized. In particular, attempts have been made to assess the putative proinflammatory role of interstitial macrophages in disease progression and the impact of therapeutic blockade of chemokine receptor CCR1 in COL4A3-deficient mice with Alport disease and type 2 diabetic db/db mice with advanced diabetic nephropathy.

We hypothesized that blocking CCR1-dependent interstitial macrophage recruitment might prolong survival of COL4A3-deficient mice and reduce tubulointerstitial inflammation and tubular injury in COL4A3-deficient mice and type 2 diabetic db/db mice.

3. MATERIAL AND METHODS

3.1 Materials

3.1.1 Equipment

Balances:

Analytic Balance, BP 110 S

Sartorius, Göttingen, Germany

Mettler PJ 3000

Mettler-Toledo, Greifensee, Switzerland

Cell Incubators:

Type B5060 EC-CO₂

Heraeus Sepatech, München, Germany

Centrifuges:

Heraeus, Minifuge T

VWR Internationl, Darmstadt, Germany

Heraeus, Biofuge primo

Kendro Laboratory Products GmbH,
Hanau, Germany

Heraeus, Sepatech Biofuge A

Heraeus Sepatech, München, Germany

ELISA-Reader

Tecan, GENios Plus

Tecan, Crailsheim, Germany

Fluorescence Microscopes

Leica DC 300F

Leica Microsystems, Cambridge, UK

Olympus BX50

Olympus Microscopy, Hamburg, Germany

Spectrophotometer

Beckman DU[®] 530

Beckman Coulter, Fullerton, CA, USA

TaqMan Sequence Detection System

ABI prism[™] 7700 sequence detector

PE Biosystems, Weiterstadt, Germany

Other Equipments

Cryostat RM2155

Leica Microsystems, Bensheim, Germany

Cryostat CM 3000

Leica Microsystems, Bensheim, Germany

Digital camera DC 300F

Leica Microsystems, Cambridge, UK

Glucometer Accu check sensor

Roche, Mannheim, Germany

Homogenizer ULTRA-TURRAX T25

IKA GmbH, Staufen, Germany

Microtome HM 340E

Microm, Heidelberg, Germany

pH meter WTW

WTW GmbH, Weilheim, Germany

Thermomixer 5436

Eppendorf, Hamburg, Germany

Vortex Genie 2[™]

Bender&Hobein AG, Zurich, Switzerland

Water bath HI 1210

Leica Microsystems, Bensheim, Germany

3.1.2 Chemicals and materials

Chemicals for the molecular biology techniques

RNeasy Mini Kit	Qiagen GmbH, Hilden, Germany
RT-PCR primers	PE Biosystems, Weiterstadt, Germany
DuoSet [®] Elisa Kit (mouse RANTES/CCL5)	R&D Systems, Minneapolis, MN, USA

Cell culture

DMEM-medium	Biochrom KG, Berlin, Germany
RPMI-1640 medium	GIBCO/Invitrogen, Paisley, Scotland, UK
FSC	Biochrom KG, Berlin, Germany
Dulbecco's PBS (1×)	PAA Laboratories GmbH, Cölbe, Germany
Trypsine/EDTA (1×)	PAA Laboratories GmbH, Cölbe, Germany
Penicillin/Streptomycin (100×)	PAA Laboratories GmbH, Cölbe, Germany

Antibodies

rat anti-F4/80	Serotec, Oxford, UK
anti-Ki-67	Dianova, Hamburg, Germany
anti-ssDNA	Chemicon, Hofheim, Germany
anti-mMECA-32	University of Iowa, Hybridoma Bank, USA
anti-mCCL5	PeptoTech, Rocky Hill, NJ, USA
goat anti-fibronectin	Santa Cruz, Heidelberg, Germany
rat anti-Mac2	Cederlane, Ontario, Canada
anti-ERHR3	DPC Biermann, Bad Nauheim, Germany
anti-CD3	BD Pharmingen, Hamburg, Germany
mouse F4/80 FITC conjugated	Caltag Laboratories, Bulingame, CA, USA

Miscellaneous

Anti-FITC MicroBeads	Miltenyi Biotec, Bergish Gladbach, Germany
CellTiter 96 Proliferation Assay	Promega, Mannheim, Germany
Fluorescence-labeled microspheres (0.96 µm FluoSpheres)	Molecular Probes [™] /Invitrogen GmbH, Karlsruhe, Germany
LS ⁺ /VS ⁺ Positive selection columns (MACS)	Miltenyi Biotec, Bergish Gladbach, Germany
Needles	BD Drogheda, Ireland

Pipette's tip 1-1000 μ L	Eppendorf, Hamburg, Germany
PKH26 Red Fluorescent Cell Linker kit	Sigma-Aldrich Chemicals, Steinheim, Germany
Plastic histosettes	NeoLab, Heidelberg, Germany
Preseparation filters	Miltenyi Biotec, Bergish Gladbach, Germany
SuperFrost® Plus microscope slides	Menzel-Gläser, Braunschweig, Germany
Silver Impregnation Kit	Bio-Optica, Milano, Italy
Syringes	Becton Dickinson GmbH, Heidelberg, Germany
Tissue culture dishes \varnothing 100x20mm	TPP, Trasadingen, Switzerland
Tissue culture dishes \varnothing 150x20mm	TPP, Trasadingen, Switzerland
Tissue culture dishes \varnothing 35x10mm	Becton Dickinson, Franklin Lakes, NJ, USA
Tissue culture flasks 150 cm ²	TPP, Trasadingen, Switzerland
Tubes 15 and 50 mL	TPP, Trasadingen, Switzerland
Tubes 1.5 and 2 mL	TPP, Trasadingen, Switzerland

Chemicals

Aceton	Merck, Darmstadt, Germany
AEC Substrat Packung	Biogenex, San Ramon, USA
Ether	Merck, Darmstadt, Germany
Bovines Serum Albumin	Roche Diagnostics, Mannheim, Germany
BX471	Berlex Biosciences, Richmond, USA
Cyclodextrin	Sigma-Aldrich Chemicals, Steinheim, Germany
DEPC	Fluka, Buchs, Switzerland
DMSO	Merck, Darmstadt, Germany
Diluent C for PKH26 dye	Sigma-Aldrich Chemicals, Steinheim, Germany
EDTA	Calbiochem, San Diego, USA
Eosin	Sigma, Deisenhofen, Germany
Ethanol	Merck, Darmstadt, Germany
Formalin	Merck, Darmstadt, Germany
Hydroxyethyl cellulose	Sigma-Aldrich, Steinheim, Germany
HCl (5N)	Merck, Darmstadt, Germany
Isopropanol	Merck, Darmstadt, Germany
Kaliumchlorid	Merck, Darmstadt, Germany
Kaliumdihydrogenphosphat	Merck, Darmstadt, Germany

Kaliumhydroxid	Merck, Darmstadt, Germany
MACS-Puffer	Miltenyi Biotec, Bergisch Gladbach, Germany
Merkaptoethanol	Roth, Karlsruhe, Germany
Natriumacetat	Merck, Darmstadt, Germany
Natriumchlorid	Merck, Darmstadt, Germany
Natriumcitrat	Merck, Darmstadt, Germany
Natriumdihydrogenphosphat	Merck, Darmstadt, Germany
Penicillin	Sigma, Deisenhofen, Germany
Roti-Aqua-Phenol	Carl Roth GmbH, Karlsruhe, Germany
SSC (Saline-sodium citrate Puffer)	Sigma, Deisenhofen, Germany
Streptomycin	Sigma, Deisenhofen, Germany
Tissue Freezing Medium	Leica, Nussloch, Germany
Trypan Blue	Sigma, Deisenhofen, Germany
Oxygenated water	DAKO, Hamburg, Germany
Xylol	Merck, Darmstadt, Germany

- BX 471 was kindly supplied by Berlex Biosciences, Richmond, California, USA;
- BL 5923 was kindly supplied by Novartis Institute for Biomedical Research, Basel, Switzerland;
- rabbit anti-laminin (gift from M. Paulsson, Cologne, Germany);
- All other reagents were of analytical grade and are commercially available from Invitrogen, SIGMA or ROTH.

3.1.3 Oligonucleotide primers and probes for RT-PCR

The following oligonucleotide primers (300 nM) and probes (100 nM) were used for studies:

- Ccr1:*** *Forward primer:* 5'-TTAGCTTCCATGCCTGCCTTATA-3'
 Reverse primer: 5'-TCCACTGCTTCAGGCTCTTGT-3'
 Internal fluorescence labeled probe (FAM): 5'-ACTCACCGTACCTGTA-
 GCCCTCATTTC-3'
- Ccr2:*** *Forward primer:* 5'- CCTTGGGAATGAGTAACTGTGTGA -3'
 Reverse primer: 5'- ACAAAGGCATAAATG-ACAGGATTAATG - 3'
 *Internal fluorescence labeled probe (FAM):*5'- TGACAAGCACTTA-
 GACCAGGCCATGCA -3'
- Ccr5:*** *Forward primer:* 5'-CAAGACAATCCTGATCGTGCAA-3'
 Reverse primer: 5'-TCCTACTCCCAAGCTGCATAGAA-3'
 Internal fluorescence labeled probe (FAM): 5'- TCTATACCCGATCC-
 ACA GGAGAACATGAAGTTT-3'
- Tgf-β1:*** *Forward primer:* 5'- CACAGTACAGCAAGGTCCTTGC-3'
 Reverse primer: 5'- AGTAGACGATGGGCAGTGGCT-3'
 Internal fluorescence labeled probe (FAM): 5'- GCTTCGGCG-
 TCACCGTGCT-3'
- collagenI-α1:*** *Forward primer:* 5'- TGCTTTCTGCCCCGGAAGA-3'
 Reverse primer: 5'- GGGATGCCATCTCGTCCA-3'
 Internal fluorescence labeled probe (FAM): 5'- CCAGGGTCTC
 CCTTGGGTCCTACATCT -3'
- mGAPDH:*** *Forward primer:* 5'-CATGGCCTTCCGTGTTCTTA-3'
 Reverse primer: 5'-ATGCCTGCTTCACCACCTTCT-3'
 Internal fluorescence labeled probe (VIC):
 5'-CCCAATGTGTCCGTCGTGGATCTGA-3'
- Ccl2*** predeveloped TaqMan assay reagent from PE Biosystem

Ccl5 predeveloped TaqMan assay reagent from PE Biosystem

18s rRNA predeveloped TaqMan assay reagent from PE Biosystem

3.1.4 Computer programs

- Adobe Acrobat Writer 6.0
- Internet Explorer
- Office XP, 2003
- Photoshop 7.0, CS
- Windows 2003 Professional
- CellQuest software
- ABI PRISM Sequence Detection software 1.0
- SPSS for Windows 13.0

3.1.5 Solutions

40% Cyclodextrin

40g of cyclodextrin was weighed into a 100 ml sterile plastic bottle. 0.9% NaCl was added portionwise. The mixture was shaken and mixed overnight to dissolve. 0.9% NaCl was added to a total volume of 100ml. The solution was filtered through a 0.22 um filter into a sterile bottle, labeled and stored at 4 °C.

0.5 % Hydroxyethyl cellulose

0.5g of hydroxyethyl cellulose was weighed into a 100 ml sterile plastic bottle. Unbuffered saline was added portionwise. The mixture was shaken and mixed overnight to dissolve. Saline was added to a total volume of 100 ml. The solution labeled and stored at ambient temperature.

BX 471

25mg/ml solution of BX471 in cyclodextrin was prepared in the following manner:

1.25g of BX471 was weighed into a 100 ml plastic erlenmeyer flask. 50 ml of 40% cyclodextrin in 0.9% NaCl was added to the flask. The mixture was stirred during the addition of 250µl of conc HCl. The mixture was stirred to dissolve. After dissolution was complete (1 hour) the pH of the solution was measured at pH=3.3 and 1N KOH was added to raise the pH to 4.5. The solution was filtered through a 0.22 um filter into a clean plastic erlenmeyer. The solution was labeled and stored at ambient temperature.

BL 5923

30mg/ml solution of BL5923 in 0.5% hydroxyethyl cellulose was prepared in the following manner:

1g of BL5923 was weighed into a 50 ml plastic erlenmeyer flask. 33.3 ml of 0.5% hydroxyethyl cellulose unbuffered saline was added to the flask. The mixture was shaken and mixed overnight to dissolve in a waterbath at 37°C. The solution was labeled and stored at ambient temperature.

Anesthesia mixture

10 ml Midazolam (1mg/ml)

2 ml Fentanyl (0.05 mg/ml)

1 ml Dormitor (1 mg/ml)

Antagonist mixture

5 ml Annexate (0.1mg/ml)

0.5 ml Antisedan (5 mg/ml)

3 ml Naloxon (0.4 mg/ml)

MACS Buffer

PBS pH 7.2

0.5% bovine serum albumin

2 mM EDTA

10x Citratpuffer

110 mM Natriumcitrat
in ddH₂O
with 2N NaOH to pH 6

20x PBS

2.74 M NaCl
54 mM KCl
30 mM KH₂PO₄
130 mM Na₂HPO₄
in ddH₂O
with HCl to pH 7.5

Solution D

4M Guanidinium Thiocyanat
25mM Natriumcitrat, pH 7
0.5% Sarcosyl
0.1M β-Mercaptoethanol

3.2 Methods

3.2.1 Animal studies

3.2.1.1 Homing conditions and animal procedures

Mice were housed in filter top cages with a 12 hour dark/light cycle and unlimited access to food (Sniff, Soest, Germany) and water for the duration of the study. Cages, bedding, nestles, food, and water were sterilized by autoclaving before use. The genotype of each mouse was confirmed by PCR using genomic DNA extracted from tail tips. COL4A3-deficient mice on a 129/SvJ genetic background were bred under specific-pathogen-free housing conditions. Male 5 week old C57BLKS db/db or C57BLKS wild-type mice were obtained from Taconic (Ry, Denmark) and maintained on a normal diet under standard animal house conditions as described above.

All experimental procedures were performed according to the German animal care and ethics legislation and had been approved by the local government authorities.

3.2.1.2 Study design and experimental procedures

COL4A3-deficient mice: COL4A3-deficient mice develop glomerulosclerosis with renal fibrosis progress to uremia-related death at about 10 weeks of age (165, 166). At the age of 6 weeks COL4A3-deficient mice were divided in two groups that received either BX471 (25 mg/kg body weight) in the vehicle 40% cyclodextrin or vehicle only by subcutaneous injections at 8 hour intervals (160). Treatment was continued until death for assessment of survival or until day 63 of age (9 weeks) in a subgroup of mice which were sacrificed for histopathological evaluation. Urine samples were obtained at weekly intervals and analyzed for protein/creatinine ratios using an automatic autoanalyzer (Integra 800, Roche Diagnostics, Germany). Blood samples were collected from each animal under general anaesthesia at the end of study as described below.

Db/db mice: At the age of 6 weeks uninephrectomy (1K mice) or sham surgery (2K mice) was performed under general anesthesia with midazolam 5mg/kg and 0.05 mg/kg fentanyl in db/db and wild-type mice. Anesthetized mice were positioned on the dissection border. After this 1.5 cm flank incision was performed. Silk suture (2-0) was placed around the right kidney and after tying off the vessels and ureter the kidney was rapidly removed. In sham

group of mice the kidney was manipulated but not ligated. Skin incision was closed with silk suture and wound clamps (Figure 10). After surgery all mice received analgetic (1 drop of Novaminsulfon-ratiopharm, Ratiopharm GmbH, Germany, 1:200, orally administered) and were allowed free access to water and food.

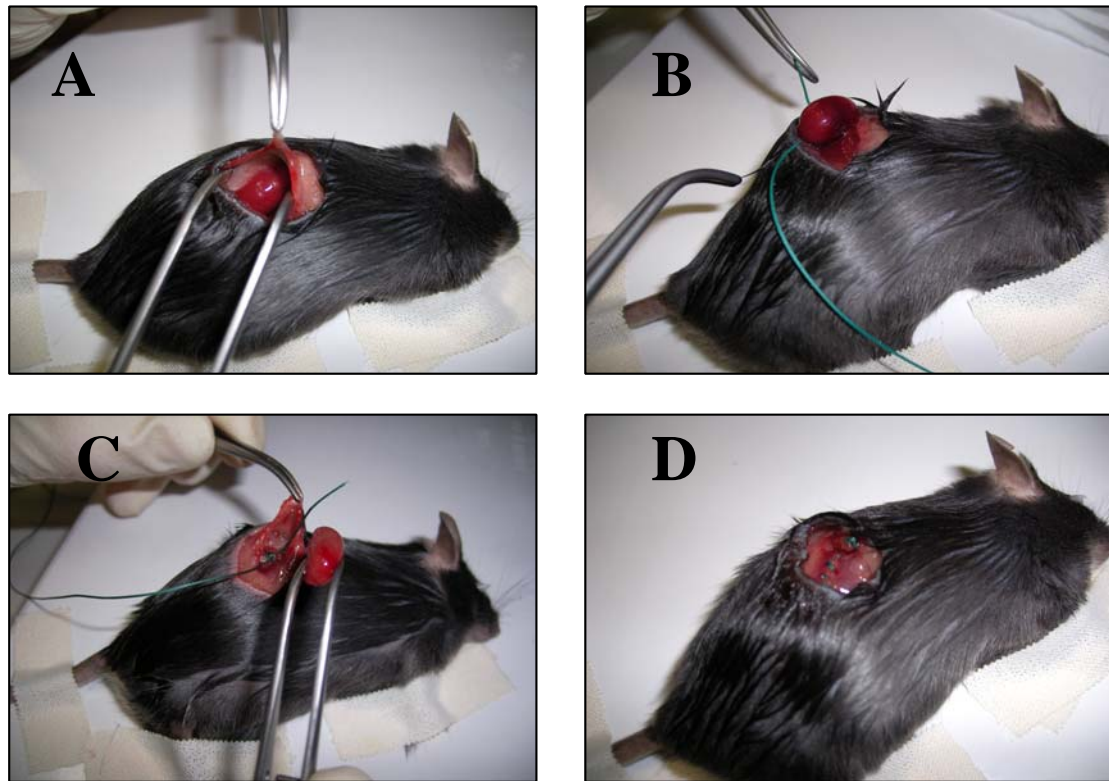


Figure 10. Schematic representation of uninephrectomy.

A: Making flank incision. **B:** Tying off the kidney's vessels and ureter with silk suture. **C:** Removing of the kidney after ligation. **D:** Wound closing with silk suture and wound clamps.

At the age of 5 months uninephrectomized (1K mice) db/db mice were divided in three groups that received either BL5923 (60 mg/kg, b.i.d.) in the vehicle 0.5% hydroxyethyl cellulose, vehicle only or nil by oral gavage. Treatment was continued for 4 weeks when tissue was obtained for histopathological evaluation. Mice were examined for diabetes from 2 months old and blood glucose levels were determined at monthly intervals using a glucometer (Accu check sensor, Roche, Mannheim, Germany). White blood counts were determined with a Coulter counter (Beckmann Coulter GmbH, Krefeld, Germany). Urine samples were obtained at monthly intervals and analyzed for albumin/creatinine ratios using an automatic autoanalyzer (Integra 800, Roche Diagnostics, Germany). Blood was drawn

from the retroorbital sinus under general anesthesia before sacrifice. For obtaining serum the whole blood was centrifuged at 3000 x g for 5 minutes at 4 °C and stored at -20 °C. Serum was analyzed for creatinine and BUN using an automatic analyzer as described above.

After completion of the treatment period the mice were sacrificed by cervical dislocation and the kidneys were collected and processed for RNA isolation, immunostaining or paraffin fixed for histological analysis (section 3.2.3). For histological analysis kidneys were fixed with 10% formalin and processed for periodic acid Schiff staining for the examining histomorphological changes (section 3.2.3).

3.2.1.3 Determination of BL5923 blood levels

Blood samples (45 µl) were spiked with an internal standard (5 µl) and extracted with 200 µl acetonitrile. After centrifugation, 220 µl of the supernatant were dried and redissolved in 60 µl methanol and 40 µl 0.1% formic acid. The solution was centrifuged and 10 µl of the supernatant were analyzed by HPLC/MS using the Rheos LC HPLC system. Eluent A was water with 1.5 % formic acid plus 0.02 % TFA, eluent B was acetonitrile/methanol (50:50, V/V) with 1.5 % formic acid plus 0.02 % TFA. Column efflux was directly introduced into the ion source of a Finnigan Quantum Ultra MS detector. Quantitative analysis was performed by selected ion monitoring over the respective quasi-molecular ions. The calibration curve was performed in triplicate. Data from blood samples were calculated along the calibration curve and are expressed in ng/ml. Determination of BL5923 blood levels was performed in collaboration with Novartis Institutes for BioMedical Research, Basel, Switzerland.

3.2.1.4 Cremaster muscle intravital microscopy

The surgical preparation of cremaster muscles was performed as originally described by Baez (ref. 167) with minor modifications. Mice were anesthetized using a ketamine/xylazine mixture (100 mg/kg of ketamine and 10 mg/kg of xylazine) administered by intraperitoneal injection. The left femoral artery was cannulated in a retrograde manner for continuous blood pressure monitoring and the administration of substances to the cremaster vasculature (Figure 11A-B). The right cremaster muscle was exposed through a ventral incision of the scrotum. The muscle was opened ventrally in a relatively avascular zone, using careful electrocautery to stop any bleeding, and spread over the transparent pedestal of a custom-made microscope

stage (Figure 11C-D). Epididymis and testicle were detached from the cremaster muscle and placed into the abdominal cavity. Throughout the procedure, the muscle was superfused with buffered Ringer's injection. To minimize induction of inflammation by the surgical trauma, the muscle was handled as little as possible. After surgical preparation, which typically required 30 min, the stage was transferred to the microscope and the temperature of the superfusion buffer was maintained at 37 °C by an infrared heating lamp and a digital thermometer with a thermocouple small enough to allow for placement of the probe in close vicinity of the cremaster muscle (168).

Intravital microscopy was performed using an Olympus BX50 upright microscope equipped for stroboscopic fluorescence epi-illumination microscopy and microscopic images as well as real-time recordings. Three hours after intrascrotal injection of CCL3 (600 ng in 0.3 ml PBS; R&D Systems Europe Ltd.), intravital microscopic analysis was performed in wild-type and CCR1-deficient mice as well as in wild-type mice injected subcutaneously with the CCR1 antagonist BX471 (25 mg/kg body weight) 1 hour before intrascrotal injection of CCL3. Wild-type mice treated with PBS were used as controls (n=7 each group).

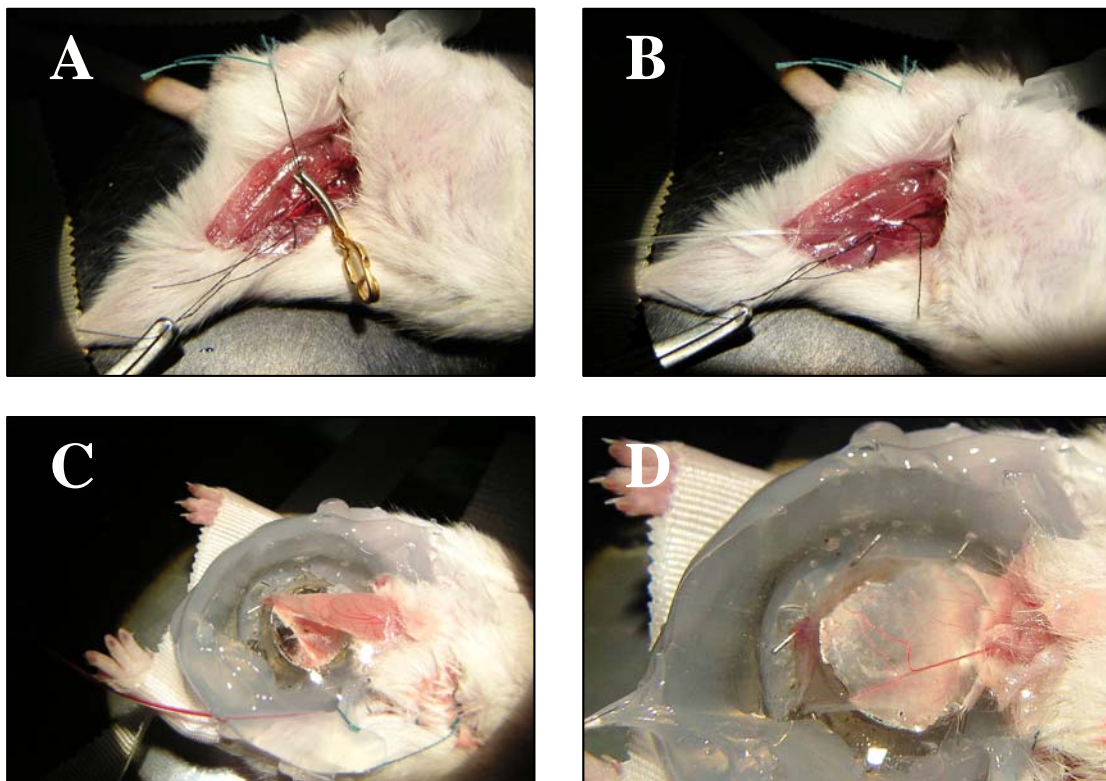


Figure 11. Preparing cremaster muscle for intravital microscopy.

A-B: Preparation of left femoral artery for continuous blood pressure monitoring and the administration of substances to the cremaster vasculature.

C-D: Cremaster muscle exposing and spreading for intravital microscopy.

Leukocyte migration parameters were determined in five postcapillary venules (inner diameter 17-35 μm) per animal. Rolling leukocytes were defined as those moving slower than the associated blood flow and quantified for 30 s. Firmly adherent leukocytes were defined as leukocytes that remained stationary for at least 30 s and related to the luminal surface per 100- μm vessel length. Emigrated leukocytes were counted in *regions of interest* (ROIs) covering a width of 75 μm on both sides of a vessel over 100 μm vessel length. For the analysis of interstitial migration of leukocytes, these ROIs were divided into two sub-areas, respectively: One adjacent to the vessel (25 μm in length x 100 μm in width) and one distant to the vessel (50 μm in width x 100 μm in length. Blood flow velocity was measured after intraarterial administration of fluorescence-labeled microspheres (0.96 μm FluoSpheres, Molecular Probes). Intravital studies were performed in collaboration with Prof. Krombach's group (Institute for Surgical Research, Munich, Germany).

3.2.1.5 Cell transfer study

3.2.1.5.1 Cell isolation

F4/80 positive macrophages were prepared by immunomagnetic selection from spleens of 8 weeks Collagen4A3-deficient mice or 6 months old db/db male mice. The mice were sacrificed by cervical dislocation and spleens were isolated for obtaining cultures of spleen macrophages. After isolation total spleens were placed in a petri-dish containing MACS buffer on ice and mashed with the help of forceps, this coarse suspension was then passed through a 30 micron steel wire mesh and collected in a sterile petri-dish. Then suspension was centrifuged at 1500 RPM at 4 °C to obtain a pellet. The pellet thus obtained was washed with sterile PBS and resuspended in an arbitrary volume of MACS buffer. This was followed by a washing steps (2x), passed through a preseparation filter to obtain single cell suspension. Finally the cells were centrifuged, supernatant was discarded and the pellet was resuspended in 1 ml volume of MACS buffer and cell counts were done.

Magnetic labeling was performed following the manufacturer's protocol in which the cell pellet obtained from total spleen was resuspended in 100 μl MACS buffer 10^7 total cells, 2 μl of F4/80 FITC conjugated antibody was added, mixed well and incubated for 10 min at RT. The cells were then washed twice after incubation and centrifuged at 300 x g for 10 min. Supernatant was discarded and cell pellet was resuspended in 90 μl of MACS buffer per 10^7 total cells. 10 μl of MACS Anti-FITC Microbeads was added per 10^7 total cells, mixed well and incubated for 15 min in refrigerator at 6-12°C. The cells were washed by adding 10-20x

labeling volume of MACS buffer, centrifuged at 300 x g for 10 minutes and supernatant was discarded. The cell pellet was then resuspended in 500 μ l per 10^8 total cells and this suspension was applied on LS⁺/VS⁺ positive selection columns, that were pre-rinsed with 3 ml MACS buffer and the remaining effluent was collected. Purity of isolated cells was verified by flow-cytometric analysis.

3.2.1.5.2 Fluorescent labeling

Separated F4/80 positive macrophages were labeled with PKH26, the red fluorescent cell linker, following the manufacturer's protocol. PKH26 has been characterized in a wide variety of systems and found to be useful for *in vitro* and *ex vivo* labelling (169, 170), *in vitro* cell proliferation studies (171, 172), and *in vitro* and *in vivo* cell tracking applications (169-172). All steps have been performed at 25 °C. Single cell suspension (2×10^7 cells/probe) was placed in a conical bottom polypropylene tube, washed once using RPMI medium without serum and centrifuged at 400 x g for 5 minutes into a loose pellet. After centrifuging cells, supernatant was carefully aspirated leaving no more 25 μ l of supernatant on the pellet. The cell pellet was resuspended in 1 ml of Diluent C by pipetting the suspension manually. 1 ml fresh prepared 4×10^{-6} M PKH26 dye was added to the cell suspension, mixed well and incubated 3 minutes at 25 °C. Periodically, the tube was inverted gently to assure mixing during this staining period. The staining reaction was stopped by adding an equal volume of serum (1ml of FSC) and incubated 1 minute. The serum-stopped sample was diluted by adding an equal volume of complete medium (3 ml of RPMI+10% FSC) and centrifuged at 400 x g for 10 minutes to remove cells from staining solution. Supernatant was removed and the cell pellet was transferred to a new tube for further washing (3 times by adding 10 ml of complete RPMI medium). Finally the cells were centrifuged, supernatant was discarded and the pellet was resuspended in an arbitrary volume of complete RPMI medium and cell counts were done. Labeling efficacy was assessed by flow cytometry.

3.2.1.5.3 Intravenous injection protocol

Collagen4A3-deficient mice: 8 weeks old collagen4A3-deficient mice were injected with 2.0×10^5 F4/80 macrophages in 200 μ l isotonic saline through the tail vein. Two groups of mice were injected with macrophages that had been preincubated with either 600 μ M of BX471 or vehicle (40% Cyclodextrin) for 30 minutes. The respective mice received a single

subcutaneous injection of either BX471 (25 mg/kg) or vehicle 3 hours before the injection of the cells.

Db/db mice: 3.5×10^5 F4/80 macrophages in 200 μ l isotonic saline were injected into the tail vein of 6 months old db/db that had received a single dose of either BL5923 or vehicle (0.5 % hydroxyethyl cellulose) 3 hours before injection.

In both experiments renal tissues were obtained after 3 hours, snap frozen by using *Tissue Freezing Medium*, and prepared for fluorescence microscopy. The number of interstitial fluorescent cells was determined in 15 high power fields.

3.2.2 In vitro methods

3.2.2.1 Culture of mammalian cells

The murine macrophage cell line *J774* (American Type Culture Collection, Rockville, MD, USA) was grown in RPMI 1640 medium containing 10% heat-inactivated fetal calf serum, penicillin 100 U/ml and streptomycin 100 μ g/ml (complete RPMI medium) under standard culture conditions (in an incubator set at 37 °C supplied with 5 % CO₂/air). A proximal tubular epithelial cell line was maintained in DMEM medium (GIBCO/Invitrogen, Carlsbad, CA, USA) containing 10% FCS and 1% penicillin-streptomycin under standard culture conditions as described above (173). *J774* mouse macrophages and proximal tubular epithelial cells double every 24-36 h and were normally subcultured twice a week according to the following procedure: After removing the old medium, cells were washed twice with PBS. Subsequently, the appropriate volume of EDTA-trypsin solution was added to the culture flasks and the cells were incubated at RT for 5 min. Trypsinization was stopped by resuspending the cells in complete medium and cell suspension was transferred to new falkon tube. Cells were centrifuged at 1000 RPM for 3 min at RT, supernatant was discarded and the pellet was resuspended in 5 ml of complete RPMI or DMEM medium. Cells counts were done and desired number of cells was plated in 6 well plates and incubated at 37 °C for 24 h under standard culture conditions.

3.2.2.2 Cell freezing and thawing

Cells were spun down under sterile conditions for 3 min at 1000 RPM. The cell pellet was maintained on ice and carefully resuspended in cold freezing medium (90 % FCS and 10 % DMSO) by pipetting the suspension repeatedly up and down. 1.5 ml aliquots were quickly

dispensed into freezing vials (4 °C). The cells were slowly frozen at –20 °C for 1 h and then at –80 °C overnight. The next day, they were transferred to liquid nitrogen.

In order to thaw cells a freezing vial was removed from liquid nitrogen and put in a waterbath at 37 °C. The cells were then dispensed in 5 ml of warm complete growth medium and spun down at 1000 RPM for 5-7 min. Then the old medium was removed and the cells were resuspended in fresh medium. The medium was changed once more after 24 h.

3.2.2.3 Stimulation experiments

J774 mouse macrophages were maintained in RPMI 1640 supplemented with 10% heat inactivated fetal calf serum and 1% penicillin-streptomycin. Cells were kept at a density of 5×10^5 cells/ml for 24 hours in standard medium without supplements before being stimulated with 200 U/ml IFN- γ (PeproTech Inc, Rocky Hill, NJ, USA), 500 U/ml TNF- α (ImmunoTools, Friesoythe, Germany) and 500 ng/ml CCL3 (Cell Sciences Inc, Canton, MA, USA) for 24 hours. In some wells BX471 was added to a final concentration of 1 μ M. Supernatants were collected and assayed for CCL5 by ELISA.

Cell proliferation assay has been carried out in *J774* mouse macrophages and murine tubular epithelial cells by following methodology. Initially cells were grown in medium (RPMI or DMEM) with or without fetal calf serum 24 h in 96 wellplate prior incubation with BL5923 (10 μ g/ml, or 50 μ g/ml) for 48 hours. Subsequently 20 μ l of CellTiter 96 Aqueous One Solution (Promega, Mannheim, Germany) was added to each well and incubated for 1.5 h at 37 °C. The optical density was measured at 492 nm.

3.2.2.4 Cytokine Elisa

Cytokine levels in cell culture supernatants were determined using commercial Elisa kit for CCL5 following the protocol provided by the respective manufactures. The 96-well plate was first coated with 100 μ l/well capture antibody (anti-mouse cytokine) at recommended dilution in 0.2 M Sodium phosphate buffer of specified pH and placed overnight at 4 °C. The wells were then aspirated, washed with >200 μ l wash buffer (PBS pH 7 with 0.05% Tween-20) and the plate was blocked with >200 μ l/well assay diluent (PBS pH 7 with 10% FCS) and incubated at RT for 1 hour. This was followed by aspiration, 2 washes as described above, and 100 μ l of standard or sample was pipetted to appropriate well and the plate was

incubated for 2 hours at RT. The plate was then aspirated, washed five times and 100 μ l working detector (biotinylated anti-mouse cytokine or detection antibody with avidin-horse radish peroxidase conjugate) was added to each well and incubated at room temperature for 1 hour. This was followed by an aspiration and wash steps (>5 washes). The TMB substrate solution (BD Biosciences, Hamburg, Germany) was added to each well at the volume of 100 μ l and incubated for 30 minutes. The stop solution (1M Phosphoric or 2N Sulphuric acid) was then added to each well, and absorbance was measured at prescribed wavelength (nm), using an automatic plate reader. Note: reagents and buffers used in all experimental protocols, double distilled water (ddH₂O) was used unless stated otherwise.

3.2.3 Immunohistochemical methods and histopathological evaluation

All immunohistological studies were performed on paraffin embedded sections. From each mouse parts of the kidneys were isolated, placed in plastic histosettes and fixed in 10% formalin in PBS. 2 μ m thick paraffin-embedded sections were cut and processed for immunohistochemical staining. Deparaffinisation followed by dehydration was carried out by incubating the sections in xylene, 100% absolute ethanol, 95%, 80% and 50% ethanol followed by rinsing with PBS (2 changes, 3 minutes each).

The following rat and rabbit antibodies were used as primary antibodies: rat anti-Mac2 (glomerular macrophages, Cederlane, Ontario, Canada, 1:50), rat anti-F4/80 (macrophages, Serotec, Oxford, UK, 1:50), anti-Ki-67 (cell proliferation, Dianova, Hamburg, Germany, 1:25), rat anti-CD3 (lymphocytes, Serotec, 1:50), anti-ssDNA (apoptotic cells, Chemicon, Hofheim, Germany, 1:50), anti-mMECA-32 (endothelial cells, Iowa Hybridoma Bank, USA, 1:50), anti-mCCL5 (Peprotech, Rocky Hill, NJ, 1:50), rabbit anti-laminin (gift from M. Paulsson, Cologne, Germany, 1:100), goat anti-fibronectin (St. Cruz, Heidelberg, Germany, 1:100). Negative controls included incubation with a respective isotype antibody.

For quantitative analysis 2 μ m sections were stained with periodic acid-Schiff reagent or silver following the instructions of the supplier (Bio-Optica, Milano, Italy). Glomerular sclerotic lesions were assessed using a semiquantitative score by a blinded observer as follows: 0 = no lesion, 1 = <25% sclerotic, 2 = 25-49% sclerotic, 3 = 50-74% sclerotic, 4 = 75-100% sclerotic, respectively. 15 glomeruli were analysed per section. The indices for interstitial volume, interstitial collagen deposition, tubular cell damage, and tubular dilatation were determined by superposing a grid containing 100 (10 x 10) sampling points on photographs of 10 nonoverlapping cortical fields of silver-stained tissue (x 20) of each kidney. Interstitial laminin and fibronectin staining was graded by semiquantitative scoring

of 12 different kidney sections from each animal into 0, 1+ and 2+ by a blinded observer (166). Interstitial cell counts were determined in 15 high power fields (hpf, 400x) by a blinded observer.

3.2.5 RNA analysis

3.2.5.1 RNA isolation

From each animal aliquots of the kidneys were snap frozen in liquid nitrogen and stored at -80 °C. The RNA isolation protocol was suitably modified from Chomczynski's method (174). 3 ml of solution D containing 8 µl of β-mercaptoethanol/ml was taken in 15 ml falcon tube, to which a small piece of tissue from which RNA had to be isolated, was placed. The tissue was homogenized using ULTRA-TURRAX T25 at speed level 2 and placed on ice. To this 300 µl 2M sodium acetate solution was added and mixed gently, followed by addition of 3 ml Roti-Aqua-Phenol and gentle mixing. A 1.6 ml mixture of chloroform/isoamylalcohol (49:1) was added to the contents of the falcon and vortexed for 20 seconds until milky white suspension resulted. The falcon tube was then placed on ice for 15 min and centrifuged at 4000 x g at 4 °C. The upper phase (approximately 3 ml) was collected carefully in a fresh falcon tube, to which 3 ml isopropanol was added, incubated for 30 minutes at -20 °C and centrifuged for 15 minutes at 4000 x g at 4 °C. The supernatant was then discarded carefully to avoid loss of pellet and falcon tube was inverted on a tissue paper to drain of the remaining isopropanol and 1 ml solution. The pellet was dissolved in 0.5 ml solution D and the solution was transferred to fresh DEPC-treated tubes and 0.8 ml isopropanol was added to it, mixed and placed at -20 °C for 30 minutes. This was followed by centrifugation for 15 minutes at 4000 x g at 4 °C; the supernatant was discarded carefully to retain the pellet. The pellet then was washed with 80% ethanol made in DEPC water, and vortexed again for 15 min and centrifuged at 4000xg at 4 °C. The supernatant was discarded and the tubes were inverted to drain of residual ethanol and the semi-dried pellet was dissolved in 100 µl DEPC water. A 10 µl aliquot was used for the quality check and remaining RNA solution was stored at -80 °C until cDNA synthesis. The RNA was quantified and quality was determined by taking 2 µl of RNA solution diluted 50 times in DEPC water for calculating ratios 260/280 nm spectrophotometric OD measurement. The formula used was Extinction x dilution to obtain number of µl/ml of RNA per sample and ratio value approximately close to 1.6 was considered to be of acceptable quality. Further quality check (if necessary) was performed using a denaturing RNA gel, ran at 70-100 V for 1 hour and the gel was read on a gel documentation apparatus.

3.2.5.2 cDNA synthesis and real-time RT-PCR

The RNA samples isolated according to the procedure detailed above were diluted in DEPC water to the concentration of 1 µg/20µl. A master mix was prepared with reagents such as 9 µl of 5x buffer (Invitrogen, Karlsruhe, Germany), 1 µl of 25 mM dNTP mixtute (Amersham Pharmacia Biotech, Freiburg, Germany), 2 µl of 0.1 M DTT (Invitrogen, Karlsruhe, Germany), 1 µl of 40U/ µl RNasin (Promega, Mannheim, Germany), 0.5 µl of Hexanucleotide (Roche, Mannheim, Germany), 1 µl of Superscript (Invitrogen, Karlsruhe, Germany) or ddH₂O in the case of the control. The master mix was made to the volume of 15 µl and added to 1 µg/ 20µl RNA samples were taken in separate DEPC treated microcentrifuge tubes, which were mixed and placed at 42 °C on a thermal shaker incubator for 1 hour. After 1 hour the cDNA samples were collected at placed at -20 °C until use for real-time RT-PCR analysis.

The cDNA samples prepared as described above were diluted 1:10 a dilution for the real-time RT-PCR. The real-time RT-PCR was performed on a TaqMan® ABI 7700. The quantitative PCR for mRNA is based on the employment of sequence-specific primers and likewise sequence-specific probes. The latter is tagged at both ends with a fluorescent molecule. The quencher absorbs TAMRA (at the 3'- End) the fluorescence of the other reporter tagged material such as FAM or VIC at the 5'- End. The TaqMan® universal PCR master mix (Applied Biosystems, Darmstadt, Germany) contained Taq polymerase possessing a 5'→ 3' polymerase activity and a 5'→ 3' exonuclease activity. During the elongation phase of the PCR, specifically bound probe was hydrolyzed by the exonuclease and the 5'-tag was set free. With every newly synthesized DNA strand fluorescent tag material was set free and the resulting fluorescence was measured at 488 nm. The resulting fluorescence signal is directly proportional to the quantity of DNA synthesized. The CT value (= "Cycle Threshold") was computed for each sample. This is the cycle number, with which the reporter fluorescence signal breaks through a user-defined threshold. The TaqMan® universal PCR master mix containing, the forward primers and reverse primers (final concentration of 300 nM) and the probe (final concentration of 100 nM) was placed on ice. In the TaqMan® universal PCR master mix contained are the PCR buffers, dNTPs and the AmpliTaqGold® previously mentioned (Taq polymerase without 3'→ 5' exonuclease activity). 18 µl of the mastermix was pipetted into each well of a 96-well plate and 2 µl of template (DNA dilution) was added to each of these wells. The plate was sealed and centrifuged at 280 xg and analyzed using TaqMan® ABI 7700. For the TaqMan® RT-PCR the following temperature settings were used: The first incubation was carried out for 2 minutes at 50 °C followed by 95 °C for 10 minutes so as to activate the polymerase. Templates were amplified during 40 cycles each

comprising 15 seconds incubation at 95 °C followed by 1 minute incubation at 60 °C. The RT-PCR for the housekeepers (18S rRNA or GAPDH) was carried out under similar conditions. The CT values were recorded using the ABI PRISM Sequence Detection software (version 1.0) and the results were evaluated in relation the respective housekeepers. In all cases controls consisting of ddH₂O were negative for target and housekeeper genes. Oligonucleotide primer (300 nM) and probes (100 nM) were used for RT-PCR described in section C.1.3. Primers and probes for murine Ccl2, Ccl5 and 18S rRNA were obtained as predeveloped assay reagents from PE Biosystems.

3.2.6 Statistical analysis

Data are presented as mean ± SEM. Intravital microscopy data were analysed using one-way ANOVA followed by Student-Newman-Keuls test, using SigmaStat Software (Jandel Scientific, Erkrath, Germany). Comparison of groups was performed using univariant analysis of variance and post-hoc Bonferroni's correction was used for multiple comparisons (*in vitro* data). Paired Student's t-test was used for the comparison of single groups (*in vivo* data of Alport model). A value of $p < 0.05$ was considered to indicate statistical significance. Survival curves were compared by Kaplan-Meier analysis using log-rank two-tailed testing.

4. RESULTS

4.1 Role of CCR1 for the progression of Alport disease

4.1.1 CCR1 blockade and survival of COL4A3-deficient mice

Alport disease is characterized by glomerulosclerosis and subsequent progressive tubulointerstitial injury, leading to ESRD. In human Alport disease and in COL4A3-deficient mice, disease progression is associated with considerable interstitial inflammatory monocytic cell infiltrates, but their functional role for disease progression remains unclear (175, 176, 177).

We hypothesized that CCR1 blockade can reduce interstitial leukocyte recruitment and activation during progressive renal fibrosis and prolong survival in COL4A3-deficient mice. This question was addressed by treating COL4A3-deficient mice and wild-type mice with either BX471 in vehicle or vehicle only. Vehicle-treated COL4A3-deficient mice showed a mean survival of 69 days (95% confidence interval 64 to 74 days) while daily treatment with BX471 from week 6 increased mean survival to 86 days (95% confidence interval 80 to 92 days, $p = 0.0002$, Figure 12). Mortality of COL4A3-deficient mice was likely to be related to uremic death as within the last week of life the physical activity of COL4A3-deficient mice continuously declined until death as noted in previous studies (165, 166). Wild-type control mice remained healthy until the end of the study at week 20.

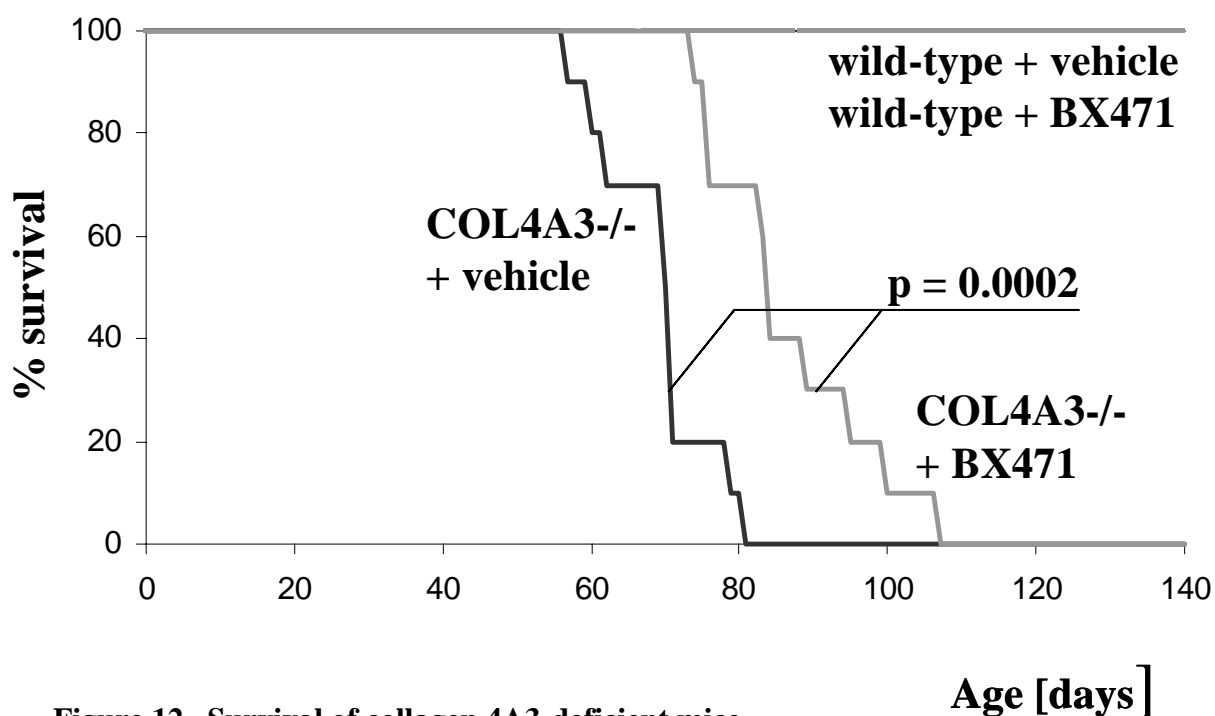


Figure 12. Survival of collagen 4A3-deficient mice.

Mice were treated with either BX471 in vehicle or vehicle alone as indicated. Survival is illustrated as Kaplan-Meier curve.

4.1.2 Interstitial macrophages and tubulointerstitial injury in COL4A3-deficient mice

We hypothesized that improved survival in BX471-treated COL4A3-deficient mice was caused by prevention of renal disease progression. Some additional studies were performed using the same treatment protocol as before but where COL4A3-deficient mice were sacrificed at the age of 9 weeks, for collection of renal tissue.

Glomerular injury: In vehicle-treated COL4A3-deficient mice proteinuria increased over time until the end of the study. By contrast in BX471-treated mice proteinuria did not increase from week 6 and showed a significant reduction of protein/creatinine ratios in urines compared to vehicle-treated mice at week 9 (Figure 13). This was consistent with a reduced number of glomeruli with severe glomerulosclerotic lesions in BX471-injected COL4A3-deficient mice (Table 5, Figure 14).

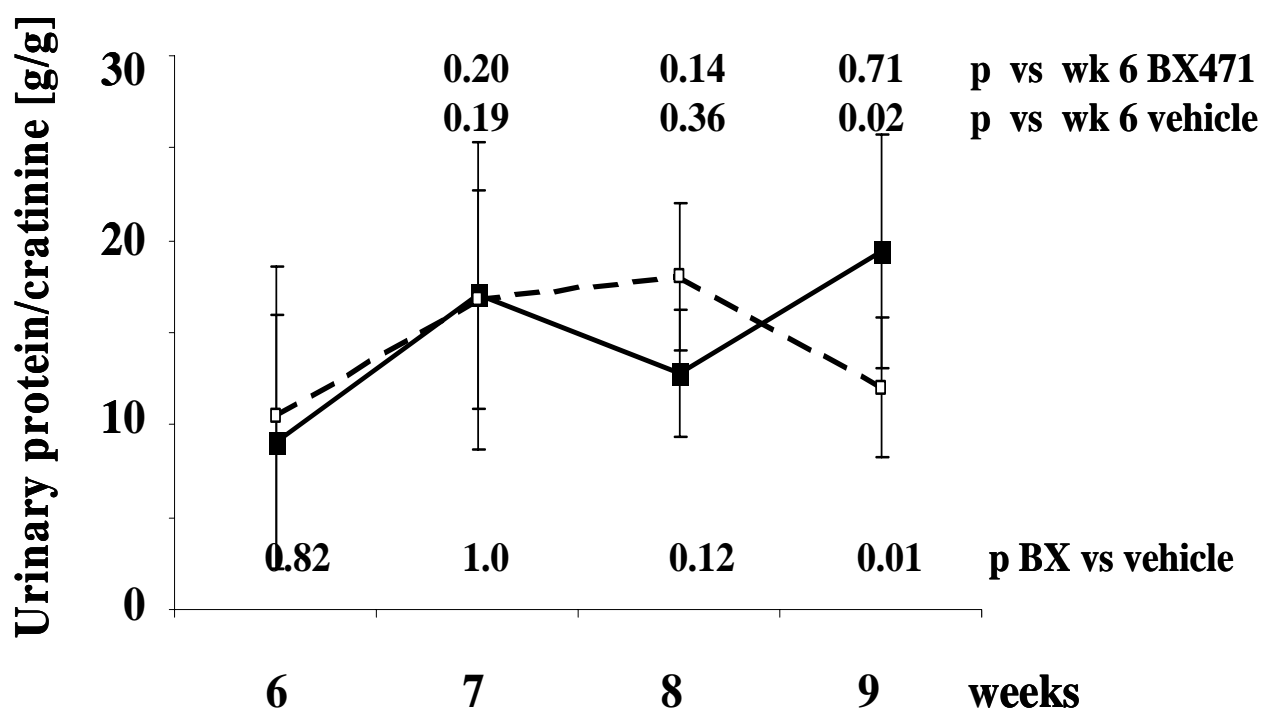


Figure 13. Proteinuria of collagen 4A3-deficient mice.

Urinary protein/creatinine ratios from urine samples taken at weekly intervals in vehicle-treated (black line) and BX471-treated COL4A3-deficient mice (dotted line). Values represent means \pm SEM.

BX471 did not affect the number of Ki-67 positive proliferating glomerular cells (Table 5, Figure 14). No statistical significant differences were noted in BUN and serum creatinine levels in vehicle- and BX471-treated COL4A3-deficient mice at week 9.

Table 5. Serum, urinary, and histological findings in Collagen4A3-deficient mice.

	Wild-type + vehicle (n = 7)	COL4A3 ^{-/-} + vehicle (n = 8)	COL4A3 ^{-/-} + BX471 (n = 10)
Renal function			
BUN [mg/dl]	23.1 ± 2.8	69.5 ± 19.8 [*]	65.9 ± 13.4 [*]
serum creatinine [mg/dl]	0.39 ± 0.05	0.52 ± 0.11 [*]	0.50 ± 0.04 [*]
Glomerulosclerosis score			
0 (no lesion in %)	89 ± 7	6 ± 5 [*]	20 ± 9 ^{*#}
1 [1 - 24%]	11 ± 10	10 ± 4	23 ± 11 ^{*#}
2 [25 - 49%]	0 ± 0	10 ± 4 [*]	12 ± 9 [*]
3 [50 - 74%]	0 ± 0	25 ± 9 [*]	18 ± 7 [*]
4 [75 - 100%]	0 ± 0	49 ± 11 [*]	27 ± 13 ^{*#}
Cellular response [cells/glom. or hpf]			
Glom. Ki-67+	0.1 ± 0.1	1.0 ± 0.3 [*]	1.2 ± 0.4 [*]
Interst. F4/80+	1.9 ± 0.7	24.3 ± 2.3 [*]	17.9 ± 3.2 ^{a#}
Tubular Ki-67+	0.4 ± 0.2	1.6 ± 0.8 [*]	3.2 ± 0.7 ^{*#}
ssDNA+	0.1 ± 0.0	1.8 ± 0.4 [*]	0.7 ± 0.4 ^{*#}
Peritubular capillaries [capillary cross sections/hpf]			
MECA-32 +	66.7 ± 10.3	33.8 ± 8.6 [*]	59.3 ± 9.0 ^{*#}
Interstitial matrix deposition			
Fibronectin [% hpf]	0.0 ± 0.0	1.1 ± 0.4 [*]	1.2 ± 0.4 [*]
Laminin [% hpf]	0.0 ± 0.0	1.8 ± 0.3 [*]	1.3 ± 0.2 ^{*#}

Values are means ± SEM, ^{*} p < 0.05 vs. wild-type, [#] p < 0.05 BX471 vs. vehicle

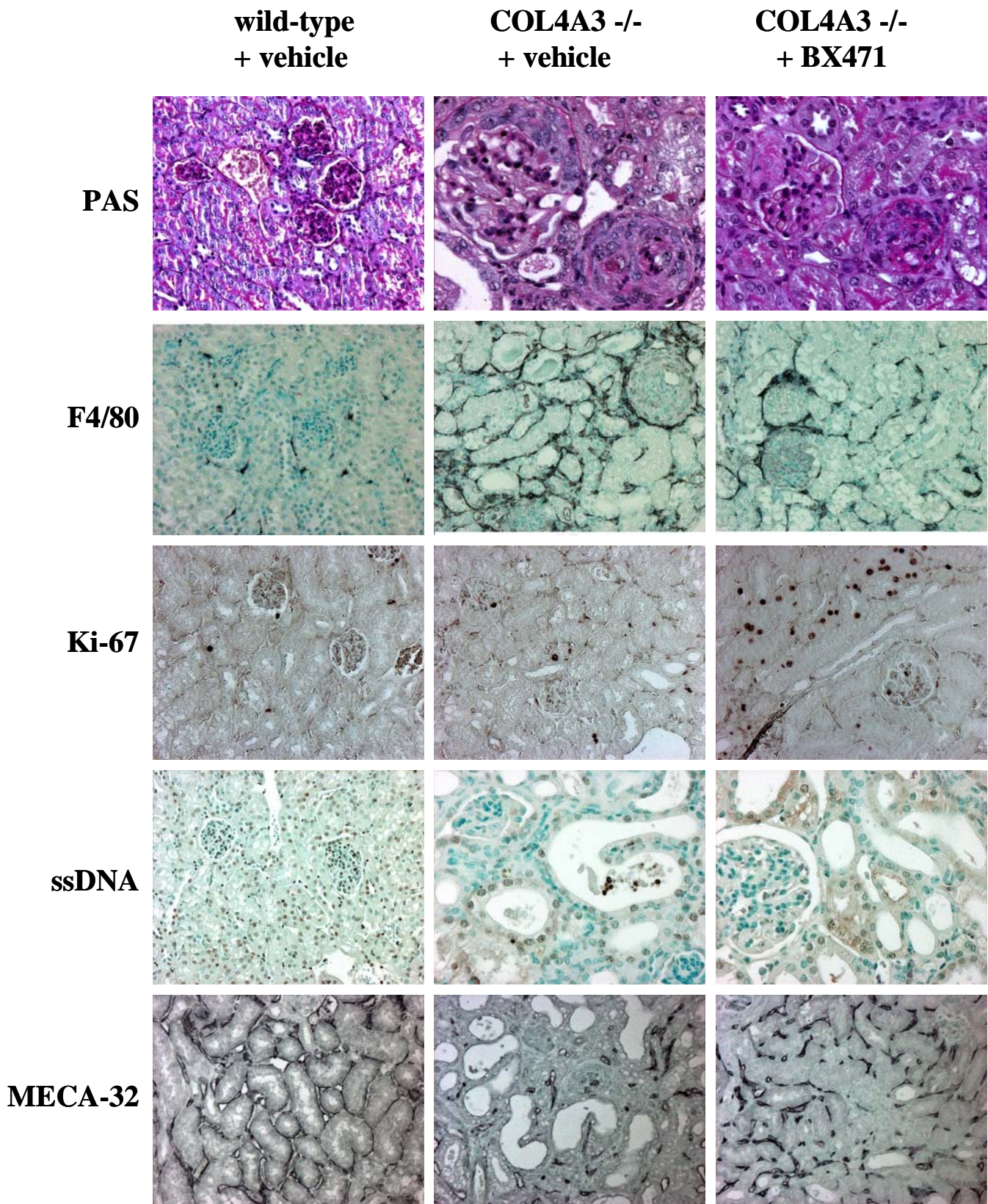


Figure 14. Renal histopathology in COL4A3-deficient mice.

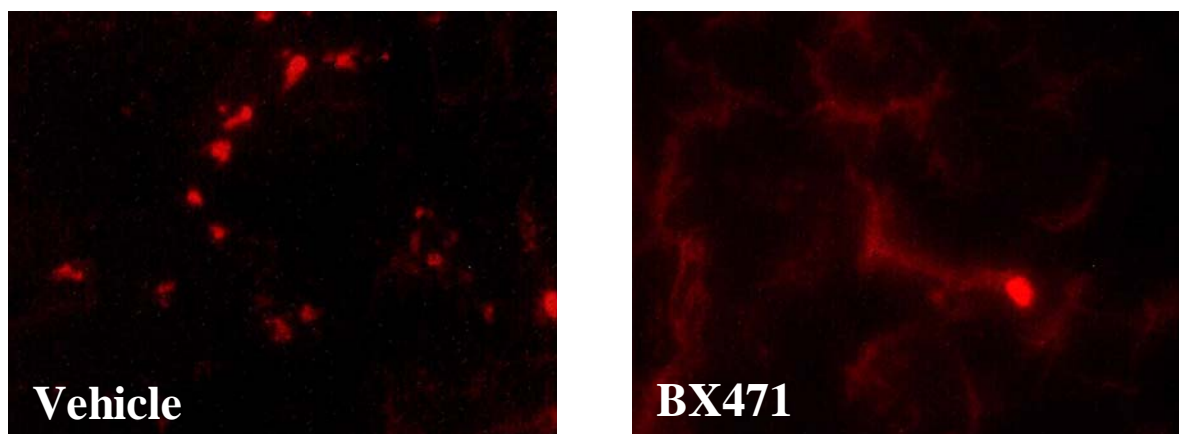
Renal sections of wild-type and COL4A3-deficient mice were stained with periodic acid Schiff solution or for the indicated markers as described in methods. For quantification see table 5, original magnification 400x.

Tubulointerstitial injury: Vehicle-treated COL4A3-deficient mice had diffuse tubular atrophy and interstitial fibrosis as compared to age-matched wild-type mice (Figure 14, Table 5). COL4A3-deficient mice had increased numbers of Ki-67 positive proliferating and apoptotic tubular epithelial cells (Table 5, Figure 14). Interstitial damage in COL4A3-deficient mice was associated with a robust increase of interstitial F4/80 positive macrophages. BX471 markedly reduced the numbers of interstitial F4/80 positive macrophages compared to vehicle-treated COL4A3-deficient mice (Figure 14, Table 5). This reduction of interstitial macrophages was associated with reduced numbers of ssDNA positive apoptotic tubular epithelial cells. By contrast, BX471 increased the numbers of Ki-67 positive proliferating tubular epithelial cells, suggesting a role of interstitial macrophages for the balance of apoptotic cell death and tubular cell regeneration (Figure 14, Table 5). BX471 prevented the reduction in peritubular capillary cross sections observed in untreated COL4A3-deficient mice (Table 5, Figure 14), suggesting that CCR1-dependent macrophage recruitment is involved in interstitial microvascular injury of COL4A3-deficient mice.

4.1.3 Renal infiltration of labeled macrophages in kidneys of COL4A3-deficient mice

In order to confirm that BX471-induced reduction of interstitial macrophage counts is caused by blocking macrophage recruitment, we performed cell transfer studies with labeled macrophages. After injection fluorescently labeled F4/80 macrophages localized to the interstitial compartment of 8 weeks of COL4A3-deficient mice, while glomeruli and perivascular fields were negative (Figure 15A). Pretreatment with BX471 significantly reduced the numbers of labeled F4/80 macrophages that infiltrated into the renal interstitium of COL4A3-deficient mice (Figure 15B).

A



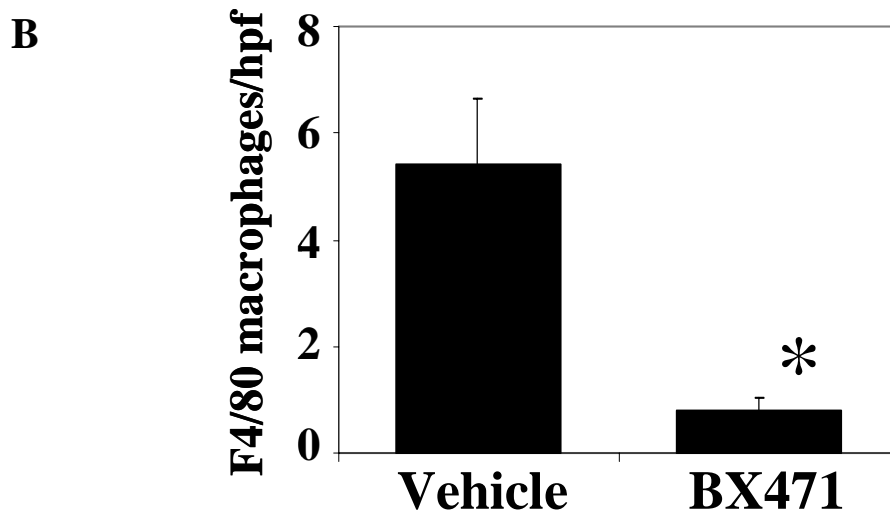


Figure 15. Renal infiltration of labeled macrophages in kidneys of COL4A3-deficient mice.

A. COL4A3-deficient mice 8 weeks of age were injected intravenously with PKH26-labeled F4/80 macrophages isolated from spleens of donor mice. The cells were pretreated with either vehicle or BX471 as indicated. Recipient mice received subcutaneous injections with either vehicle or BX471 before injection of the respective cells and kidneys were obtained 3 hours after injection of cells and examined by fluorescence microscopy. Fluorescence-labeled cells locate to the renal interstitium, original magnification 400x.

B. Cell counts for interstitial labeled F4/80 macrophages were determined by fluorescence microscopy from 15 hpf. Values are means \pm SEM. * $p < 0.001$.

4.1.4 Interstitial renal fibrosis

The degree of interstitial renal fibrosis was compared in kidneys of mice from all groups. Vehicle-treated COL4A3-deficient mice showed an increase of the respective indices for damaged tubular cells, tubular dilatation, interstitial matrix, and interstitial volume when compared to age-matched wild-type mice (Figure 16). BX471 significantly reduced all these markers compared to vehicle-treated COL4A3-deficient mice (Figure 16). BX471 reduced the amount of interstitial laminin deposits as compared to vehicle-treated COL4A3-deficient mice, but BX471 had no effect on interstitial fibronectin deposits (Table 5).

A

**Wild-type
+ vehicle**

**COL4A3 -/-
+ vehicle**

**COL4A3 -/-
+ BX471**

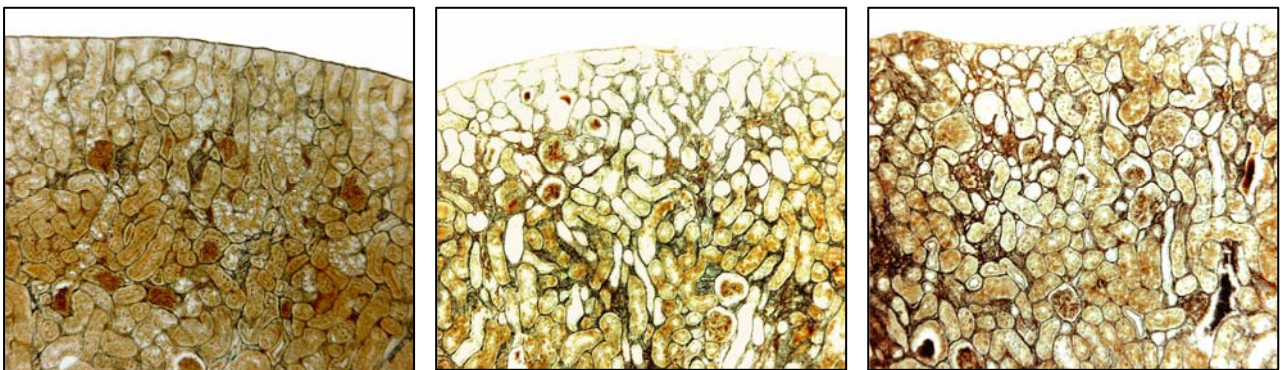


Figure 16. Renal fibrosis in COL4A3-deficient mice.

A. Renal sections of wild-type and COL4A3-deficient mice were stained with silver. Images illustrate representative sections of kidneys from the respective groups at week 9 of age (original magnification 100x).

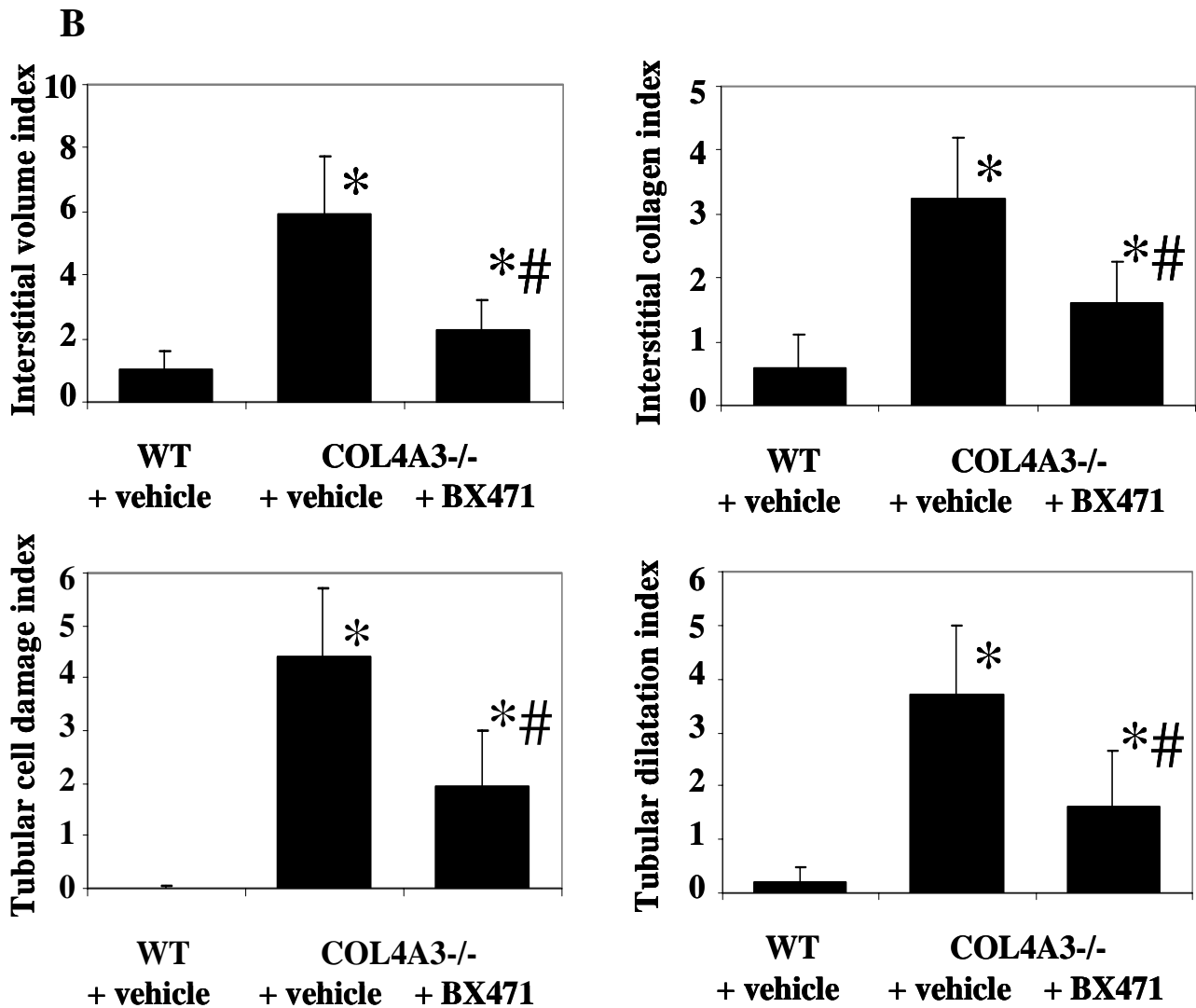


Figure 17. Renal fibrosis in COL4A3-deficient mice.

B. Morphometric analysis of cortical renal sections was performed as described in methods. Values represent means \pm SEM of the respective index in 7-10 mice in each group. * $p < 0.001$ vs vehicle-treated COL4A3-deficient mice, # $p < 0.002$ vs vehicle-treated wild-type mice.

4.1.5 Renal CCL5 expression in COL4A3-deficient mice

For examining whether BX471 treatment affected the production of proinflammatory mediators, e.g. the CC-chemokine CCL5 in kidneys COL4A3-deficient mice we performed real-time RT-PCR for *Ccl5* mRNA on total renal isolates from vehicle- and BX471-treated COL4A3-deficient mice at 9 weeks of age. We found that BX471 somewhat reduced renal *Ccl5* mRNA expression although this was not statistically significant (Figure 18A).

A

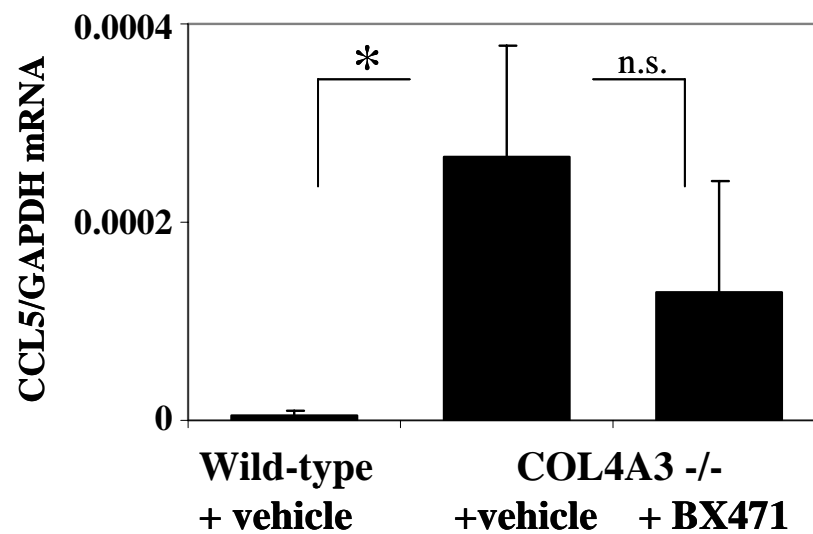


Figure 18. Renal CCL5 expression in COL4A3-deficient mice.

A. *Ccl5* mRNA expression was determined by real-time RT-PCR using total renal RNA from 5-7 mice of each group. *Ccl5* mRNA levels for vehicle- and BX471-treated COL4A3-deficient mice are expressed per respective *Gapdh* mRNA expression of each kidney.

* $p < 0.05$.

Immunostaining localized CCL5 in vehicle-treated COL4A3-deficient mice to single periglomerular and interstitial cells but not to tubular epithelial cells or glomeruli. Treatment with BX471 markedly reduced the amount of CCL5 positive cells in the renal interstitium of COL4A3-deficient mice (Figure 18B). Together these data suggest that BX471 modulates the expression of CCL5 in kidneys of COL4A3-deficient mice, either by impairing recruitment of CCL5 producing cells to the kidney or possibly by directly inhibiting CCL5 production in resident renal macrophages.

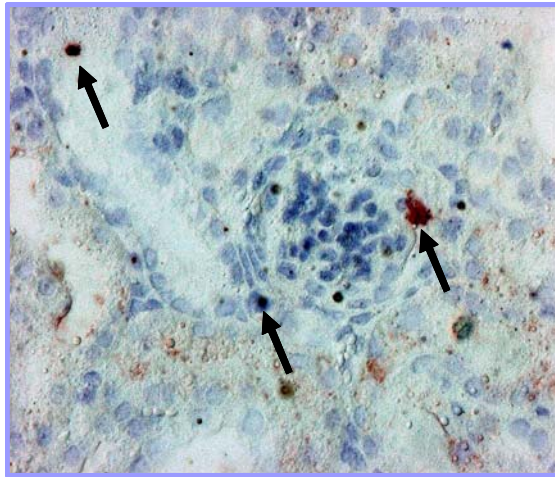
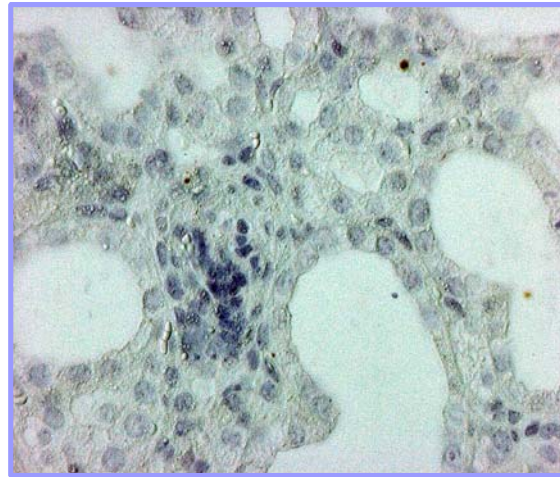
B**COL4A3 -/-
+ vehicle****COL4A3 -/-
+ BX471**

Figure 18. Renal CCL5 expression in COL4A3-deficient mice.

B. Immunostaining for CCL5 was performed on paraffin-embedded renal sections as described in methods. Arrows indicate CCL5 positive cells in the renal interstitium and the periglomerular area in vehicle-treated COL4A3 mice. No CCL5 staining was detected in kidneys of BX471-treated COL4A3-deficient mice. Images illustrate representative sections of kidneys from the respective groups at week 9 of age (original magnification 400x).

4.1.6 CCL5 production by J774 macrophages

The role of cytokines such as TNF- α or IFN- γ for macrophage activation and CCL5 production is well established. However, it is unknown whether CCR1 ligation contributes to the activation of tissue macrophages. We evaluated CCL5 production in cultured murine J774 macrophages after incubation with various cytokine combinations for 24 hours. A combination of IFN- γ and TNF- α induced marked CCL5 secretion by J774 macrophages. Adding the CCR1 ligand CCL3 to this cytokine combination increased CCL5 protein production by 50% (Figure 19). The CCR1 antagonist BX471 completely blocked the CCL3-induced increase of CCL5 secretion, indicating that CCL3 mediates its effect on CCL5 secretion through CCR1. CCL3 alone did not induce CCL5 secretion in J774 macrophages. These data suggest that CCR1 ligation by its chemokine ligand CCL3 contributes to macrophage CCL5 production, which may facilitate additional leukocyte recruitment and local inflammation *in vivo*.

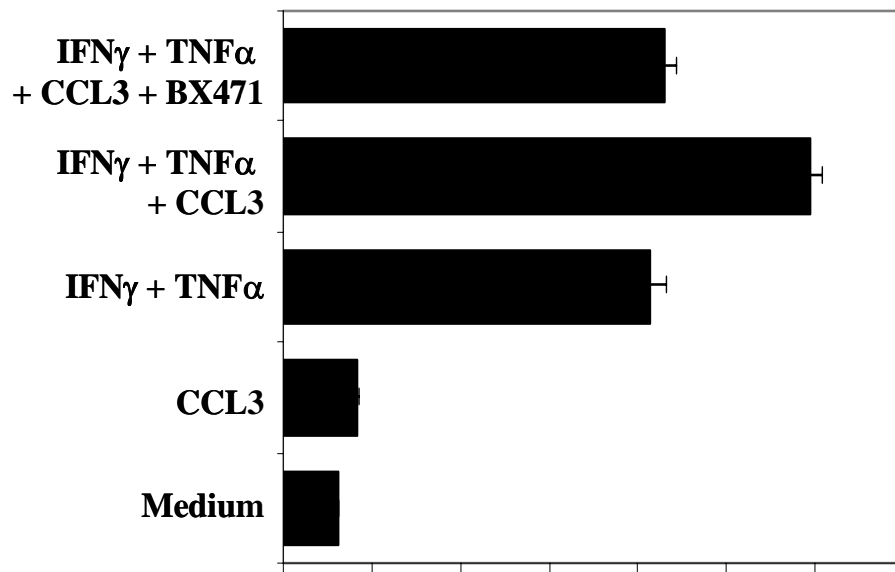


Figure 19. CCL5 production by J774 macrophages.

J774 cells were stimulated with either 200 ng/ml IFN- γ , 500U/ml TNF- α , 500ng/ml CCL3, 1 μ M BX471 or standard medium without supplements for 24 hours as indicated. CCL5 protein production was determined in supernatants by ELISA. Results shown are from one of three comparable experiments, each performed in duplicate. Values are expressed as CCL5 concentrations \pm SEM. * $p < 0.05$.

4.1.7 CCR1 mediates intravascular adhesion and transendothelial migration of leukocytes

In order to assess the role of CCR1 during the multistep recruitment process of intravascular leukocytes into inflamed tissues *in vivo*, we applied intravital microscopy of cremaster muscles in wild-type and CCR1-deficient mice, as well as in wild-type mice treated with the CCR1 antagonist BX471. Analysis was performed 3 hours after intrascrotal administration of CCL3. This technique allowed us to visualize and quantify the four following stages of leukocyte recruitment: rolling, adhesion, transendothelial diapedesis, and interstitial migration (Figure 20A).

A

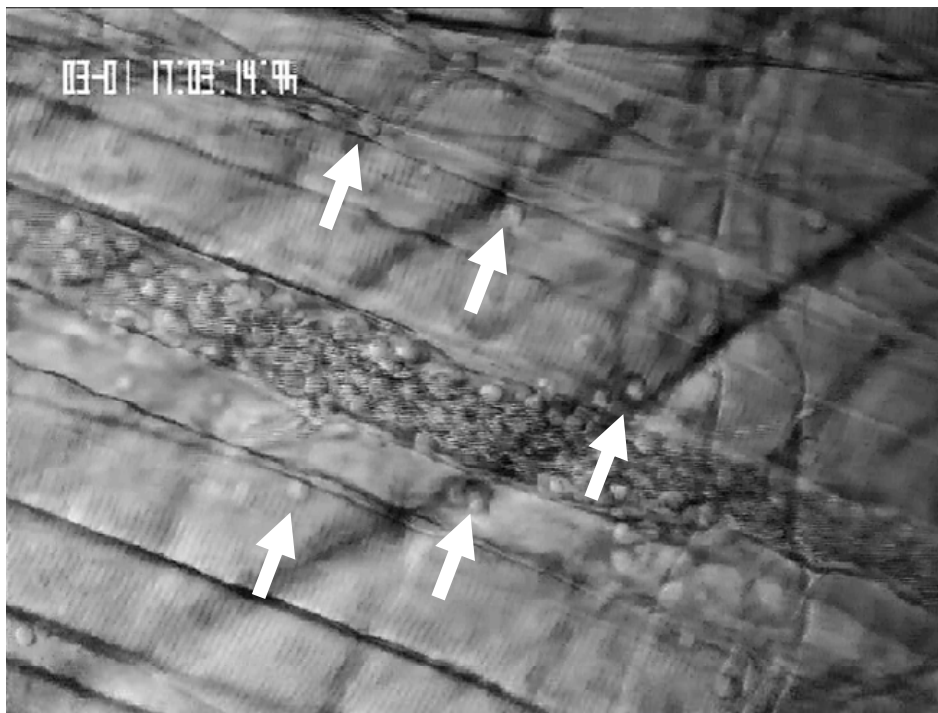


Figure 20. Intravital microscopy.

A. Microscopic image of a CCL3-stimulated cremasteric postcapillary venule that is surrounded by leukocytes emigrated into the interstitial tissue (arrows). Objective magnification 400x.

Rolling phase: In the rolling phase transient interactions between activated endothelial cells and leukocyte surface molecules slow down circulating leukocytes. CCL3 prestimulation did not affect leukocyte rolling in wild type mice (Figure 20B) and no statistical significant differences were detected between the four groups of mice studied.

Adherence phase: Leukocyte arrest on activated vascular endothelial cells is mediated by chemokine-driven activation of adhesion molecules and is a prerequisite for transendothelial migration. CCL3 prestimulation significantly increased leukocyte adhesion in wild-type mice (Figure 20C). CCL3-induced increase of leukocyte adhesion was not observed in CCR1-deficient mice or in mice treated with the CCR1 antagonist BX471.

Transendothelial migration phase: After adhesion leukocytes have to transmigrate through vascular endothelia and basement membranes in order to enter the interstitial compartment. CCL3 prestimulation significantly increased transendothelial migration of leukocytes in wild-type mice (Figure 20D). Lack of CCR1 or BX471 treatment reduced but did not completely block CCL3-induced leukocyte transmigration when compared to wild-type control mice.

Interstitial migration phase: In interstitial tissue compartments leukocyte continue to migrate, but the role of CCR1 for this process is unknown. Interestingly, there was no significant difference between migration distances in cremaster muscles from either group, indicating that CCR1 does not play a role for interstitial migration of leukocytes (Figure 20E). Systemic leukocyte counts, inner diameters of the postcapillary venules studied, cell velocity and shear rates were unaltered by CCL3 prestimulation, as these factors could compromise the comparison between CCL3-treated and control mice (data not shown).

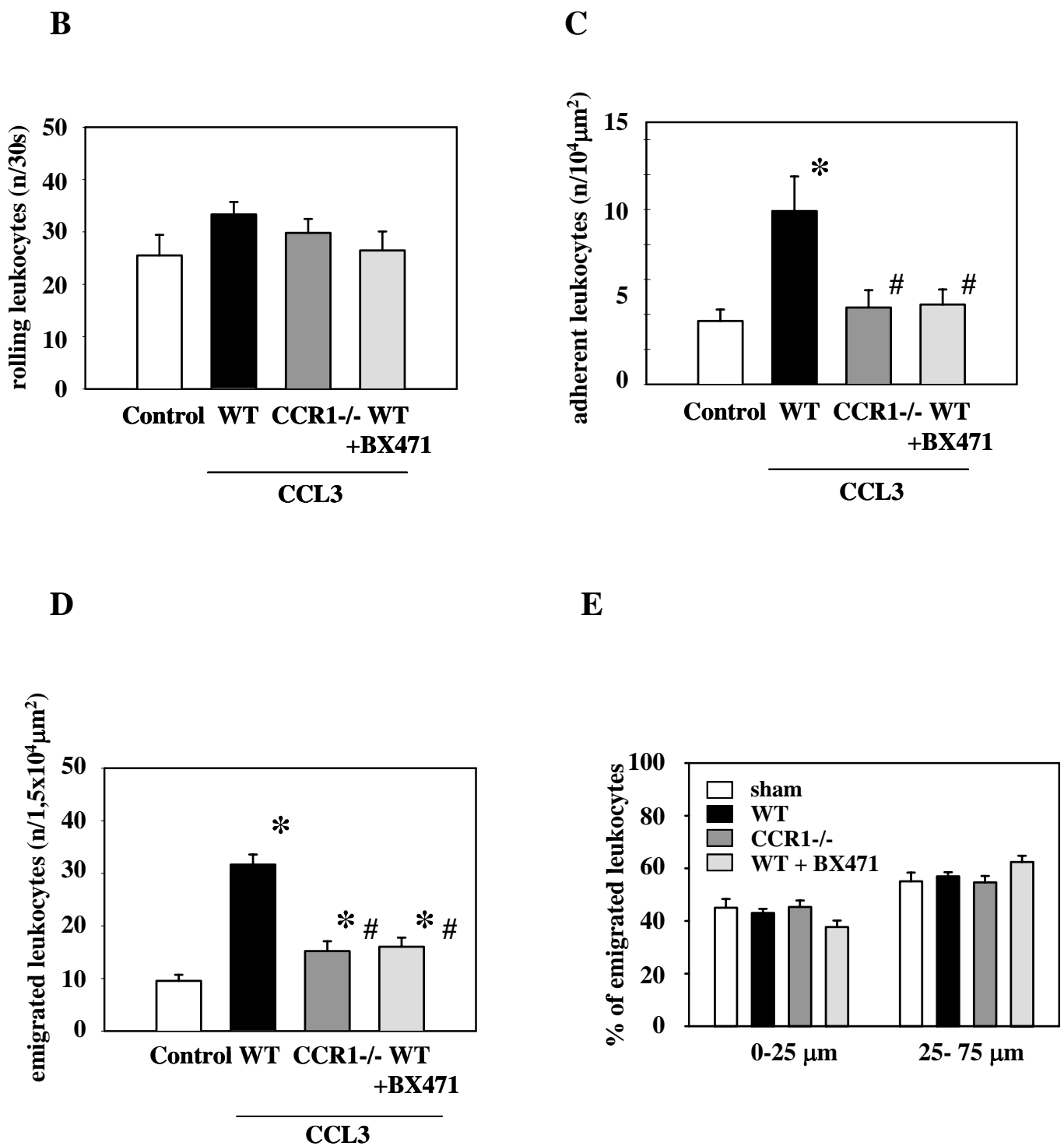


Figure 20. Intravital microscopy.

B-E. Quantitative analysis of the respective parameters of leukocyte-endothelial cell interactions and leukocyte emigration as determined by intravital microscopy. Values represent means \pm SEM in 7 mice of each group, * $p < 0.05$ vs sham, # $p < 0.05$ vs. wild-type mice.

4.2 Role of CCR1 for the progression of type 2 diabetic nephropathy

4.2.1 Effect of uninephrectomy on diabetic nephropathy of db/db mice

Albuminuria is the first functional marker of diabetic nephropathy in humans and db/db mice. In fact, 2 months old db/db mice revealed increased albuminuria as compared to wild-type mice of the same age (Figure 21A). Uninephrectomy performed in db/db (1K) mice at 6 weeks of age was associated with higher albuminuria levels as compared to sham-operated (2K) db/db mice.

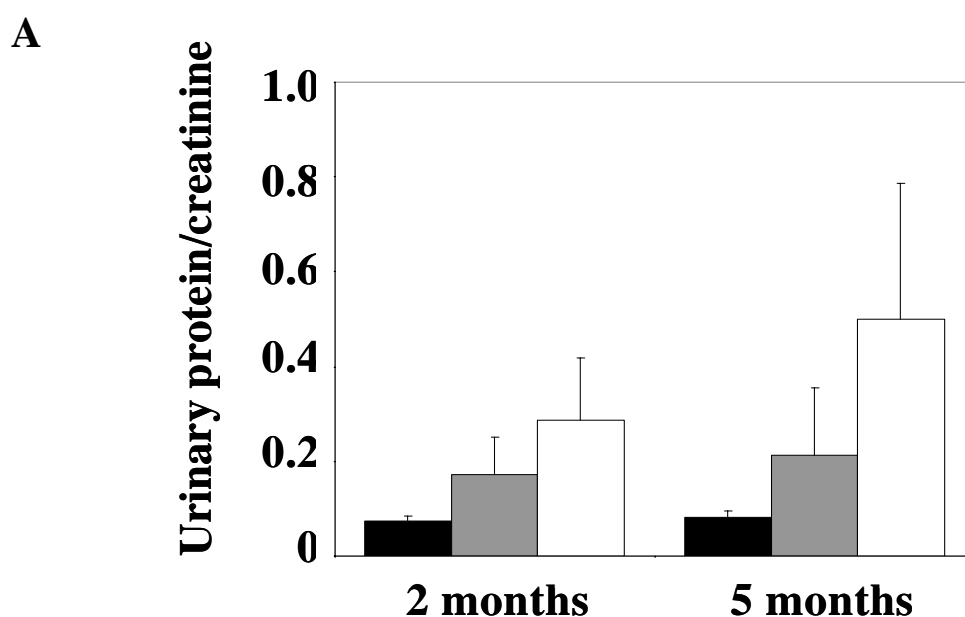


Figure 21. Effect of uninephrectomy on diabetic nephropathy of db/db mice.

A. Urinary albumin/creatinine ratios were determined in 2K wild-type mice (black bars), 2K db/db mice (grey bars), and 1K db/db mice (white bars). Values represent means \pm SEM from 7-10 mice in each group.

The nephrectomy-related impact on albuminuria further increased until 5 months of age, consistent with uninephrectomy accelerating diabetic nephropathy in db/db mice (178). Uninephrectomy may simply increase albuminuria by hyperfiltration and not necessarily via a CCR1-dependent mechanism. Therefore, we examined the renal expression of CCR1 in 1K and 2K db/db mice. We have previously shown that intrinsic renal cells do not express the

chemokine receptor CCR1 in the mouse kidney and that renal CCR1 expression originates from infiltrating macrophages and T cells (153). As appropriate antibodies that allow detection of CCR1 protein by cell fluorescence or immunostaining in mice are not available, we used real-time RT-PCR in order to determine the expression of *Ccr1* mRNA in kidneys of db/db mice. Kidneys of 2 months old 2K db/db mice showed low *Ccr1* mRNA expression which markedly increased until 6 months of age (Figure 21B). Renal *Ccr1* mRNA expression further increased in 1K db/db mice.

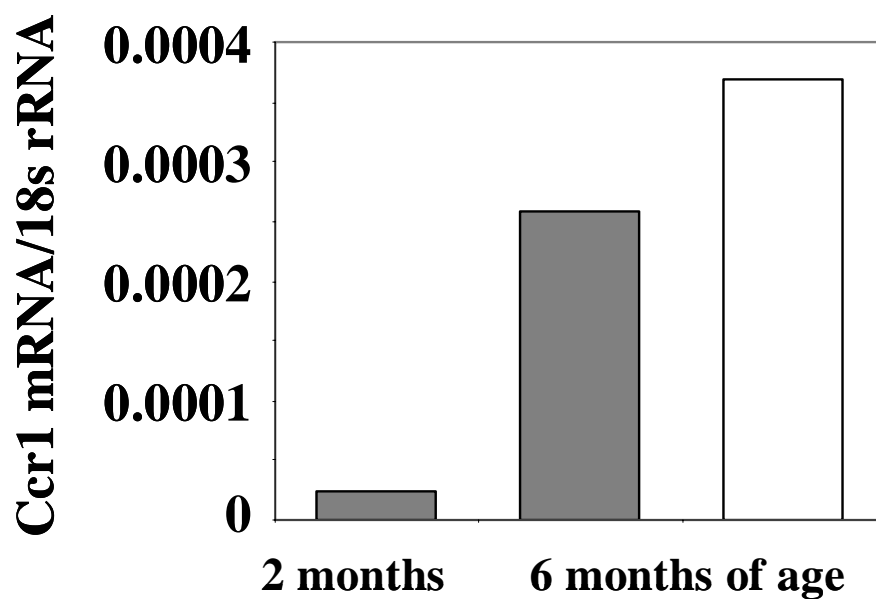
B

Figure 21. Effect of uninephrectomy on diabetic nephropathy of db/db mice.

B. Quantitative real time RT-PCR analysis was performed on total cDNA derived from kidneys of 2 or 6 months old 2K db/db mice (grey bars) or 6 months old 1K db/db mice (white bars). The cDNA was amplified using primers specific for mCCR1 for 40 PCR cycles. The data shown are derived from pooled cDNA samples from 6-10 mice of each group and are expressed as ratio to respective 18s rRNA expression.

4.2.2 CCR1 antagonist reduces recruitment of macrophages to the renal interstitium of uninephrectomized db/db mice

Next we tested whether the pharmacokinetic profile of the CCR1 antagonist BL5923 is affected by uninephrectomy and whether BL5923 can block macrophage recruitment to the renal interstitium of 1K db/db mice. The pharmacokinetic data show that the half-life of BL5923 is not prolonged in 1K db/db mice. The plasma compound levels were identical in sham-operated and uninephrectomized db/db mice (Figure 22A).

A

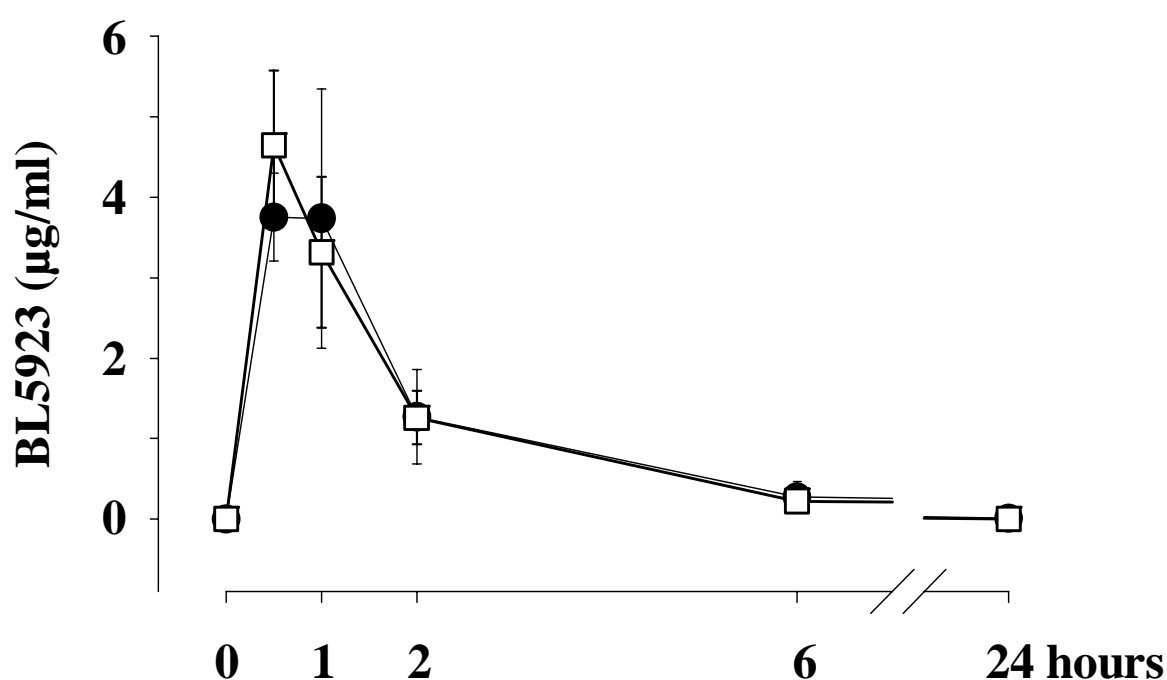


Figure 22. Pharmacokinetic profile of BL5923 and recruitment of monocytes into the renal interstitium of db/db mice.

A. BL5923 was applied once orally at 60 mg/kg p.o. to groups of six 2K db/db mice (closed circles) or 1K db/db mice (open squares). Blood samples were obtained at 30 min, 1, 2, 6, and 24 hours and the plasma level of BL5923 were determined by HPLC/MS and expressed as mean \pm SEM in $\mu\text{g/ml}$.

Next, we performed cell transfer studies with ex vivo fluorescently labeled F4/80 positive monocytes into 6 months old 1K db/db mice that had been pretreated with a single dose of either BL5923 or vehicle. 3 hours after injection F4/80 cells were found to localize to the interstitial compartment of 1K db/db mice (Figure 22B). Pretreatment with BL5923 significantly reduced the numbers of labeled F4/80 cells that infiltrated into the renal interstitium of 1K db/db mice (Figure 22C). Next we assessed white blood counts in mice treated with BL5923. A single dose of BL5923 decreased white blood counts in sham-operated and uninephrectomized db/db mice ($6.1 \pm 0.6 \times 10^3/\mu\text{l}$ vs. $3.2 \pm 0.8 \times 10^3/\mu\text{l}$ [sham-operated] or vs. $3.4 \pm 0.6 \times 10^3/\mu\text{l}$ [uninephrectomized], $p < 0.001$, respectively). These data provide the rationale for using BL5923 to block interstitial macrophage recruitment in 1K db/db mice, an accelerated model of diabetic nephropathy.

B

F4/80 macrophages

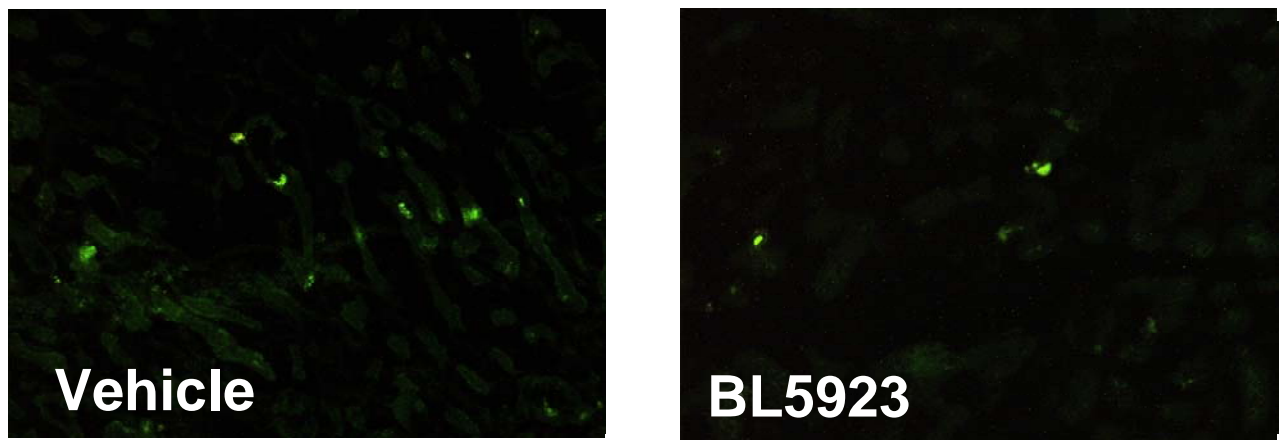


Figure 22. Pharmacokinetic profile of BL5923 and recruitment of monocytes into the renal interstitium of db/db mice.

B. 1K db/db mice 6 months of age were injected intravenously with PKH26-labeled F4/80 macrophages isolated from spleens of donor db/db mice. Recipient mice received subcutaneous injections with either vehicle or BL5923 before injection of the respective cells and kidneys were obtained 3 hours after injection of cells and examined by fluorescence microscopy. Fluorescence-labeled cells locate to the renal interstitium, original magnification 400x.

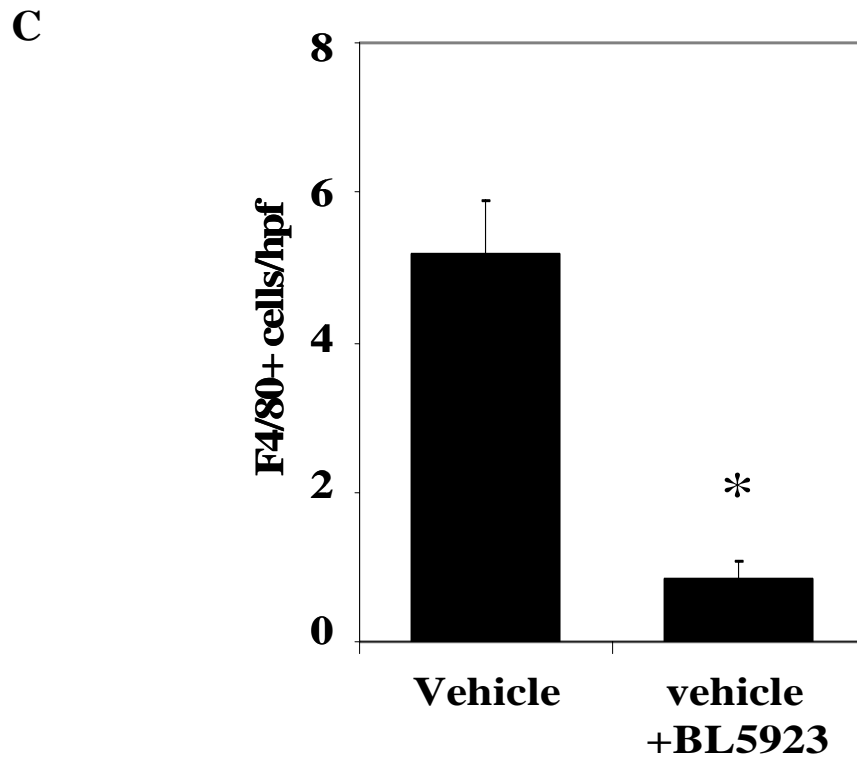


Figure 22. Pharmacokinetic profile of BL5923 and recruitment of monocytes into the renal interstitium of db/db mice.

C. Cell counts for interstitial labeled F4/80 monocytes were determined by fluorescence microscopy from 15 hpf. Values are means \pm SEM. * $p < 0.001$.

4.2.3 BL5923 reduces interstitial macrophage counts and tubulointerstitial injury in uninephrectomized db/db mice

As BL5923 can block interstitial macrophage recruitment in 1K db/db mice, BL5923 treatment may have beneficial effects on the progression of diabetic nephropathy associated with tubulointerstitial injury and interstitial fibrosis. We initiated oral administration of BL5923 (60 mg/kg, b.i.d.) or vehicle at an age of 5 months in 1K db/db mice. Treatment was continued for 4 weeks when urine samples and tissues were collected for the assessment of diabetic nephropathy. During that period BL5923 treatment did not significantly affect blood glucose levels or body weight which were both markedly elevated in all groups of db/db mice as compared to non-diabetic wild type mice (Figure 23A and B).

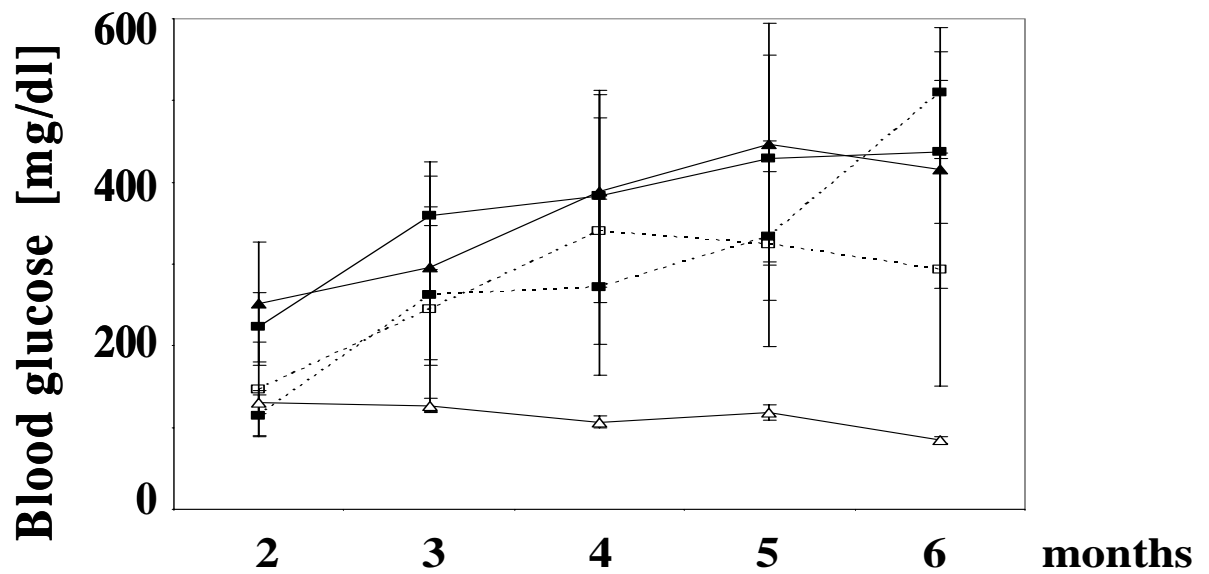
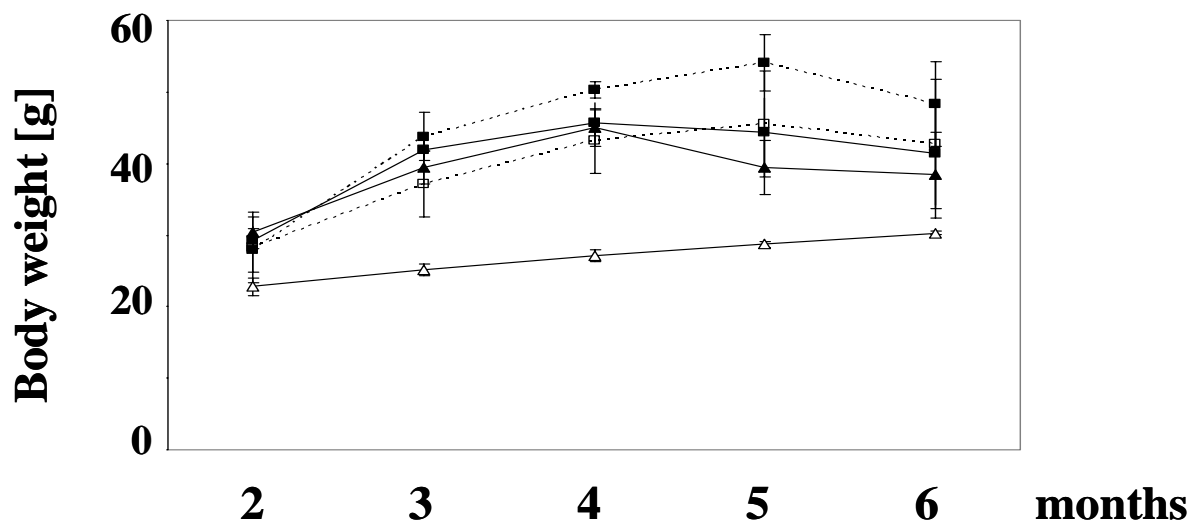
A**B**

Figure 23. Blood glucose levels and body weight in db/db and wild-type mice.

Blood glucose levels (**A**) and body weight (**B**) were determined at monthly intervals in 2K wild-type mice (open triangles), 2K db/db mice (black triangles), and 1K db/db mice (nil: black squares, dashed line; vehicle: black squares; BL5923: open squares). Values represent means \pm SEM.

Glomerular injury: At 6 months of age diabetic glomerulosclerosis was more prominent in 1K db/db mice as compared to 2K db/db mice (Table 6, Figure 24). BL5923 had no effect on glomerulosclerosis or urinary albumin/creatinine ratios of 6 months old db/db mice (Table 6, Figure 24). BL5923 did not affect the number of Mac-2 positive glomerular macrophages or Ki-67 positive proliferating glomerular cells (Table 6, Figure 24). BUN levels were comparable in vehicle- and BL5923-treated 1K db/db mice.

Table 6. Serum, urinary, and histological findings in sham-operated (2K) and uninephrectomized (1K) mice.

	2K		1K		
	Wild-type + nil (n = 7)	db/db + nil (n = 7)	db/db + nil (n= 9)	db/db + vehicle (n = 7)	db/db + BL5923 (n=8)
Renal function					
Urine albumin/creatinine	0.1 ± 0.1	0.4 ± 0.1	0.3 ± 0.9	0.2 ± 0.1	0.2 ± 0.1
BUN [mg/dl]	27 ± 5	42 ± 18	51 ± 10	37 ± 6	37 ± 7
Glomerulosclerosis score					
0 [no lesion]	90 ± 1	12 ± 6	0 ± 0	0 ± 0	0 ± 0
1 [1 - 24%]	5 ± 2	20 ± 2	4 ± 5	3 ± 4	3 ± 5
2 [25 - 49%]	4 ± 4	31 ± 9	23 ± 8	27 ± 4	29 ± 6
3 [50 - 74%]	1 ± 2	26 ± 11	32 ± 3	39 ± 5	33 ± 4
4 [75 – 100%]	0 ± 0	11 ± 3	40 ± 10	31 ± 9	34 ± 7
Cellular response [cells/glom. or hpf]					
Glom. Ki-67+			0.8 ± 0.4		0.8 ± 0.3
Mac-2+	0.2 ± 0.1	1.7 ± 0.1	2.4 ± 0.7	2.6 ± 0.3	2.2 ± 0.5
Interst. F4/80+	2.8 ± 0.3	8.4 ± 1.3	14.4 ± 2.1	14.1 ± 2.2	2.3 ± 1.5*
Ki-67+			6.2 ± 4.0		0.6 ± 0.3*
Tubular Ki-67+			5.7 ± 1.5		2.2 ± 0.5*
Peritubular capillaries [capillary cross sections/hpf]					
MECA-32 +			81 ± 10		103 ± 11*

Values are means ± SEM, * p < 0.05 vs. vehicle

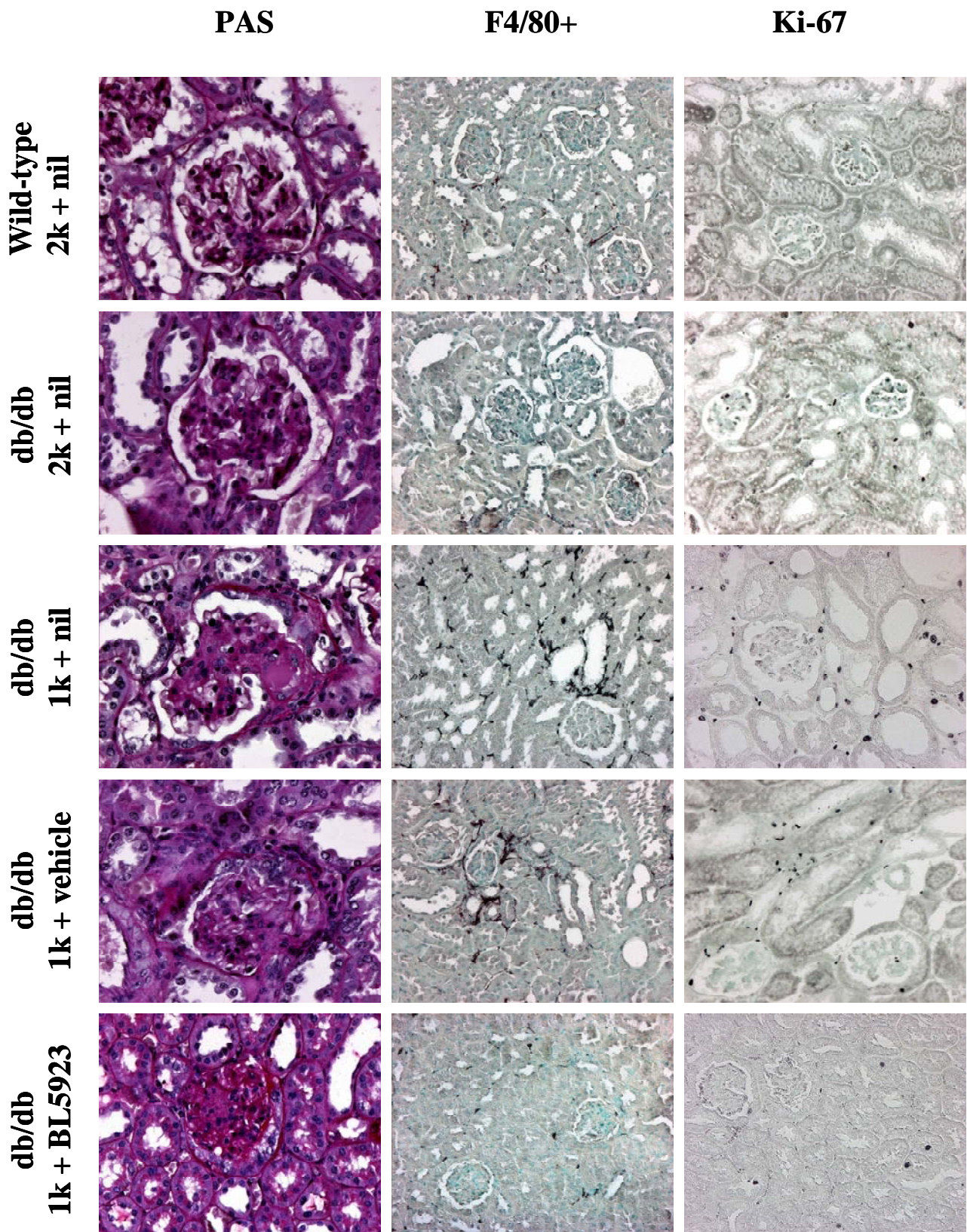


Figure 24. Renal histopathology in db/db mice.

Renal sections from mice of all groups were stained with periodic acid Schiff solution or for the indicated markers as described in methods. For quantification see table 6. Original magnification 200-400x.

Tubulointerstitial injury: Indices for flattened or necrotic tubular cells, tubular dilatation, interstitial matrix, and interstitial volume as markers of tubulointerstitial damage and renal fibrosis were assessed in mice of all groups by morphometry. BL5923 significantly reduced all these markers in 1K db/db mice (Figure 25).

Interstitial disease in vehicle-treated 1K db/db mice was associated with a robust increase of interstitial F4/80 positive macrophages which were markedly reduced by BL5923 (Figure 24, Table 6). CD3 positive lymphocytes were absent in kidneys of 6 months old db/db mice (not shown). The reduction of interstitial macrophages was associated with reduced numbers of Ki-67 positive proliferating tubular epithelial cells as well as proliferating cells in the interstitial compartment (Table 6, Figure 24). BL5923 prevented the reduction in MECA32 positive peritubular capillary cross sections which was observed in vehicle-treated 1K db/db mice (Table 6). These findings show that blocking CCR1-dependent interstitial macrophage recruitment preserves tubulointerstitial injury in db/db mice.

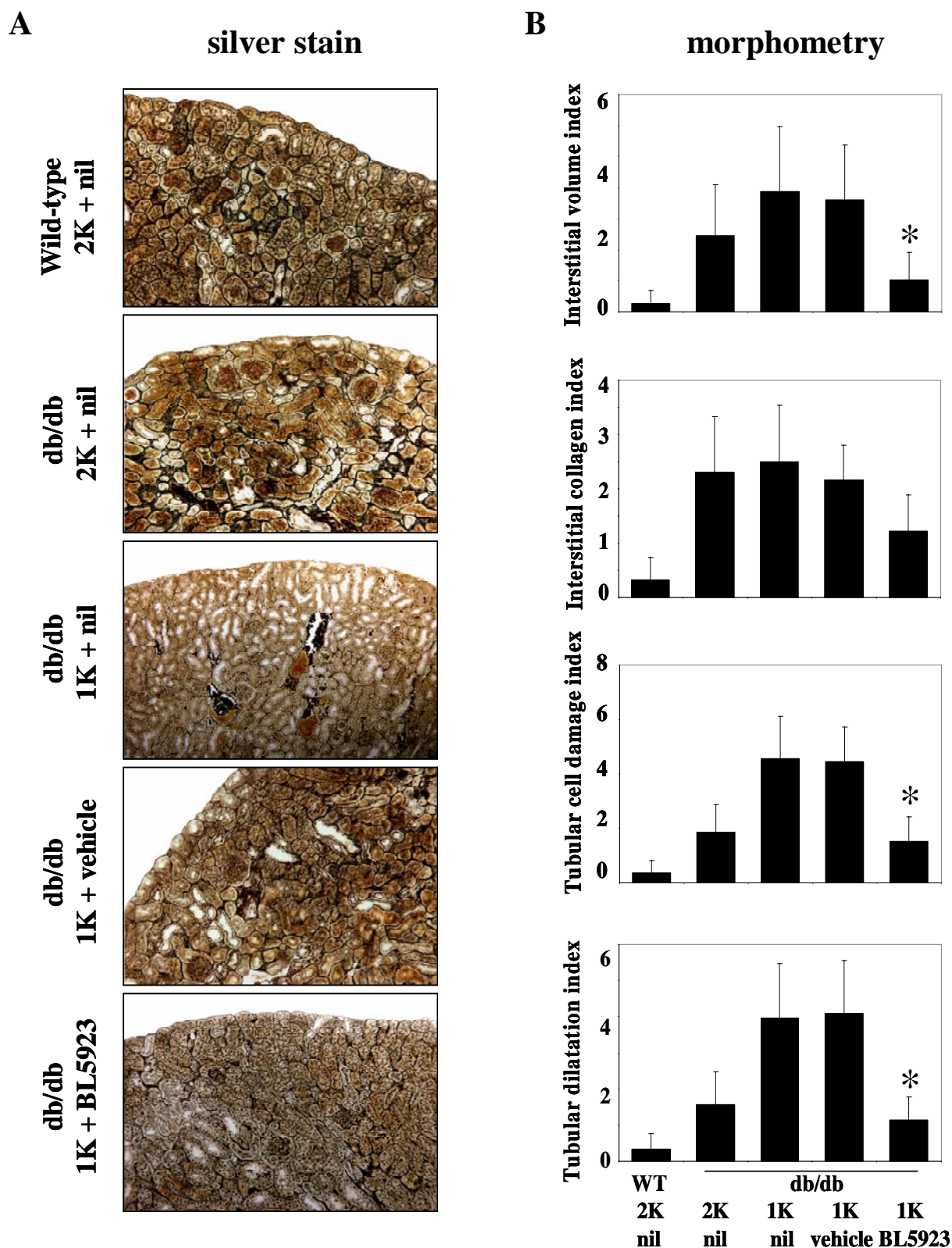


Figure 25. Renal fibrosis in db/db mice.

A. Renal sections from mice of all groups were stained with silver. Images illustrate representative sections of kidneys from the respective groups at 6 months of age (original magnification 100x). **B.** Morphometric analysis of cortical renal sections was performed as described in methods. Values represent means \pm SEM of the respective index in 10 mice in each group. * $p < 0.05$ vs vehicle-treated 1K db/db mice.

4.2.4 CCR1 blockade reduces renal expression of proinflammatory mediators in uninephrectomized db/db mice

Macrophages are a major source of proinflammatory and profibrotic mediators in renal injury. Therefore, we assessed whether the BL5923-induced reduction of interstitial macrophage infiltrates affects the expression levels of proinflammatory mediators in kidneys of 1K db/db mice. We used real-time RT-PCR to quantify the mRNA expression of chemokines and chemokine receptors which drive renal leukocyte recruitment in chronic kidney disease (106). BL5923 reduced mRNA levels of Ccl2, Ccr1, Ccr2, and Ccr5 in kidneys of 6 months old 1K db/db mice (Figure 26). Ccl5 mRNA expression levels were undetectable in kidneys of all groups. In addition, BL5923 reduced renal mRNA expression of Tgf- β 1 and collagen I- α 1, two markers of interstitial fibrosis in mice (Figure 26). These data indicate that blocking CCR1-dependent interstitial macrophage recruitment reduces the renal expression of proinflammatory mediators, i.e. Ccr1, Ccr2, Ccr5, and markers of interstitial fibrosis, e.g. Tgf- β 1 and collagen I- α 1 in 1K db/db mice.

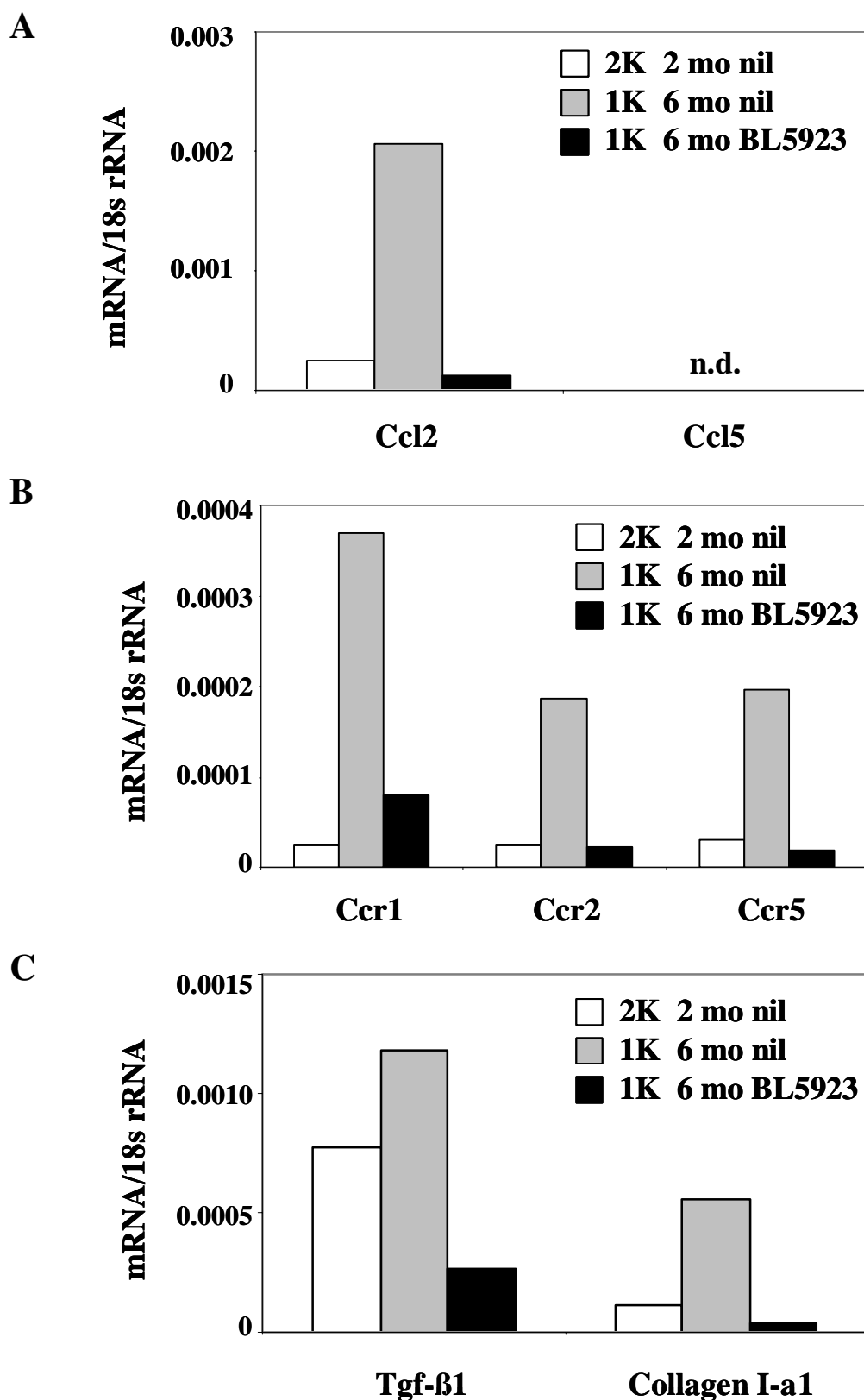


Figure 26. Renal mRNA expression of proinflammatory mediators and markers of fibrosis.

mRNA expression for the CC-chemokines Ccl2 and Ccl5 (A), their respective CC-chemokine receptors Ccr1, Ccr2, and Ccr5 (B), Tgf-β1, and collagen I-α1 (C) was determined by real-time RT-PCR using total renal RNA pooled from 6-10 mice of each group. mRNA levels for each group of mice are expressed per respective 18s rRNA expression.

4.2.5 CCR1 blockade inhibits the proliferation of J774 cells but not of tubular epithelial cells

Our finding that BL5923 reduces the number of proliferating cells in the tubular as well as interstitial compartment raises the question whether these effects are directly mediated via CCR1 on these cells. We used J774 cells, a murine monocyte/macrophage cell line, and a murine tubular epithelial cell line (173) to assess Ccr1 mRNA expression and to study the impact of BL5923 on the proliferation rate of these cells. Ccr1 mRNA was not detectable in cultured tubular epithelial cells, while J774 expressed Ccr1 mRNA at high levels (Figure 27A). The proliferation rate of both cell lines was low within 48 hours in the absence of FCS but markedly increased when FCS was added to the culture dishes (Figure 27B). When BL5923 was added the proliferation rate of Ccr1 positive J774 cells significantly declined. By contrast, BL5923 had no effect on the proliferation rate of Ccr1 negative tubular epithelial cells.

A

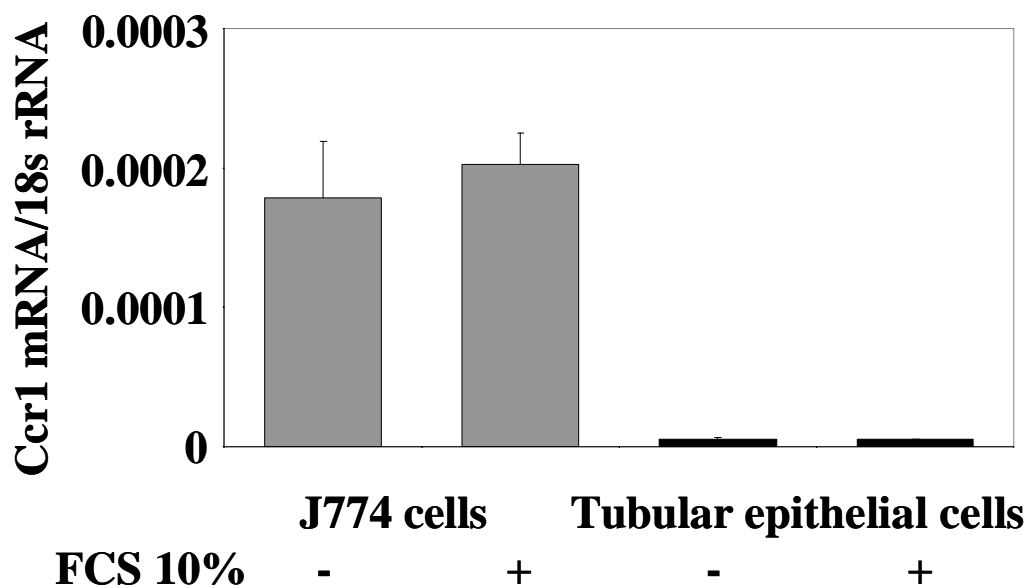


Figure 27. BL5923 and the proliferation of J774 macrophages or tubular epithelial cells.

A. The Ccr1 mRNA expression levels were determined in cultured J774 macrophages and tubular epithelial cells as described in methods. Data are expressed as means \pm SEM of the ratio of Ccr1 mRNA and the respective 18s rRNA level.

B

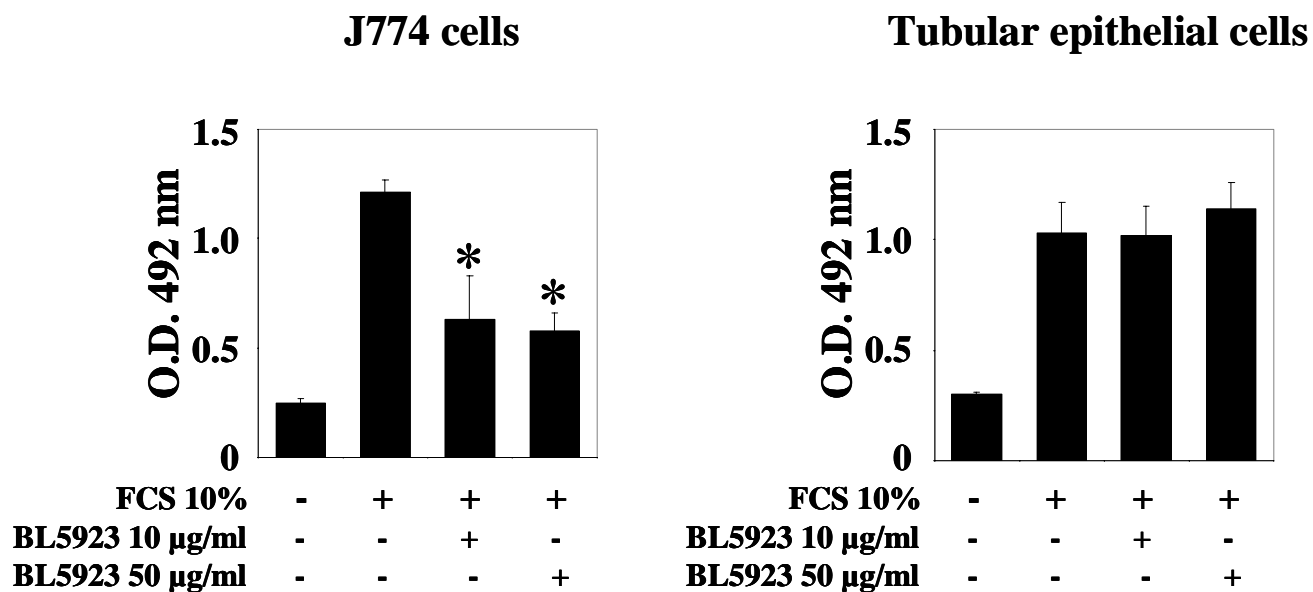


Figure 27. BL5923 and the proliferation of J774 macrophages or tubular epithelial cells.

B. The proliferation of cultured J774 macrophages and tubular epithelial cells was assessed after 72 hours using the CellTiter 96 Proliferation Assay as described in methods. Data are expressed at means \pm SEM of the optical density (O.D.) read at a wavelength of 492 nm. * $p < 0.05$ vs. medium + 10% fetal calf serum (FCS).

5. DISCUSSION

Different types of chemokine receptors are expressed in a restricted manner on specific leukocyte subsets. In the context of CKD, the leukocyte subsets of interest include monocyte/macrophages (97, 179). Alport disease and diabetic nephropathy are associated with interstitial macrophage infiltrates but their contribution to disease progression is unclear. We addressed this question by blockade of interstitial macrophage recruitment with specific CCR1 antagonists in COL4A3-deficient mice, a mouse model for human Alport disease and uninephrectomized db/db mice, an accelerated model for advanced nephropathy of type 2 diabetes, because CCR1 mediates the macrophage recruitment to the renal interstitium.

Effect of CCR1 blockade in COL4A3-deficient mice

COL4A3-deficient mice develop CKD similar to human autosomal recessive Alport syndrome. CCR1 blockade was found to prolong survival in COL4A3-deficient mice. This survival benefit was associated with a reduction of interstitial macrophages, apoptotic tubular cells, and in morphometric indices of tubular atrophy, interstitial fibrosis, and preservation of peritubular capillaries. These data suggest a role for CCR1 for the progression of kidney disease in COL4A3-deficient mice. Macrophages are known to secrete mediators that induce apoptosis of tubular epithelial cells *in vitro* (180). In fact, a set of recent studies provided indirect evidence that interstitial macrophages may account for tubular epithelial cell apoptosis in COL4A3-deficient mice (176, 177). For example, in these mice disease progression is independent to TGF- β -dependent myofibroblast proliferation and interstitial matrix deposition as previously anticipated (177), but rather to macrophage-induced tubular atrophy (181). Our data now provide direct evidence that lower numbers of interstitial macrophages are associated with less apoptotic tubular epithelial cells in kidneys of COL4A3-deficient mice. In addition, increased numbers of proliferating tubular cells in BX471-treated COL4A3-deficient mice suggest that lower numbers of interstitial macrophages support tubular cell regeneration in COL4A3-deficient mice. These mechanisms may also explain our finding that BX471 preserved the loss of peritubular

microvasculature in COL4A3-deficient mice. Loss of peritubular capillaries is a known marker for advanced interstitial injury, and thought to cause ischemia, a stimulus for fibroblast proliferation and production of extracellular matrix (182). The beneficial effects of BX471 treatment on the renal microvasculature of COL4A3-deficient mice may also contribute to our observation that BX471 reduced severe glomerulosclerotic lesions and proteinuria in COL4A3-deficient mice. All these factors should account for prolonged survival seen with CCR1 blockade. However, serum creatinine and BUN levels did not differ between vehicle and BX471-treated mice which is consistent with the moderate effect of BX471 on survival and the high variability of these measures at 9 weeks of age.

Furthermore, we showed a role of CCR1 for leukocyte adhesion to vascular endothelial cells using the technique of intravital microscopy which allowed to study the specific roles of CCR1 during the multiple steps of leukocyte recruitment. Our finding that, CCR1 is required for firm adhesion of leukocytes to activated vascular endothelium *in vivo*, is consistent with previously reported data with human macrophages and T cells in an *in vitro* flow chamber model (105). CCR1 does also contribute to transendothelial leukocyte migration but as lack of CCR1 or CCR1 blockade only partially impaired this process other factors appear to be involved. *In vitro* data from Weber et al. argue for CCR5 being one of these factors as BX471 in combination with a neutralizing antibody against CCR5 completely blocked transendothelial migration of human monocytes and T cells *in vitro* (141). Organ or compartment specificity of single chemokines or CCRs is a common finding in chemokine biology. Therefore, we have to consider the possibility, that our intravital microscopical data derived from the M. cremaster do not allow a conclusion about the role of CCR1 for leukocyte recruitment in mouse kidneys. We have addressed this question by injecting fluorescently-labeled macrophages into COL4A3-deficient mice. BX471 blocked the recruitment of macrophages into the renal interstitium of these mice suggesting that, reduced numbers of renal macrophages observed with BX471 treatment is caused by the mechanisms identified by intravital microscopy.

Activated resident and infiltrating macrophages are a major source of renal chemokine secretion (103), which adds on the chemokines expressed by intrinsic renal cells (reviewed by ref. 98). By this mechanism renal macrophages support further leukocyte recruitment and renal inflammation (90). In fact, the CC-chemokine CCL5 can activate renal macrophages in a way that kidney disease progresses even independent of the total number of renal macrophages (104). We therefore questioned whether CCR1 does also contribute to the activation state of macrophages. We found that a combination of TNF- α , IFN- γ , and CCL3 increased the production of CCL5. This mimics the *in vivo* situation of an inflammatory

microenvironment where CC-chemokines occur in concert with other proinflammatory cytokines. As BX471 completely blocked the CCL3-induced production of CCL5 in vitro we relate this effect exclusively to CCR1 and not to other CCRs that can bind CCL3. These data give rise to the hypothesis that CCR1 blockade can modulate the activation state of renal macrophages that are already present in the diseased kidney. This would occur in addition to the impaired recruitment of CCL5 producing cells which was demonstrated by decreased numbers of CCL5 positive cells in kidneys of BX471-treated mice.

Effect of CCR1 blockade in type 2 diabetic db/db mice

Available rodent models of diabetic nephropathy are frequently used to study the early glomerular changes of diabetic nephropathy (183). However, rodents usually do not develop advanced interstitial lesions as they occur in late stages of human diabetic nephropathy (184). Experimentally, in our study uninephrectomy was used to enhance the development of advanced diabetic nephropathy (185).

CCR1 blockade reduced interstitial macrophage infiltrates in uninephrectomized (1K) db/db mice most likely by interfering with macrophage adhesion to activated endothelial cells of peritubular capillaries in the renal interstitium. BL5923, the orally available CCR1 antagonist used in our study, showed comparable activity in 1K db/db mice in blocking the recruitment of fluorescently labeled macrophages into the renal interstitial compartment of 1K db/db mice. Adhesion is an early and critical event in the multistep process of leukocyte evasion from the circulation (136). Thus, consistent with the low numbers of fluorescently labeled intrarenal macrophages in BL5923-treated 1K db/db mice, labeled macrophages could not retain at activated peritubular capillaries but were carried away with the peritubular blood flow. In addition, we found that CCR1 blockade reduces the proliferation of murine monocyte/macrophages in the presence of serum. This may represent another mechanism by which BL5923 reduced the number of interstitial macrophages in db/db mice. In fact, the number of interstitial proliferating cells was found to be reduced in BL5923-treated db/db mice. Furthermore, we found that a single dose of the CCR1 antagonist reduces the white blood count in db/db mice. Chemokine receptors do not only mediate leukocyte recruitment to peripheral tissues but are also involved in mobilizing monocytes from the bone marrow into the intravascular compartment (186). The role of CCR1 in this process needs to be explored in future studies. Together, CCR1 blockade is modulating the number of renal

interstitial macrophages by multiple mechanisms, e.g. lowering the number of white blood cells in the intravascular compartment, blocking extravasation into the renal interstitial compartment, and inhibiting macrophage proliferation.

Selectively manipulating the number of interstitial macrophages in 1K db/db mice should allow to conclude on their functional role for the progression of diabetic nephropathy. Most interestingly, reduced numbers of interstitial macrophages were associated with improved peritubular vasculature and the extent of tubulointerstitial injury and interstitial fibrosis, all important predictors of disease progression in diabetic nephropathy (187, 188). These data indicate that the presence of macrophages in diabetic nephropathy contributes to renal injury, a mechanism that may be referred to as “inflammation” (83, 189, 190). Inflammatory or antiinflammatory phenotypes of renal macrophages are difficult to determine by immunostaining but best by their function *in vivo* (191). For example, interstitial macrophages produce large amounts of proinflammatory mediators, i.e. cytokines and chemokines, which add to the mediators produced by renal cells, i.e. in a positive amplification loop (162, 105). This observation made in non-diabetic types of kidney disease is likely also to apply to diabetic nephropathy in humans, because 1. Interstitial macrophage infiltrates are common in diabetic nephropathy (192) and 2. Patients with diabetic nephropathy excrete high levels of CC-chemokines into the urine. For example, the urinary excretion of CCL2 (formerly named as monocyte chemoattractant protein-1) indicates intrarenal inflammation (193, 137). Chemokine expression involves activation of protein kinase C in renal cells as well as immune cells infiltrates. Therapeutic intervention targeting protein kinase C can disrupt this positive amplification loop by reducing renal chemokine expression, subsequent recruitment of immune cells, and tubular injury in experimental and human diabetic nephropathy (194, 195). However, protein kinase C blockade cannot address the role of single chemokine ligands in the inflammatory lesion in diabetic nephropathy. Chow, et al. addressed the role of CCL2 in the pathogenesis of experimental diabetic nephropathy by inducing type I diabetes in CCL2-deficient mice (196). CCL2-deficient mice were largely protected from renal injury after streptozotocin injection which was associated with markedly reduced macrophage infiltrates in the glomerular and the tubulointerstitial compartments. While this study supports an important role of CCL2 in the pathogenesis of experimental diabetic nephropathy the role of interstitial macrophages for progression of diabetic nephropathy remains unclear. The selective recruitment of a certain immune cell subset can better be achieved by delayed blockade of a single chemokine receptor that mediates the recruitment of this cell type to the compartment of interest, i.e. CCR1 for the recruitment of macrophages to the renal interstitium. Our data indicate that interstitial macrophages are a

major source and trigger of intrarenal cytokine and chemokine production in experimental diabetic nephropathy. Blocking CCR1-dependent interstitial macrophage recruitment reduced the mRNA expression of the CC-chemokine CCL2 in kidneys of 1K db/db mice, for which a crucial role in the progression of DN was recently demonstrated (193, 196). As a consequence of reduced intrarenal chemokine signaling and CCR1 blockade subsequent leukocyte recruitment was impaired in association with reduced renal mRNA expression of the proinflammatory chemokine receptors Ccr1, -2, and -5, factors not expressed by non-immune renal cells *in vivo*.

Blocking CCR1-dependent interstitial macrophage recruitment was also associated with less interstitial fibrosis. This was indicated by less renal Tgf- β 1 and collagen I- α 1 mRNA expression as well as interstitial collagen deposits in BL5923-treated 1K db/db mice. Direct effects of BL5923 on intrinsic renal cells in the renal tubulointerstitium are unlikely. We did not observe detect direct effects of BL5923 on tubular epithelial cells *in vitro* as these cells lack CCR1 expression.

Together, these data identify a previously unrecognized role for interstitial macrophages for tubulointerstitial injury, loss of peritubular microvasculature, interstitial inflammation and fibrosis in type 2 diabetic db/db mice.

Summary and future perspectives

CCR1 antagonism with specific small-molecule antagonists can effectively prevent recruitment of macrophages into the renal interstitial compartment. CCR1 blockade proved to be effective in COL4A3-deficient mice, a mouse model for human Alport disease and uninephrectomized db/db mice, an accelerated model for advanced nephropathy of type 2 diabetes. Remarkably, CCR1 blockade was even effective when treatment was initiated after the disease process was established. It remains to be evaluated whether CCR1 blockade has additive effects to current treatments of CKD. However, our data show that glomerular pathology and proteinuria remain almost unaffected by CCR1 blockade. Thus, chemokine receptors other than CCR1 (e.g. CCR2) may mediate to glomerular leukocyte infiltration. Based on the experimental data available, we propose that the therapeutic effects of CCR1 antagonists –in combination with established therapies – should be evaluated in an attempt to slow down the progression of human chronic kidney diseases, which are associated with interstitial macrophage infiltrates.

6. REFERENCES

1. Zandi-Nejad K, Brenner BM: Primary and secondary prevention of chronic kidney disease. *J Hypertens* 10:1771-1776, 2005
2. Vielhauer V, Schlöndorff D, Anders HJ: Disease mechanisms of glomerulonephritis: chemokines and chemokine receptor. *Drug Discovery Today: Disease Mechanisms* 1 (1):83-90, 2004
3. US Renal Data System. Experts from the United States Renal Data System 2004 Annual Data Report: Atlas of End-Stage Renal Disease in the United States. *Am J Kidney Dis* 45, 2005
4. Go AS, Chertow GM, Fan D, McCulloch CD, Hsu CY: Chronic kidney disease and the risk of death, cardiovascular events and hospitalization. *N Engl J Med* 351:1296-1305, 2005
5. Pereira AA, Weiner DE, Scott T, Sarnak MJ: Cognitive function in dialysis patients. *Am J Kidney Dis* 45:448-462, 2005
6. Monk RD, Bennet DA: Reno-cerebrovascular disease? The incognito kidney in cognition and stroke. *Neurology* 67:196-198, 2006
7. K/DOQI clinical practice guidelines for chronic kidney disease: evaluation, classification, and stratification, http://www.kidney.org/professionals/kdoqi/guidelines_ckd/toc.htm/
8. Levey AS, Eckardt KU, Tsukamoto Y, Levin A, Coresh J, Rossert J, Zeeuw D, Hostetter TH, Lameire N, Eknoyan G: Definition and classification of chronic kidney disease: a position statement from Kidney Disease: Improving Global Outcomes (KDIGO). *Kidney Int* 67:2089-100, 2005
9. MacGregor MS, Boag DE, Innes A: Chronic kidney disease: evolving strategies for detection and management of impaired renal function. *QJM* 99(6):365-375, 2006
10. Alport AC: Hereditary familial congenital haemorrhagic nephritis. *BMJ* 1:504-506, 1927
11. Kashtan CE, Gubler MC, Sisson-Ross S, Mauer M: Chronology of renal scarring in males with Alport syndrome. *Pediatr Nephrol* 12:269-274, 1998
12. Floege J, Kunter U, Weber M, Gross O: Bone marrow transplantation rescues Alport mice. *Nephrol Dial Transplant* 21(10):2721-2723, 2006
13. Sohar E: Renal disease, inner ear deafness and ocular changes. *Arch Intern Med* 97:627-630, 1956
14. Perrin D, Jungers P, Grunfeld JP, Delons S, Noël LH, Zenatti C: Perimacular changes in Alport's syndrome. *Clin Nephrol* 13:163-167, 1980

15. Cochat P, Guibaud P, Torres R, Roussel B, Guarner V, Larbre F: Diffuse leiomyomatosis in Alport syndrome. *J Pediatr* 113:339–343, 1998
16. Garcia-Torres R, Orozco L: Alport-leiomyomatosis syndrome: An update. *Am J Kidney Dis* 22:641–648, 1993
17. Epstein CJ, Sahud MA, Piel CF, Goodman JR, Bernafeld MR, Kushner JH, Ablin AR: Hereditary macrothrombocytopenia, nephritis and deafness. *Am J Med* 52:299–310, 1972
18. Peterson LC, Rao VK, Crosson JT, White JG: Fechtner syndrome— A variant of Alport's syndrome with leukocyte inclusions and macrothrombocytopenia. *Blood* 65:397–406, 1985
19. Atkin CL, Hasstedt SJ, Menlove L, Cannon L, Kirschner N, Schwartz C, Nguyen K, Skolnick MH: Mapping of Alport syndrome to the long arm of the X chromosome. *Am J Hum Genet* 42:249–255, 1988
20. Hasstedt SJ, Atkin CL, San Juan AC: Genetic heterogeneity among kindreds with Alport syndrome. *Am J Hum Genet* 38:940–953, 1986
21. Flinter FA, Cameron JS, Chantler C, Houston I, Bobrow M: Genetics of classic Alport syndrome. *Lancet* 2:1005–1007, 1988
22. Cameron JS: Recurrent primary disease and de novo nephritis following renal transplantation. *Pediatr Nephrol* 5:412–421, 1991
23. Kleppel MM, Kashtan C, Santi PA, Wieslander J, Michael AF: Distribution of familial nephritis antigen in normal tissue and renal basement membranes of patients with homozygous and heterozygous Alport familial nephritis. *Lab Invest* 61:278–289, 1989
24. Savage COS, Noel LH, Crutcher E, Price SRG, Grunfeld JP, Lockwood CM: Hereditary nephritis: Immunoblotting studies of the glomerular basement membrane. *Lab Invest* 60:613–618, 1989
25. Kleppel MM, Kashtan CE, Butkowski RJ, Fish AJ, Michael AF: Alport familial nephritis: Absence of 28 kilodalton non-collagenous monomers of type IV collagen in glomerular basement membrane. *J Clin Invest* 80:263–266, 1987
26. Thorner P, Baumal R, Eddy A, Marrano PM: A study by immunofluorescence of the NC1 domain of collagen type IV in glomerular basement membranes of two patients with hereditary nephritis. *Virchow Arch A Pathol Anat* 416:205–212, 1990
27. Van den Heuvel LPWJ, Schröder CH, Savage COS, Menzel D, Assmann KJM, Monnens LAH, Veerkamp JH: The development of anti-glomerular basement membrane nephritis in two children with Alport's syndrome: Characterization of the antibody target. *Pediatr Nephrol* 3:406–413, 1989
28. Kashtan CE, Butkowski RJ, Kleppel MM, Roy First M, Michael AF: Posttransplant anti-glomerular basement membrane nephritis in related males with Alport syndrome. *J Lab Clin Med* 116:508–515, 1990
29. Hudson BG, Tryggvason K, Sundaramoorthy M, Neilson EG: Alport's syndrome, Goodpasture's syndrome, and type IV collagen. *N Engl J Med* 348:2543–2556, 2003

30. Boutaud A, Borza DB, Bondar O, Gunwar S, Netzer KO, Singh N, Ninomiya Y, Sado Y, Noelken ME, Hudson BG: Type IV collagen of the glomerular basement membrane: evidence that the chain specificity of network assembly is encoded by the noncollagenous NC1 domains. *J Biol Chem* 275:30716-24, 2000
31. Borza DB, Bondar O, Ninomiya Y, Sado Y, Naito I, Todd P, Hudson BG: The NC1 domain of collagen IV encodes a novel network composed of the alpha 1, alpha 2, alpha 5, and alpha 6 chains in smooth muscle basement membranes. *J Biol Chem* 276:28532-40, 2001
32. Borza DB, Bondar O, Todd P, Sundaramoorthy M, Sado Y, Ninomiya Y, Hudson BG: Quaternary organization of the Goodpasture autoantigen, the $\alpha 3(\text{IV})$ collagen chain: sequestration of two cryptic autoepitopes by intraprotomer interactions with the $\alpha 4$ and $\alpha 5$ NC1 domains. *J Biol Chem* 277: 40075-83, 2002
33. Timpl R, Wiedemann H, van Delden V, Furthmayr H, Kuhn K: A network model for the organization of type IV collagen molecules in basement membranes. *Eur J Biochem* 120:203-11, 1981
34. Sundaramoorthy M, Meiyappan M, Todd P, Hudson BG: Crystal structure of NC1 domains: structural basis for type IV collagen assembly in basement membranes. *J Biol Chem* 277:31142-53, 2002
35. Than ME, Henrich S, Huber R, Ries A, Mann K, Kuhn K, Timpl R, Bourenkov GP, Bartunik HD, Bode W: The 1.9-Å crystal structure of the noncollagenous (NC1) domain of human placenta collagen IV shows stabilization via a novel type of covalent Met-Lys cross-link. *Proc Natl Acad Sci U S A* 99:6607-12, 2002
36. Langeveld JP, Noelken ME, Hard K, Todd P, Vliegenthart JF, Rouse J, Hudson BG: Bovine glomerular basement membrane: location and structure of the asparagine-linked oligosaccharide units and their potential role in the assembly of 7 S collagen IV tetramer. *J Biol Chem* 266:2622-31, 1991
37. Nayak BR, Spiro RG: Localization and structure of the asparagine-linked oligosaccharides of type IV collagen from glomerular basement membrane and lens capsule. *J Biol Chem* 266:13978-87, 1991
38. Kalluri R, Shield CF, Todd P, Hudson BG, Neilson EG: Isoform switching of type IV collagen is developmentally arrested in X-linked Alport syndrome leading to increased susceptibility of renal basement membranes to endoproteolysis. *J Clin Invest* 99:2470-8, 1997
39. Guo XD, Johnson JJ, Kramer JM: Embryonic lethality caused by mutations in basement membrane collagen of *C. elegans*. *Nature* 349:707-9, 1991
40. Zhang X, Hudson BG, Sarras MP Jr. Hydra cell aggregate development is blocked by selective fragments of fibronectin and type IV collagen. *Dev Biol* 64:10-23, 1994
41. Netzer KO, Suzuki K, Itoh Y, Hudson BG, Khalifah RG: Comparative analysis of the noncollagenous NC1 domain of type IV collagen: identification of structural features important for assembly, function, and pathogenesis. *Protein Sci* 7:1340-51, 1998

42. Fowler SJ, Jose S, Zhang X, Deutzmann R, Sarras MP Jr, Boot-Handford RP: Characterization of hydra type IV collagen: type IV collagen is essential for head regeneration and its expression is up-regulated upon exposure to glucose. *J Biol Chem* 275: 39589-99, 2000
43. Kalluri R, Gattone VH II, Hudson BG: Identification and localization of type IV collagen chains in the inner ear cochlea. *Connect Tissue Res* 37:143-50, 1998
44. Cosgrove D, Samuelson G, Meehan DT, Miller C, McGee J, Walsh EJ, Sigel M: Ultrastructural, physiological, and molecular defects in the inner ear of a geneknockout mouse model for autosomal Alport syndrome. *Hear Res* 121:84-98, 1998
45. Yoshioka K, Hino S, Takemura T, Maki S, Wieslander J, Takekoshi Y, Makino H, Kagawa M, Sado Y, Kashtan CE: Type IV collagen $\alpha 5$ chain. Normal distribution and abnormalities in X-linked Alport syndrome revealed by monoclonal antibody. *Am J Pathol* 144:986-996, 1994
46. Ninomiya Y, Kagawa M, Iyama K-I, Naito I, Kishoro Y, Seyer JM, Sugimoto M, Oohashi T, Sado Y: Differential expression of two basement membrane collagen genes, COL4A6 and COL4A5, demonstrated by immunofluorescence staining using peptide-specific monoclonal antibodies. *J Cell Biol* 130:1219-1229, 1995
47. Brunner HG, Schröder CH, van Bennekom C, Lambermon E, Tuerlings J, Menzel D, Olbing H, Monnens LAH, Wieringa B, Ropers HH: Localization of the gene for X-linked Alport's syndrome. *Kidney Int* 34:507-510, 1988
48. Flinter FA, Abbs S, Bobrow M: Localization of the gene for classic Alport syndrome. *Genomics* 4:335-338, 1989
49. Hostikka SL, Eddy RL, Byers MG, Höyhtya M, Shows TB, Tryggvason K: Identification of a distinct type IV collagen α chain with restricted kidney distribution and assignment to the locus of the X chromosome-linked Alport syndrome. *Proc Natl Acad Sci USA* 87:1606-1610, 1990
50. Chan B, Antignac C, Gubler MC, Deschênes G, Mariyama M, Mochizuki M, Reeders ST: A new locus for Alport syndrome: Linkage of autosomal recessive Alport syndrome to the gene encoding the $\alpha 3$ chain of type IV collagen. In Proceedings of the Second International Workshop on Alport Syndrome, New Haven, p 3, 1993
51. Mochizuki T, Lemmink HH, Mariyama M, Antignac C, Gubler M-C, Pirson Y, Verellen-Dumoulin C, Schröder CH, Smeets HJM, Reeders ST: Identification of mutations in the $\alpha 3(\text{IV})$ and $\alpha 4(\text{IV})$ collagen genes in autosomal recessive Alport syndrome. *Nature Genet* 8:77-82, 1994
52. Lemmink HH, Nillesen WN, Mochizuki T, Schröder CH, Brunner HG, van Oost BA, Monnens LAH, Smeets HJM: Benign familial hematuria due to mutation of the type IV collagen $\alpha 4$ gene. *J Clin Invest* 98 (5):1114-1118, 1996
53. Kashtan CE: Renal transplantation in patients with Alport syndrome. *Pediatr Transplantation* 10:651-657, 2006

-
54. Kashtan CE: Animal models of Alport syndrome. *Nephrol Dial Transplant* 17:1359-1361, 2002
55. Report of the Expert Committee on the Diagnosis and Classification of Diabetes Mellitus. *Diabetes Care* 21(1):S5-19, 1998
56. Uusitupa MI, Niskanen LK, Siitonen O, Voutilainen E, Pyorala K: Ten-year cardiovascular mortality in relation to risk factors and abnormalities in lipoprotein composition in type 2 (non-insulin-dependent) diabetic and non-diabetic subjects. *Diabetologia* 36:1175-84, 1993
57. Amos A, McCarty D, Zimmet P: The rising global burden of diabetes and its complications: estimates and projections to the year 2010. *Diabetic Med* 14: S1-S85, 1997
58. King H, Aubert R, Herman W: Global burden of diabetes, 1995-2025. Prevalence, numerical estimates and projections. *Diabetes Care* 21: 1414-1431, 1998
59. Zimmet P: Diabetes epidemiology as a trigger to diabetes research. *Diabetologia* 42:499-518, 1999
60. Zimmet P: Globalization, coca-colonization and the chronic disease epidemic: can the doomsday scenario be averted? *J Intern Med* 247: 301-310, 2000
61. American Diabetes Association. Economic consequences of diabetes mellitus in the U.S. in 1997. *Diabetes Care* 21: 296-309, 1998
62. Ritz E, Tarnag DC: Renal disease in type 2 diabetes. *Nephrol Dial Transplant* 16 (5):11-18, 2001
63. Remuzzi G, Schieppati A, Ruggenenti P: Nephropathy in patients with Type 2 diabetes. *N Eng J Med* 346:1145-1151, 2002
64. Mason RM, Wahab NA: Extracellular matrix metabolism in diabetic nephropathy. *J Am Soc Nephrol* 14, 1358-1373, 2003
65. Steffes MW, Osterby R, Chavers B, Mauer SM: Mesangial expansion as a central mechanism for loss of kidney function in diabetic patients. *Diabetologia* 36:1064-1070, 1993
66. Gilbert RE, Cooper ME: The tubulointerstitium in progressive diabetic kidney disease: more than an aftermath of glomerular injury? *Kidney Int* 56:1627-1637, 1999
67. Moriya T, Tanaka K, Moriya R: Glomerular structural changes and structural-functional relationships at early stage of diabetic nephropathy in Japanese Type 2 diabetic patients. *Med Electron Microsc* 32:115-122, 2000
68. Ramage IJ, Howatson AG, McColl JH, Maxwell H, Murphy AV, Beattie TJ: Glomerular basement membrane thickness in children: a stereological assessment. *Kidney Int* 62:895-900, 2002

69. Osterby R, Gundersen HJG: Fast accumulation of basement membrane material and the rate of morphological changes in acute experimental diabetic glomerular hypertrophy. *Diabetologia* 18:493–500, 1980
70. Hirose K, Osterby R, Nozawa M, Gundersen HJ: Development of glomerular lesion in experimental long-term diabetes in the rat. *Kidney Int* 21, 689–695, 1982
71. Nyengaard JR, Rasch R: The impact of experimental diabetes mellitus in rats on capillary number and sizes. *Diabetologia* 36:189–194, 1993
72. Yoshida H, Fogo A, Ichikawa I: Glomerular hemodynamic changes vs. hypertrophy in experimental glomerular sclerosis. *Kidney Int* 35, 654–660, 1989
73. Doi T, Striker LJ, Gibson CG, Agodoa LYC, Brinster RL, Striker GE: Glomerular lesions in mice transgenic for growth hormone and insulin-like growth factor-1. *Am J Pathol* 137:541–552, 1990
74. Fogo A, Hawkins EP, Berry PL, Glick AD, Chiang ML, MacDonell RC Jr, Ichikawa I: Glomerular hypertrophy in minimal change disease predicts subsequent progression to focal glomerular sclerosis. *Kidney Int* 38:115–123, 1990
75. McKay K, Striker LJ, Pinkert CA, Brinster RL, Striker GE: Relationship of glomerular hypertrophy and sclerosis: studies in SV40 transgenic mice. *Kidney Int* 37:741–748, 1990
76. Osterby R: Glomerular structural changes in Type 1 (insulin-dependent) diabetes mellitus: causes, consequences, and prevention. *Diabetologia* 35:803–812, 1992
77. Nagata M, Scharer K, Kriz W: Glomerular damage after uninephrectomy in young rats. Hypertrophy and distortion of capillary architecture. *Kidney Int* 42:136–147, 1992
78. Cahill MM, Ryan GB, Bertram JF: Biphasic glomerular hypertrophy in rats administered puromycin aminonucleoside. *Kidney Int* 50:768–775, 1996
79. Guo M, Ricardo SD, Deane JA, Shi M, Cullen-McEwen L, Bertram JF: A stereological study of the renal glomerular vasculature in the *db/db* mouse model of diabetic nephropathy. *J Anat* 207:813–821, 2005
80. Andersen AR, Christiansen JS, Andersen JK, Kreiner S, Deckert T: Diabetic nephropathy in type 1 (insulin-dependent) diabetes: An epidemiological study. *Diabetologia* 25:496–501, 1983
81. Rossing P, Rossing K, Jacobsen P, Parving HH: Unchanged incidence of diabetic nephropathy in IDDM patients. *Diabetes* 44:739–743, 1995
82. Bakris GL, Williams M, Dworkin L, Elliott WJ, Epstein M, Toto R, Tuttle K, Douglas J, Hsueh W, Sowers J: Preserving renal function in adults with hypertension and diabetes: A consensus approach. National Kidney Foundation Hypertension and Diabetes Executive Committees Working Group. *Am J Kidney Dis* 36:646–661, 2000
83. Galkina E, Ley K: Leukocyte Recruitment and Vascular Injury in Diabetic Nephropathy. *J Am Soc Nephrol* 17:368–377, 2006

84. Furuta T, Saito T, Ootaka T, Soma J, Obara K, Abe K, Yoshinaga K: The role of macrophages in diabetic glomerulosclerosis. *Am J Kidney Dis* 21:480-485, 1993
85. Lavaud S, Michel O, Sassy-Prigent C, Heudes D, Bazin R, Bariety J, Chevalier J: Early influx of glomerular macrophages precedes glomerulosclerosis in the obese Zucker rat model. *J Am Soc Nephrol* 7:2604-2615, 1996
86. Coimbra TM, Janssen U, Grone HJ, Ostendorf T, Kunter U, Schmidt H, Brabant G, Floege J: Early events leading to renal injury in obese Zucker (fatty) rats with type II diabetes. *Kidney Int* 57:167-182, 2000
87. Phillips AO, Baboolal K, Riley S, Grone H, Janssen U, Steadman R, Williams J, Floege J: Association of prolonged hyperglycemia with glomerular hypertrophy and renal basement membrane thickening in the Goto Kakizaki model of non-insulin dependent diabetes mellitus. *Am J Kidney Dis* 37:400-410, 2001
88. Young BA, Johnson RJ, Alpers CE, Eng E, Gordon K, Floege J, Couser WG, Seidel K: Cellular events in the evolution of experimental diabetic nephropathy. *Kidney Int* 47:935-944, 1995
89. Sassy-Prigent C, Heudes D, Mandet C, Belair MF, Michel O, Perdereau B, Bariety J, Bruneval P: Early glomerular macrophage recruitment in streptozocin-induced diabetic rats. *Diabetes* 49:466-475, 2000
90. Nolic-Paterson DJ, Atkins RC: The role of macrophages in glomerulonephritis. *Nephrol Dial Transplant* 16 (5):3-7, 2001
91. Chow F, Ozols E, Nolic-Paterson DJ, Atkins RC, and Tesch GH: Macrophages in mouse type 2 diabetic nephropathy: Correlation with diabetic state and progressive renal injury. *Kidney Int* 65:116-128, 2004
92. Hummel KP, Dickie MM, Coleman DL: Diabetes, a new mutation in the mouse. *Science* 153:1127-1128, 1966
93. Chen, H, Charlat O, Tartaglia LA, Woolf EA, Weng X, Ellis SJ, Lakey ND, Culpepper J, Moore KJ, Breitbart RE, Duyk GM, Tepper RI, and Morganstern JP: Evidence that the diabetes gene encodes the leptin receptor: identification of a mutation in the leptin receptor gene in *db/db* mice. *Cell* 84:491-495, 1996
94. Lee GH, Proenca R, Montez JM, Carroll KM, Darvishzadah JG, Lee GI, Freidman JM: Abnormal splicing of the leptin receptor in diabetic mice. *Nature* 379:632-635, 1996
95. Becker GJ, Hewitson TD: The role of tubulointerstitial injury in chronic renal failure. *Curr Opin Nephrol Hypertens* 10:133-138, 2000
96. Zeisberg M, Strutz F, Müller GA: Role of fibroblast activation in inducing interstitial fibrosis. *J Nephrol* 3:111-120, 2000
97. Eddy AA: Molecular basis of renal fibrosis. *Pediatr Nephrol* 15:290-301, 2000

98. Segerer S, Nelson PJ, Schlöndorff D: Chemokines, chemokine receptors, and renal disease: from basic science to pathophysiologic and therapeutic studies. *J Am Soc Nephrol* 11:152–176, 2000
99. Tsuboi N, Yoshikai Y, Matsuo S, Kikuchi T, Iwami K, Nagai Y, Takeuchi O, Akira S, Matsuguchi T: Roles of toll-like receptors in C-C chemokine production by renal tubular epithelial cells. *J Immunol* 169:2026–2033, 2002
100. Wang Y, Rangan GK, Tay YC, Wang Y, Harris DC: Induction of monocyte chemoattractant protein-1 by albumin is mediated by nuclear factor- κ B in proximal tubule cells. *J Am Soc Nephrol* 10:1204–1213, 1999
101. Zoja C, Donadelli R, Colleoni S, Figliuzzi M, Bonazzola S, Morigi M, Remuzzi G: Protein overload stimulates RANTES production by proximal tubular cells depending on NF- κ B activation. *Kidney Int* 53:1608–1615, 1998
102. Umekawa T, Chegini N, Khan SR: Increased expression of monocyte chemoattractant protein-1 by renal epithelial cells in culture on exposure to calcium oxalate, phosphate and uric acid crystals. *Nephrol Dial Transplant* 18:664–669, 2003
103. Anders HJ, Frink M, Linde Y, Banas B, Wornle M, Cohen CD, Vielhauer V, Nelson PJ, Grone HJ, Schlöndorff D: CC chemokine ligand 5/RANTES chemokine antagonists aggravate glomerulonephritis despite reduction of glomerular leukocyte infiltration. *J Immunol* 170:5658–5666, 2003
104. Vielhauer V, Eis V, Schlöndorff D, Anders HJ: Identifying chemokines as therapeutic targets in renal disease: lessons from antagonist studies and knockout mice. *Kidney Blood Press Res* 27:226–238, 2004
105. Haberstroh U, Pocock J, Gomez-Guerrero C, Helmchen U, Hamann A, Gutierrez-Ramos JC, Stahl RA, Thaiss F: Expression of the chemokines MCP-1/CCL2 and RANTES/CCL5 is differentially regulated by infiltrating inflammatory cells. *Kidney Int* 62:1264–1276, 2002
106. Anders HJ, Vielhauer V, Schlöndorff D: Chemokines and chemokine receptors are involved in the resolution or progression of renal disease. *Kidney Int* 63:401–415, 2003
107. Segerer S, Regele H, Mack M, Kain R, Cartron JP, Colin Y, Kerjaschki D, Schlöndorff D: The Duffy antigen receptor for chemokines is upregulated during acute renal transplant rejection and crescentic glomerulonephritis. *Kidney Int* 58:1546–1556, 2000
108. Liu ZH, Chen SF, Zhou H, Chen HP, Li LS: Glomerular expression of C-C chemokines in different types of human crescentic glomerulonephritis. *Nephrol Dial Transplant* 18:1526–1534, 2003
109. Cockwell P, Chakravorty SJ, Girdlestone J, Savage CO: Fractalkine expression in human renal inflammation. *J Pathol* 196:85–90, 2002
110. Furuichi K, Wada T, Sakai N, Iwata Y, Yoshimoto K, Shimizu M, Kobayashi K, Takasawa K, Kida H, Takeda SI, Mukaida N, Matsushima K, Yokoyama H: Distinct expression of CCR1 and CCR5 in glomerular and interstitial lesions of human glomerular diseases. *Am J Nephrol* 20:291–299, 2000

111. Anders HJ, Vielhauer V, Kretzler M, Cohen CD, Segerer S, Luckow B, Weller L, Grone HJ, Schlöndorff D: Chemokine and chemokine receptor expression during initiation and resolution of immune complex glomerulonephritis. *J Am Soc Nephrol* 12:919–931, 2001
112. Akira S, Hemmi H: Recognition of pathogen associated molecular patterns by TLR family. *Immunol Lett* 85:85–95, 2003
113. Anders HJ, Banas B, Linde Y, Weller L, Cohen CD, Kretzler M, Martin S, Vielhauer V, Schlöndorff D, Grone HJ: Bacterial CpGDNA aggravates immune complex glomerulonephritis: role of TLR9-mediated expression of chemokines and chemokine receptors. *J Am Soc Nephrol* 14:317–326, 2003
114. Vielhauer V, Anders HJ, Mack M, Cihak J, Strutz F, Stangassinger M, Luckow B, Grone HJ, Schlöndorff D: Obstructive nephropathy in the mouse: Progressive fibrosis correlates with tubulointerstitial chemokine expression and accumulation of CC chemokine receptor 2 and 5 positive leukocytes. *J Am Soc Nephrol* 12:1173–1187, 2001
115. Segerer S, Mack M, Regele H, Kerjaschki D, Schlöndorff D: Expression of the C–C chemokine receptor 5 in human kidney diseases. *Kidney Int* 56:52–64, 1999
116. Daha MR: Mechanisms of mesangial injury in glomerular diseases. *J Nephrol* 13(3): 89–95, 2000
117. Strutz F, Zeisberg M, Ziyadeh FN, Yang CQ, Kalluri R, Muller GA, Neilson EG: Role of basic fibroblast growth factor-2 in epithelial-mesenchymal transformation. *Kidney Int* 61:1714–1728, 2002
118. Bucala R, Spiegel LA, Chesney J, Hogan M, Cerami A: Circulating fibrocytes define a new leukocyte subpopulation that mediates tissue repair. *Mol Med* 1:71–81, 1994
119. Abbate M, Zoja C, Corna D, Capitanio M, Bertani T, Remuzzi G: In progressive nephropathies, overload of tubular cells with filtered proteins translates glomerular permeability dysfunction into cellular signals of interstitial inflammation. *J Am Soc Nephrol* 9:1213–1224, 1998
120. Kriz W, Hartmann I, Hosser H, Hahnel B, Kranzlin B, Provoost A, Gretz N: Tracer studies in the rat demonstrate misdirected filtration and peritubular filtrate spreading in nephrons with segmental glomerulosclerosis. *J Am Soc Nephrol* 12:496–506, 2001
121. Pawluczyk IZ, Harris KP: Macrophages promote prosclerotic responses in cultured rat mesangial cells: A mechanism for the initiation of glomerulosclerosis. *J Am Soc Nephrol* 8: 1525–1536, 1997
122. Kriz W, Kretzler M, Nagata M, Provoost AP, Shirato I, Uiker S, Sakai T, Lemley KV: A frequent pathway to glomerulosclerosis: Deterioration of tuft architecture-podocyte damage-segmental sclerosis. *Kidney Blood Press Res* 19:245–253, 1996
123. Ljungquist A: The intrarenal arterial pattern in the normal and diseased human kidney. *Acta Med Scand* 174(401):5–34, 1963

-
124. Kang DH, Kanellis J, Hugo C, Truong L, Anderson S, Kerjaschki D, Schreiner GF, Johnson RJ: Role of the microvascular endothelium in progressive renal disease. *J Am Soc Nephrol* 13:806–816, 2002
125. Marcussen N: Tubulointerstitial damage leads to atubular glomeruli: Significance and possible role in progression. *Nephrol Dial Transplant* 15(6):74–75, 2000
126. Norman JT, Clark IM, Garcia PL: Hypoxia promotes fibrogenesis in human renal fibroblasts. *Kidney Int* 58:2351–2366, 2000
127. Norman JT, Orphanides C, Garcia P, Fine LG: Hypoxia-induced changes in extracellular matrix metabolism in renal cells. *Exp Nephrol* 7:463–469, 1999
128. Zlotnik A, Yoshie O: Chemokines: A new classification system and their role in immunity. *Immunity* 12:121–127, 2000
129. Horuk R: Chemokine receptors. *Growth Factor Rev* 12:313–335, 2001
130. Murphy PM, Baggiolini M, Charo IF, Hebert CA, Horuk R, Matsushima K, Miller LH, Oppenheim JJ, Power CA: International union of pharmacology. XXII. Nomenclature for chemokine receptors. *Pharmacol Rev* 52:145–176, 2000
131. Cotter R, Williams C, Ryan L, Erichsen D, Lopez A, Peng H, Zheng J: Fractalkine (CX3CL1) and brain inflammation: Implication for HIV-1-associated dementia. *Journal of NeuroVirology* 8: 585–598, 2002
132. Salcedo R, Oppenheim JJ: Role of chemokines in angiogenesis: CXCL12/SDF-1 and CXCR4 interaction, a key regulator of endothelial cell responses. *Microcirculation* 10:359–370, 2003
133. Carter PH: Chemokine receptor antagonism as an approach to anti-inflammatory therapy: ‘Just right’ or plain wrong? *Curr Opin Chem Biol* 6:510–525, 2002
134. Nelson PJ, Krensky AM: Chemokines, chemokine receptors, and allograft rejection. *Immunity* 14:377–386, 2001
135. Moser B, Loetscher P: Lymphocyte traffic control by chemokines. *Nat Immunol* 2:123–128, 2001
136. Baggiolini M: Chemokines and leukocyte traffic. *Nature* 392:565–568, 1998
137. Luster AD: Chemokines – chemotactic cytokines that mediate inflammation. *N Engl J Med* 338:436–445, 1998
138. Horn F, Bettler E, Oliveira L, Campagne F, Cohen FE, Vriend G: GPCRDB information system for G protein-coupled receptors. *Nucleic Acids Res* 31:294–297, 2003
139. Gerard C, Rollins BJ: Chemokines and disease. *Nat Immunol* 2:108–115, 2001
140. Maurer M, von Stebut E: Macrophage inflammatory protein-1. *Int J Biochem Cell Biol* 36:1882–1886, 2004

141. Weber C, Weber KS, Klier C, Gu S, Wank R, Horuk R, Nelson PJ: Specialized roles of the chemokine receptors CCR1 and CCR5 in the recruitment of monocytes and Th1-like/CD45RO(+) T cells. *Blood* 97:1144–1146, 2001
142. Mellado M, Rodriguez-Frade JM, Vila-Coro AJ, Fernandez S, Martin de Ana A, Jones DR, Toran JL, Martinez-A C: Chemokine receptor homo- or heterodimerization activates distinct signaling pathways. *EMBO J* 20:2497–2507, 2001
143. Neote K, DiGregorio D, Mak JY, Horuk R, Schall TJ: Molecular cloning, functional expression, and signaling characteristics of a C-C chemokine receptor. *Cell* 72:415–425, 1993
144. Gao JL, Kuhns DB, Tiffany HL, McDermott D, Li X, Francke U, Murphy PM: Structure and functional expression of the human macrophage inflammatory protein 1 alpha/RANTES receptor. *J Exp Med* 177:1421–1427, 1993
145. Gong X, Gong W, Kuhns DB, Ben-Baruch A, Howard OM, Wang, JM: Monocyte chemotactic protein-2 (MCP-2) uses CCR1 and CCR2B as its functional receptors. *J Biol Chem* 272:11682–11685, 1997
146. Youn BS, Zhang SM, Lee EK, Park DH, Broxmeyer HE, Murphy PM, Locati M, Pease JE, Kim KK, Antol K, Kwon BS: Molecular cloning of leukotactin-1: a novel human beta-chemokine, a chemoattractant for neutrophils, monocytes, and lymphocytes, and a potent agonist at CC chemokine receptors 1 and 3. *J Immunol* 159:5201–5205, 1997
147. Samson M, Soularue P, Vassart G, Parmentier M: The genes encoding the human CC-chemokine receptors CC-CKR1 to CC-CKR5 (CMKBR1-CMKBR5) are clustered in the p21.3-p24 region of chromosome 3. *Genomics* 36:522-526, 1996
148. Pease JE, Horuk R: CCR1 antagonists in clinical development. *Expert Opin Investig Drugs* 14:785-796, 2005
149. Onuffer JJ, Horuk R: Chemokines, chemokine receptors and small-molecule antagonists: recent developments. *Trends Pharmacol Sci* 23:459–467, 2002
150. Kaufmann A, Salentin R, Gemsa D, Sprenger H: Increase of CCR1 and CCR5 expression and enhanced functional response to MIP-1 α during differentiation of human monocytes to macrophages. *J Leukoc Biol* 69:248–252, 2001
151. Myers SJ, Wong LM and Charo IF: Signal transduction and ligand specificity of the human monocyte chemoattractant protein-1 receptor in transfected embryonic kidney cells. *J Biol Chem* 270:5786-5792, 1995
152. Pease JE, Wang J, Ponath PD and Murphy PM: The N-terminal extracellular segments of the chemokine receptors CCR1 and CCR3 are determinants for MIP-1 alpha and eotaxin binding, respectively, but a second domain is essential for efficient receptor activation. *J Biol Chem* 273:19972-19976, 1998
153. Ninichuk V, Gross O, Reichel C, Khandoga A, Pawar RD, Ciubar R, Segerer S, Belemezova E, Radomska E, Luckow B, de Lema GP, Murphy PM, Gao JL, Henger A, Kretzler M, Horuk R, Weber M, Krombach F, Schlöndorff D, Anders HJ: Delayed chemokine receptor 1 blockade prolongs survival in collagen 4A3-deficient mice with Alport

disease. *J Am Soc Nephrol* 16:977-985, 2005

154. Eis V, Luckow B, Vielhauer V, Siveke JT, Linde Y, Segerer S, Perez De Lema G, Cohen CD, Kretzler M, Mack M, Horuk R, Murphy PM, Gao JL, Hudkins KL, Alpers CE, Gröne HJ, Schlöndorff D, Anders HJ: Chemokine receptor CCR1 but not CCR5 mediates leukocyte recruitment and subsequent renal fibrosis after unilateral ureteral obstruction. *J Am Soc Nephrol* 15:337-347, 2004

155. Eis V, Vielhauer V, Anders HJ: Targeting the chemokine network in renal inflammation. *Arch Immunol Ther Exp* 52:164-172, 2004

156. Horuk R, Shurey S, Ng HP, May K, Bauman JG, Islam I, Ghannam A, Buckman B, Wei GP, Xu W, Liang M, Rosser M, Dunning L, Hesselgesser J, Snider RM, Morrissey MM, Perez HD, Green C: CCR1-specific non-peptide antagonist: efficacy in a rabbit allograft rejection model. *Immunol Lett* 76:193-201, 2001

157. Vaidehi N, Schlyer S, Trabanino RJ, Floriano WB, Abrol R, Sharma S, Kochanny M, Koovakat S, Dunning L, Liang M, Fox JM, Lopes de Mendonça F, Pease JE, Goddard WA, Horuk R: Predictions of CCR1 chemokine receptor structure and BX 471 antagonist binding followed by experimental validation. *JBC* 281(37): 27613-27620, 2006

158. Liang M, Mallari C, Rosser M, Ng HP, May K, Monahan S, Bauman JG, Islam I, Ghannam A, Buckman B, Shaw K, Wei GP, Xu W, Zhao Z, Ho E, Shen J, Oanh H, Subramanyam B, Vergona R, Taub D, Dunning L, Harvey S, Snider RM, Hesselgesser J, Morrissey MM, Perez HD: Identification and characterization of a potent, selective, and orally active antagonist of the CC chemokine receptor-1. *J Biol Chem* 275:19000-19008, 2000

159. Bedke J, Kiss E, Horuk R, Nelson PJ, Grone HJ: Blockade of rat chemokine receptor CCR1 by BX471 reduces acute rejection and is able to reduce chronic allograft nephropathy. *Kidney Blood Press Res* 5:290, 2004

160. Anders HJ, Vielhauer V, Frink M, Linde Y, Cohen CD, Blattner SM, Kretzler M, Strutz F, Mack M, Gröne HJ, Onuffer J, Horuk R, Nelson PJ, Schlöndorff D: A chemokine receptor CCR-1 antagonist reduces renal fibrosis after unilateral ureter ligation. *J Clin Invest* 109:251-259, 2002

161. Topham PS, Csizmadia V, Soler D, Hines D, Gerard CJ, Salant DJ, Hancock WW: Lack of chemokine receptor CCR1 enhances Th1 responses and glomerular injury during nephrotoxic nephritis. *J Clin Invest* 104:1549-1557, 1999

162. Anders HJ, Belemzova E, Eis V, Segerer S, Vielhauer V, Perez de Lema G, Kretzler M, Cohen CD, Frink M, Horuk R, Hudkins KL, Alpers CE, Mampaso F, Schlöndorff D: Late onset of treatment with a chemokine receptor CCR1 antagonist prevents progression of lupus nephritis in MRL-Fas(lpr) mice. *J Am Soc Nephrol* 5:1504-1513, 2004

163. Takaya K, Koya D, Isono M, Sugimoto T, Sugaya T, Kashiwagi A, Haneda M: Involvement of ERK pathway in albumin-induced MCP-1 expression in mouse proximal tubular cells. *Am J Physiol Renal Physiol* 284:1037-1045, 2003

164. Vielhauer V, Berning E, Linde Y, Kretzler M, Strutz F, Horuk R, Grone HJ, Schlöndorff D, Anders HJ: A CCR1 antagonist reduces interstitial nephritis and fibrosis, but

not proteinuria and glomerular pathology in murine adriamycin nephropathy. *Kidney Int* 66:2264–2278, 2004

165. Cosgrove D, Meehan DT, Grunkemeyer JA, Kornak JM, Sayers R, Hunter WJ, Samuelson GC: Collagen COL4A3 knockout: a mouse model for autosomal Alport syndrome. *Genes Dev* 10:2981-2992, 1996

166. Gross O, Beirowski B, Koepke ML, Kuck J, Reiner M, Addicks K, Smyth N, Schulze-Lohoff E, Weber M. Preemptive ramipril therapy delays renal failure and reduces renal fibrosis in COL4A3-knockout mice with Alport syndrome. *Kidney Int* 63:438-446, 2003

167. Baez S: An open cremaster muscle preparation for the study of blood vessels by in vivo microscopy. *Microvasc Res* 5:384-394, 1973

168. Mempel TR, Moser C, Hutter J, Kuebler WM, Krombach F: Visualization of leukocyte transendothelial and interstitial migration using reflected light oblique transillumination in intravital video microscopy. *J Vasc Res* 40:435-441, 2003

169. Horan PK, Melnicoff MJ, Jensen BD, Slezak SE: Fluorescent cell labeling for in vivo and in vitro tracking. *Methods Cell Biol* 33:469-490, 1990

170. Batard P, Monier MN, Fortunel N, Ducos K, Sansilvestri-Morel P, Phan T, Hatzfeld A, Hatzfeld JA: TGF-(beta)1 maintains hematopoietic immaturity by a reversible negative control of cell cycle and induces CD34 antigen up-modulation. *J Immunol* 230:99-112, 1999

171. Givan AL, Fisher JL, Waugh M, Ernstoff MS, Wallace PK: A flow cytometric method to estimate the precursor frequencies of cells proliferating in response to specific antigens. *J Immunol Meth* 252:99-112, 1999

172. Horan PK, Slezak SE: Stable cell membrane labelling. *Nature* 340:167-168, 1989

173. Haverty TP, Kelly CJ, Hines WH, Amenta PS, Watanabe M, Harper RA, Kefalides NA, Neilson EG: Characterization of a renal tubular epithelial cell line which secretes the autologous target antigen of autoimmune experimental interstitial nephritis. *J Cell Biol* 107:1359-1368, 1998 (o MTC)

174. Chomczynski P, Sacchi N: Single-step method of RNA isolation by acid guanidinium thiocyanate-phenol-chloroform extraction. *Anal Biochem* 162:156-159, 1987

175. Noel LH: Renal pathology and ultrastructural findings in Alport's syndrome. *Ren Fail* 22: 751–758, 2000

176. Rodgers KD, Rao V, Meehan DT, Fager N, Gotwals P, Ryan ST, Koteliansky V, Nemori R, Cosgrove D: Monocytes may promote myofibroblast accumulation and apoptosis in Alport renal fibrosis. *Kidney Int* 63:1338-1355, 2003

177. Cosgrove D, Rodgers K, Meehan D, Miller C, Bovard K, Gilroy A, Gardner H, Kotelianski V, Gotwals P, Amatucci A, Kalluri R: Integrin alpha1beta1 and transforming growth factor-beta1 play distinct roles in alport glomerular pathogenesis and serve as dual targets for metabolic therapy. *Am J Pathol* 157:1649-1659, 2000

178. Bower G, Brown DM, Steffes MW, Vernier RL, Mauer SM: Studies of the glomerular mesangium and the juxtaglomerular apparatus in the genetically diabetic mouse. *Lab Invest* 43:333-341, 1980
179. Kluth DC, Erwig LP, Rees AJ: Multiple facets of macrophages in renal injury. *Kidney Int* 66: 542–557, 2004
180. Nikolic-Paterson DJ: A role for macrophages in mediating tubular cell apoptosis? *Kidney Int* 63:1582-1583, 2003
181. Thomas SE, Anderson S, Gordon KL, Oyama TT, Shankland SJ, Johnson RJ: Tubulointerstitial disease in aging: evidence for underlying peritubular capillary damage, a potential role for renal ischemia. *J Am Soc Nephrol* 9:231-242, 1998
182. Mantovani A: The chemokine system: redundancy for robust outputs. *Immunol Today* 20:254-257, 1999
183. Allen TJ, Cooper ME, Lan HY: Use of genetic mouse models in the study of diabetic nephropathy. *Curr Diab Rep* 4: 435–440, 2004
184. Bohle A, Wehrmann M, Bogenschutz O, Batz C, Muller CA, Muller GA: The pathogenesis of chronic renal failure in diabetic nephropathy. Investigation of 488 cases of diabetic glomerulosclerosis. *Pathol Res Pract* 187: 251– 259, 1991
185. Bower G, Brown DM, Steffes MW, Vernier RL, Mauer SM: Studies of the glomerular mesangium and the juxtaglomerular apparatus in the genetically diabetic mouse. *Lab Invest* 43:333-341, 1980
186. Serbina NV, Pamer EG: Monocyte emigration from bone marrow during bacterial infection requires signals mediated by chemokine receptor CCR2. *Nat Immunol* 7:311-317, 2006
187. Bader R, Bader H, Grund KE, Mackensen-Haen S, Christ H, Bohle A: Structure and function of the kidney in diabetic glomerulosclerosis. Correlations between morphological and functional parameters. *Pathol Res Pract* 167:204-216, 1980
188. William J, Hogan D, Battle D: Predicting the development of diabetic nephropathy and its progression. *Adv Chronic Kidney Dis* 12:202-211, 2005
189. Mora C, Navarro JF: The role of inflammation as a pathogenic factor in the development of renal disease in diabetes. *Curr Diab Rep* 5:399-401, 2005
190. Tuttle KR: Linking metabolism and immunology: diabetic nephropathy is an inflammatory disease. *J Am Soc Nephrol* 16:1537-1538, 2005
191. Erwig LP, Kluth DC, Rees AJ: Macrophage heterogeneity in renal inflammation. *Nephrol Dial Transplant* 18:1962-1965, 2003
192. Bohle A, Wehrmann M, Bogenschutz O, Batz C, Muller CA, Muller GA: The pathogenesis of chronic renal failure in diabetic nephropathy. Investigation of 488 cases of diabetic glomerulosclerosis. *Pathol Res Pract* 187:251 –259, 1991

-
193. Morii T, Fujita H, Narita T, Shimotomai T, Fujishima H, Yoshioka N, Imai H, Kakei M, Ito S: Association of monocyte chemoattractant protein-1 with renal tubular damage in diabetic nephropathy. *J Diabetes Complications* 17:11-15, 2003
194. Kelly DJ, Chanty A, Gow RM, Zhang Y, Gilbert RE: Protein kinase Cbeta inhibition attenuates osteopontin expression, macrophage recruitment, and tubulointerstitial injury in advanced experimental diabetic nephropathy. *J Am Soc Nephrol* 16:1654-1660, 2005
195. Tuttle KR, Bakris GL, Toto RD, McGill JB, Hu K, Anderson PW: The effect of roxistaurin on nephropathy in type 2 diabetes. *Diabetes Care* 28:2686-2690, 2005
196. Chow FY, Nikolic-Paterson DJ, Ozols E, Atkins RC, Rollin BJ, Tesch GH: Monocyte chemoattractant protein-1 promotes the development of diabetic renal injury in streptozotocin-treated mice. *Kidney Int* 69:73-80, 2006
197. Ninichuk V, Anders HJ: Chemokine Receptor CCR1: a new target for progressive kidney disease. *Am J Nephrol* 25:365-372, 2005

7. ABBREVIATIONS

aa	amino acids
α 5(IV)	IV collagen α 5 chain
AEC	3-Amino-9-ethylcarbazole
ADAS	autosomal dominant Alport syndrome
AR	autosomal recessive
ARAS	autosomal recessive Alport syndrome
AS	Alport syndrome
BCA-1	B cell-attracting chemokine-1
b.i.d	twice daily
BM	basement membrane
BRAK	breast and kidney-expressed chemokine
BSA	bovine serum albumin
BUN	blood urea nitrogen
BX471	CCR1 antagonist, R-N-[5-chloro-2- [2-[4- [(4-fluorophenyl) methyl]-2-methyl-1 piperazinyl]2 oxoethoxy] phenyl] urea HCl
BL5923	CCR1 antagonist
cDNA	complementary DNA
CCR1	CC chemokine receptor 1
CINC	cytokine-induced neutrophil chemoattractant
CKD	chronic kidney disease
COL4A3, 4A4	collagen4A3, 4A4
COL4A5, 4A6	collagen4A5, 4A6
CRF	chronic renal failure
CT	cycle threshold
CTACK	cutaneous T-cell-attracting chemokine
DARC	Duffy antigen receptor for chemokines
DC-CK1	dendritic cell chemokine 1
ddH ₂ O	double distilled water
DEPC	Diethylpyrocarbonate
DMEM	Dulbecco's modified Eagle's medium
DMSO	dimethyl sulfoxide

DN	Diabetic nephropathy
DNA	Desoxyribonucleic acid
dsDNA	double stranded DNA
et al.	et alii = and others
e.g.	exempli gratia = for instance
ECM	extracellular matrix
EDTA	ethylenediaminetetraacetic acid
EGF	epidermal growth factor
ELC	EBI1 ligand chemokine
ELISA	Enzyme-Linked Immunosorbent Assay
ENA78	epithelial cell-derived neutrophil-activating peptide 78
ESkine	embryonic stem cell-derived chemokine
ESRD	end-stage renal disease
FACS	fluorescence activated cell sorting
FCS	fetal calf serum
FGF	fibroblast growth factor
FITC	fluorescein isothiocyanate
FSGS	focal segmental glomerulosclerosis
GAPDH	glyceraldehyd-3-phosphate-dehydrogenase
GBM	glomerular basement membrane
GCP-2	granulocyte chemotactic protein-2
GDM	Gestational diabetes mellitus
GDP	Guanosine-5'- diphosphate
GFR	glomerular filtration rate
GN	glomerulonephritis
GPCR	G protein-coupled receptor
Gro	growth-regulated oncogene
GTP	guanosine-5'-triphosphate
HCC	hemofiltrate CC chemokine
HCC-1	hemofiltrate CC-chemokine
HE	Hematoxylin-Eosin
HIV	human immunodeficiency virus
HLA	human leukocyte antigen
hpf	high-power-field
ICAM-1	intercellular adhesion molecule-1

i.e.	id est= in other words
IgA	immunoglobulin A
IL	interleukin
IL-8	interleukin-8
IFN- γ	interferon- γ
IP-10	interferoninducible protein-10
I-TAC	interferoninducible T-cell α chemoattractant
i.v.	intravenous
J774	murine macrophage cell line
JAK/STAT	Janus kinase/signal transducers and activators of transcription
KC	keratinocyte-derived chemokine
K/DOQI	<u>K</u> idney <u>D</u> isease <u>O</u> utcomes <u>Q</u> uality <u>I</u> nitiative
K _i	inhibitor constant
LARC	liver and activation-regulated chemokine
LPS	lipopolysaccharide
MACS	magnetic assisted cell sorting
MAP kinases	mitogen-activated-protein kinases
MCP	monocyte chemoattractant protein
MCP-1	monocyte chemoattractant protein-1
MCP-2	monocyte chemoattractant protein-2
MDC	macrophage derived chemokine
MEC	mucosaeassociated epithelial chemokine
Met-RANTES	N-terminal with Methionin modified CCL5/RANTES
MIG	monokine induced by interferon- γ
min	minute/minutes
MIP	macrophage inflammatory protein
MIP-1	macrophage inflammatory protein-1
ml/min	milliliter/minute
MPIF	myeloid progenitor inhibitory factor
MPIF-1	myeloid progenitor inhibitory factor-1
mRNA	messenger ribonucleic acid
n.d.	nondeteclable
NAP-2	neutrophil-activating peptide-2
NC	noncollagenous (domain)
NF- κ B	nuclear factor- κ B

O.D.	optical density
ORF	open reading frame
PBS	phosphate buffered saline
PC	peritubular capillaries
PCR	polymerase chain reaction
PDGF	platelet derived growth factor
PF4	platelet factor 4
pH	hydrogen ion exponent
PhD	Philosophiae Doctor
pmp	per million population
RRT	renal replacement therapy
RANTES	regulated on activation normal T cell expressed and secreted
Real-time RT-PCR	Real-time reverse transcription-polymerase chain reaction
RNA	ribonucleic acid
Rnase	Ribonuclease
rRNA	ribosomal ribonucleic acid
ROIs	Regions of interest
RPM	revolutions per minute
RPMI Medium	cell culture medium
RT	room temperature
s	second
SCM-1 β	single cysteine motif-1 β chemokine
SDF-1	stromal cell-derived factor-1
SLC	secondary lymphoid tissue chemokine
SMA	smooth muscle actin
SR-PSOX	scavenger receptor for phosphatidylserine and oxidized lipoprotein
SSC	saline-sodium citrate Puffer
ssDNA	single-stranded DNA
STZ	streptozotocin
TARC	thymus and activationregulated chemokine
TCA-3	T-cell activation protein-3
TECK	thymus-expressed chemokine
TIA	transient ischemic attack
TFA	trifluoroacetic acid
TGF- β	transforming growth factor- β

Th1	T helper cell type 1
TLR	Toll-like receptors
TM	transmembrane (domain)
TNF- α	tumor necrosis factor- α
U	Units
UUO	unilateral ureteral obstruction
VCAM-1	vascular cell adhesion molecule-1
vs	versus
v/v	volume/volume
WT	wild type
XLAS	X-linked Alport syndrome
1K	1 kidney
2K	2 kidneys

8. CURRICULUM VITAE

1. Personal data

NAME Volha Ninichuk
DATE OF BIRTH 16. April 1975
PLACE OF BIRTH Gomel, Belarus
CITIZENSHIP Belarus

2. Pre-university education

1982-1992 Secondary school #26, Gomel, Belarus
1992-1995 Gomel Medical School of the Ministry of Public Health of the Republic of Belarus
Qualification of a Doctor's Assistant-Hygienist, summa cum laude
Title of Diploma:
"Analysis of sick rate of parotit infection among inhabitants of Gomel and Gomel district during 1990-1994 years".

3. University studies and working experience

1996-2001 The International A.D. Sakharov Environmental University, Department of Radiobiology and Environmental Medicine, Minsk, Belarus
Qualification of a Radiobiologist-Ecologist (equivalent to M.S.)
1999-2001 Research work as a diploma student in the Laboratory of Studying of Cytogenetic Consequences in Human after Chernobyl's catastrophe, Institute of Hereditary and Inborn Diseases, 7th City Clinic Hospital, Minsk, Belarus
Title of Diploma:
"Cytogenetic status of the children, moved to Minsk from the zone of Chernobyl accident. Analysis of chromosome aberrations and sister chromatide exchanges".

4. Postgraduate studies and professional career

2001-2002 Post-Graduate Student of the International A.D. Sakharov Environmental University, Minsk, Belarus
2001-2002 Experimental work as a laboratory assistant in the Belarussian-Switzerland health-care program "Mother and child", Belarus Green Cross, Minsk, Belarus

2003 Max-Planck-Institute of Biochemistry, Martinsried/Munich, Germany
2003-present Experimental work for PhD thesis at the Department of Clinical Biochemistry of the Faculty of Medicine of the Ludwig-Maximilians University, Munich, Germany
Title of Thesis:
“The role of chemokine receptor CCR1-dependent macrophage recruitment for the progression of chronic kidney disease in murine Alport syndrome or type 2 diabetes”.

References:

PD Dr. Hans-Joachim Anders

Associate Professor
Medizinische Poliklinik der LMU
Pettenkoferstr. 8a
80336 Munich
Germany
Tel: + 49-(0)89-2180-75-846
Fax: + 49-(0)89-2180-75-860
E-mail: hjanders@med.uni-muenchen.de

Prof. Dr. med. Detlef Schlöndorff

Medical Director
Medizinische Poliklinik der LMU
Pettenkoferstr. 8a
80336 Munich
Germany
Tel: + 49-(0)89-5160-3500
E-mail: detlef.schloendorff@med.uni-muenchen.de

Dr. Anna G. Lapko

Head of Chair of Environmental Medicine and Radiobiology
International A.D. Sakharov Environmental University
Dolgobrodskaya, 23
220009 Minsk
Belarus
Tel.: +375-017-289-56-38 (work)
Fax.: +375-017-230-68-97
E-mail: alapko@isir.minsk.by
alapko2002@yahoo.com